# FATIGUE OF THICK CYLINDERS SUBJECTED TO INTERNAL AND EXTERNAL PRESSURES

by

C.T.Kendall, B.Sc.(Eng).

A thesis submitted for the degree of

MASTER OF PHILOSOPHY

of the

UNIVERSITY OF LONDON

and also for the

DIPLOMA OF IMPERIAL COLLEGE

Department of Mechanical Engineering,

Imperial College.

Written 1971

## ACKNOWLEDGMENTS

The author wishes to thank his supervisor, Dr J. Rogan, for his advice and help. Gratitude is also expressed to Dr D.J. Burns (now of Waterloo University) who supervised some of the early work.

Thanks are also due to many members of the Mechanical Engineering Department of Imperial College for their co-operation; especially appreciated is the help given by Mr R. Place, Mr F. Yeates and the workshop staff.

A grant from the Science Research Council for expenditure involved in providing apparatus and specimens is gratefully acknowledged.

The experimental work was carried out on a part-time basis whilst the author was a member of the academic staff of the North-East Essex Technical College. Appreciation is recorded of the support received from the Essex County Council and the Principal of the College.

## ABSTRACT

The object of this research was to study the effect of the following parameters on the fatigue behaviour of thick-walled cylinders of En 25 steel: maximum range of bore shear stress, maximum hoop tension, maximum normal stress on planes of maximum range of shear stress and mean shear stress.

Existing data from cylinder, torsion and push-pull fatigue tests on this steel were re-analysed to study the effect, on shear stress range, of the other parameters, at lives of $10^5$ and $10^6$ cycles. All except cylinders with cyclic internal pressure show best correlation when normal stress is considered; these cylinders have lower fatigue strengths in each case.

A new rig (E.I.P.2) was designed to test open-end cylinders with fluctuating internal, and static external, pressures and was commissioned for the present work. Use of a similar, existing, rig was discontinued after a few tests only, because of several failures.

With rig E.I.P.2 it was possible to obtain new data by performing four sets of controlled tests; these each had approximately constant values of maximum hoop tension (in the range 0 to 28 tonf/in$^2$) and constant maximum normal stress (7 tonf/in$^2$ compressive to 7 tonf/in$^2$ tensile). The cylinders, having K ratio 1.25, were made from En 25 steel of tensile strength 65.5 to 70 tonf/in$^2$. Consideration was given mainly to the life range $10^5$ to $10^6$ cycles. The results indicate that as direct stresses are decreased the endurance, for a given shear stress range, is increased. The separate effects of hoop and normal stresses were not obtained; however, mean shear stress was shown to be much less important than direct stress.

Transverse sections of cylinders have revealed that, in some cases, fatigue cracks propagated in non-radial directions.

CONTENTS


| | | Page |
|---|---|---|
| | TITLE PAGE | 1 |
| | ACKNOWLEDGMENTS | 2 |
| | ABSTRACT | 3 |
| 1.0. | INTRODUCTION | 9 |
| | 1.1. Published work on fatigue of thick cylinders | 10 |
| | 1.2. Tension and torsion fatigue tests | 16 |
| | 1.3. Semi-continuous hydrostatic extrusion | 17 |
| 2.0. | OBJECTS | 20 |
| 3.0. | APPARATUS | 21 |
| | 3.1. Bristol fatigue machine | 21 |
| | 3.2. High base pressure system | 22 |
| | 3.3. External and internal pressure rigs | 22 |
| | 3.4. Material and specimens | 24 |
| | 3.5. External pressure supply | 26 |
| | 3.6. Measurement of internal pressure range | 27 |
| | 3.7. Calibration of pressure gauges | 28 |
| | 3.8. Trip system | 29 |
| | 3.9. Setting up procedure | 31 |
| | 3.10. Comments on pressures | 31 |
| 4.0. | RESULTS AND DISCUSSION | 34 |
| | 4.1. Important parameters and further analysis of previous work | 34 |
| | 4.2. Test series 1 - E.I.P. 1 rig | 37 |
| | 4.3. Test series 2 - preliminary tests with E.I.P. 2 rig | 39 |
| | 4.4. Strain gauge tests - E.I.P. 2 specimen | 40 |
| | 4.5. Ancillary tests - E.I.P. 2 specimens for test series 3 | 42 |
| | 4.6. Allowance for variation in tensile strength | 44 |
| | 4.7. Test series 3 - main tests with E.I.P. 2 rig | 45 |
| | 4.8. Comparison of results with other investigations | 47 |
| | 4.9. Fractures of cylinders | 49 |

| | | Page |
|---|---|---|
| 5.0. | CONCLUSIONS | 51 |
| 6.0. | RECOMMENDATIONS FOR FUTURE WORK | 52 |
| 7.0. | THEORY - THICK CYLINDERS WITH INTERNAL AND EXTERNAL PRESSURES - ELASTIC STRESSES | 53 |
| 7.1. | Symbols used | 53 |
| 7.2. | Cylinder with longitudinal stress | 54 |
| 7.3. | Cylinder without longitudinal stress | 55 |
| 7.4. | Tests with constant $\hat{\sigma}_\theta$ and constant $\sigma_z$ | 56 |
| 7.5. | Tests with constant $\hat{\sigma}_\theta$ and constant $\tau_m$ | 58 |
| 7.6. | Strain gauge tests | 59 |
| 8.0. | REFERENCES | 60 |
| 9.0. | TABLES | 64 |
| 10.0. | PHOTOGRAPHS | 82 |
| 11.0. | FIGURES | 85 |


Lists of Tables and Figures are given on pages 6, 7 and 8.

## LIST OF TABLES


| | | Page |
|---|---|---|
| 1. | Results of test series 1. En 31 and Kayser Ellison tool steel specimens | 64 |
| | Remarks on results in table 1 | 65 |
| 2. | Results of test series 1. En 25 specimens | 66 |
| | Remarks on results in table 2 | 67 |
| 3. | Results of test series 2 | 68 |
| | Remarks on results in table 3 | 69 |
| 4. | Strain gauge tests on E.I.P. 2 specimen | 70 |
| 5. | Strain gauge tests on E.I.P. 2 specimen | 71 |
| 6. | Ancillary tests. Longitudinal tension specimens | 72 |
| 7. | Ancillary tests. Transverse tension specimens | 73 |
| 8. | Ancillary tests. Hardness tests on cylinder specimens | 74 |
| 9. | Results of test series 3, specimens 1 to 7 | 75 |
| 10. | Results of test series 3, specimens 8 to 14 | 76 |
| 11. | Results of test series 3, specimens 15 to 20 | 77 |
| 12. | Results of test series 3, specimens 21 to 26 | 78 |
| | Remarks on results in tables 9 to 12 | 79 & 80 |
| 13. | Fractures of cylinders in test series 3 | 81 |


## LIST OF FIGURES


| | | |
|---|---|---|
| 1. | General arrangement of Bristol fatigue testing machine | 85 |
| 2. | Layout of Bristol fatigue testing machine reciprocating mechanism | 86 |
| 3. | Sectional view of high pressure system. Bristol fatigue testing machine | 87 |
| 4. | Sectional view of high pressure system for 0.375 in bore cylinders. Bristol fatigue testing machine | 88 |
| 5. | Schematic of high base pressure system | 89 |
| 6. | Rig E.I.P. 1 | 90 |
| 7. | Rig E.I.P. 2 | 91 |
| 8. | Specimens for rig E.I.P. 1 | 92 |
| 9. | Specimens for rig E.I.P. 2 | 93 |
| 10. | Schematic of external pressure system | 94 |

## LIST OF FIGURES (CONTINUED)


| | | Page |
|---|---|---|
| 11. | Schematic of Tecquipment direct reading strain bridge | 95 |
| 12. | Schematic of Peekel strain bridge and associated equipment | 96 |
| 13. | Calibration of P.P.I. tube | 97 |
| 14. | Calibration of top pressure gauge | 98 |
| 15. | Calibration of bottom pressure gauge | 99 |
| 16. | P.P.I. tube microstrain against airhydropump and base pressure gauge readings | 100 |
| 17. | Loading procedure | 101 |
| 18. | Effect of tensile stress on fatigue strength of En 25 steel for life of $10^6$ cycles | 102 |
| 19. | Effect of mean shear stress on fatigue strength of En 25 steel for life of $10^6$ cycles | 103 |
| 20. | Effect of normal stress on fatigue strength of En 25 steel for life of $10^6$ cycles | 104 |
| 21. | Effect of tensile stress on fatigue strength of En 25 steel for life of $10^5$ cycles | 105 |
| 22. | Effect of mean shear stress on fatigue strength of En 25 steel for life of $10^5$ cycles | 106 |
| 23. | Effect of normal stress on fatigue strength of En 25 steel for life of $10^5$ cycles | 107 |
| 24. | Positions of fractures. Specimens 3, 4 and 5 of test series 1 | 108 |
| 25. | Repeated pressure tests on En 31 cylinders | 109 |
| 26. | Results of test series 2 | 110 |
| 27. | Strain gauge test 4 - E.I.P. 2 cylinder with internal pressure | 111 |
| 28. | Cutting of cylinder specimens from bars Series 3 | 112 |
| 29. | Cutting of tension specimens from bar ends Series 3 | 113 |
| 30. | Tension test results from Instron machine | 114 |
| 31. | $\Delta\tau$ against N. Specimens 1 to 7, test series 3 | 115 |
| 32. | $\Delta\tau$ against N. Specimens 8 to 14, test series 3 | 116 |
| 33. | $\Delta\tau$ against N. Specimens 15 to 26, test series 3 | 117 |

## LIST OF FIGURES (CONTINUED)


Page

34. $\Delta\tau$/tensile strength against N, test series 3. $-2 \leq \hat{\sigma}_\theta \leq 2.4$, $-8.1 \leq \sigma_z \leq -5.8$ 118
35. $\Delta\tau$/tensile strength against N, test series 3. $10.7 \leq \hat{\sigma}_\theta \leq 12.3$, $-2 \leq \sigma_z \leq -1.3$ 119
36. $\Delta\tau$/tensile strength against N, test series 3. $18.5 \leq \hat{\sigma}_\theta \leq 22.7$, $2.5 \leq \sigma_z \leq 5$ 120
37. $\Delta\tau$/tensile strength against N, test series 3. $27 \leq \hat{\sigma}_\theta \leq 28.4$, $6.5 \leq \sigma_z \leq 7.1$ 121
38. $\Delta\tau$/tensile strength against $\hat{\sigma}_\theta$, test series 3, for lives of $10^5$, $5 \times 10^5$ and $10^6$ cycles. 122
39. $\Delta\tau$/tensile strength against $\sigma_z$, test series 3, for lives of $10^5$, $5 \times 10^5$ and $10^6$ cycles 123
40. $\Delta\tau$/tensile strength against N, test series 3, specimens 1 to 26, showing effect of $\tau_m$ 124
41. Effect of tensile stress on fatigue strength of En 25 steel cylinders. $10^6$ cycles 125
42. Effect of normal stress on fatigue strength of En 25 steel cylinders. $10^6$ cycles 126
43. Effect of tensile stress on fatigue strength of En 25 steel cylinders. $10^5$ cycles 127
44. Effect of normal stress on fatigue strength of En 25 steel cylinders. $10^5$ cycles 128
45. Notation for figures 18 to 23 and 41 to 44 129
46. Notation for figures 18 to 23 and 41 to 44 130
47. Internal pressure against external pressure. Cylinder with longitudinal stress 131
48. Internal pressure against external pressure. Cylinder without longitudinal stress. Tests at constant $\hat{\sigma}_\theta$ and $\sigma_z$ 132
49. Internal pressure against external pressure. Cylinder without longitudinal stress. Tests at constant $\hat{\sigma}_\theta$ and $\tau_m$ 133
50 $\phi$ against $\Delta\sigma_\theta$ 134
51 $\phi$ against $\sigma_{\theta m}$ 135
52 $\phi$ against $\sigma_\theta/\Delta\tau$ 136

## 1-0 INTRODUCTION

Many examples exist in practice of the use of the thick-walled cylinder to withstand high pressure. The earliest application was in the use of simple tubes for gun barrels. Design was mainly empirical until the work of Lamé and Clapeyron (1)*. Calculation of stresses at this time showed that it would be necessary to use the wall material more efficiently if requirements for better performance guns were to be met. Three significant methods were developed to achieve this: compound shrinking (1855), wire winding (1855-60) and autofrettage (about 1918). Modern guns are examples of very severe pressure vessel usage, damage resulting from both stress and high temperature.

In addition to ordnance, present day applications have increased interest in design of high pressure cylinders to withstand static and fatigue loading. In the chemical industry plants operate at pressures up to about 20 tonf/in$^2$. Fatigue loading of components can occur due to repeated pressure such as in the first stage, or by partial reduction in pressure such as in the second and higher stages, of ethylene compressors (2). In processes such as isostatic compaction, at pressures of 13.4 tonf/in$^2$ (3), fatigue conditions are imposed due to the batch or semi-continuous nature of the work. Hydrostatic extrusion (4) is attractive in principle and the industrial application has received attention, but engineering problems, such as the design of parts to withstand fatigue, still require solution.

Fatigue represents a major hazard in high pressure plant and the importance of avoiding failure, or at least ensuring that the mode of failure is ductile and therefore "safe", can scarcely be overrated. The study of fatigue of thick cylinders is of considerable practical industrial significance. The present research is concerned with the effect of stress parameters involved; information on the relative importance of these can be of value in predicting cylinder behaviour from other tests.

* References are given in section 8-0.

## 1-1 PUBLISHED WORK ON FATIGUE OF THICK CYLINDERS

Serious study of fatigue of thick cylinders was first undertaken by Morrison, Crossland and Parry at Bristol University about twenty years ago although some data, on guns, had been obtained earlier (5).

During the war I.C.I. had suffered some unexpected fatigue failures in the machines used in the high pressure process to produce polythene. The ethylene gas was separated from the oil transmitting the pressure by mercury lutes in U tubes formed from cylinders of alloy steel. The pressure in these tubes cycled from approximately zero to 10 tonf/in$^2$. In the absence of other information the design had been based conservatively on data from simple tests.

After the war, when it became possible to give consideration to such research, I.C.I. commissioned Morrison to consider the problem in detail. Morrison, Crossland and Parry (6) designed and developed a machine (hereafter referred to as the "Bristol machine") capable of testing thick cylinders at cyclic internal pressures of (up to) 20 tonf/in$^2$ and operating speeds of (up to) 700 rev/min. Their specimens had honed 1 in bores and outside diameter/bore ratios, K, of 1.4 to 2.0 . They were tested as "closed-ended" and the stress system, being equivalent to triaxial tension superimposed on pure shear, allowed comparison with fatigue results from torsion tests to determine the effect of the tension. The material used was a nickel-chrome molybdenum steel, En 25, hardened and tempered to a tensile strength of about 56 tonf/in$^2$. They tested specimens until they failed or survived $10^7$ cycles, results being in the range down to $5 \times 10^4$ cycles.

It was found that results of cylinders with different K ratios gave an almost constant fatigue limit when expressed in terms of shear stress and that this was a better approximation to failure than maximum hoop stress. Cylinder results were, however, much lower than had been

expected; at the fatigue limit the maximum range of bore shear stress was roughly equal to the semi-range of reversed shear stress in torsion. Some possible reasons for the lower cylinder results were mentioned: co-existence of triaxial tension, material anisotropy, corrosion fatigue, large surface area exposed to maximum stress and high pressure oil entering into interstices at the bore and penetrating to regions of lower stress level.

Although the anomolous cylinder results, when compared with torsion, suggested that triaxial tension had a marked effect on behaviour under shear it was surprising that the magnitude of the tension appeared unimportant from the observed correlation at the fatigue limit, expressed in terms of shear stress. Further results by Parry (7) for tests with K ratios 1.2 and 3.0 and triaxial tensile stresses outside the range previously considered confirmed former results. He found that cylinder fatigue strength could be increased by protecting the bores from the high pressure oil by a thin film of rubber, also by omitting the stress relieving treatment which had normally been carried out after honing. He concluded that honing possibly gave a smeared layer of metal which would prevent the fluid entering the surface or causing corrosion.

Further results were obtained by Morrison et al (8) for the 56 tonf/in$^2$ En 25 and also for En 25 in a harder state (68 tonf/in$^2$ tensile strength), mild steel, 3% chromium steel (Hykro), an austenitic stainless steel, a light alloy and a nearly pure titanium. The paper gives a summary of static and fatigue (bending, torsion and cylinder) properties of the metals used. It was found that the same relationship between fatigue limit for cylinders and torsion previously noted for 56 tonf/in$^2$ En 25 also obtained for other ferritic steels. Furthermore, for the ferritic steels, the ratios of safe repeated shear stress in the cylinders to fatigue limits in reversed bending, also to nominal tensile strength, were nearly constant. It seemed that the designer could work on

one third of the tensile strength of these materials as being equal to the limiting range of repeated shear stress in the cylinders. The beneficial effect of protecting the bore surfaces with a neoprene coating was shown. Other, more practical, methods of increasing fatigue resistance were investigated: nitriding and autofrettage (single application of pressure to cause overstrain, in this case to geometric mean radius). Nitriding raised the fatigue limit of the chromium steel by about 50%. Autofrettage increased the pressure necessary for fatigue failure by 10 and 26%, respectively, in En 25 cylinders of K ratios 1.6 and 2.0 (i.e. thicker cylinders derived more benefit).

The detrimental effect on fatigue strength of radial holes has been studied by Morrison et al (9). It was found that, in the case of a small crossbore in a thick cylinder, the shear stress concentration factor was 2.1 by experiment compared with a theoretical value of 2.5.

In the United States, at Watervliet Arsenal, Davidson, Eisenstadt and Reiner (10) worked on open-ended cylinders (K ratios between 1.4 and 2.0) subjected to internal pressure. Their results are for the range $10^3$ to $10^5$ cycles and refer to a material of 4340 type composition, similar to Morrison's En 25 but having higher tensile strength. They analysed their results by plotting logarithm of various cyclic parameters against logarithm of cycles to failure. The parameters used were maximum hoop stress, maximum difference in principal bore stress, maximum octahedral stress, all being rationalised by dividing by tensile strength of the specimen used, to allow for property variations; an unrationalised strain parameter was also used. None of these appeared to give any significant advantage over the others and the authors chose rationalised difference in principal bore stress to present other data in their report. They overstrained the entire wall thickness of cylinders and found that autofrettage substantially improves fatigue strength particularly at long lives. They also found that thicker

cylinders derived more benefit from autofrettage than those with lower K values.

The work on fatigue of thick cylinders to this stage was reviewed by Manning in the Bullied Memorial Lectures of 1963 (2).

In order to overcome the problem of insufficiently large bar material being available for 1 in bore specimens Parry (11) designed a new head for the Bristol machine. Tests on cylinders of bore diameters 1 in to 3/8 in showed no size effect. The beneficial effect of autofrettage was again demonstrated, a significant effect being that it could offset the detrimental effect of crossbores. By comparing results of "as turned" (30$\mu$in c.l.a.) with lapped bores, the latter were shown to be 20% stronger with stress relieving and 62% stronger without stress relieving. Other materials tested at the same time were En 56, a maraging steel, beryllium copper and two brittle materials, En 31 and tungsten carbide.

Austin and Crossland (12) designed a machine to apply repeated internal pressures up to 40 tonf/in$^2$ in order to supplement the work of Morrison et al. They worked in the low life region, below $10^5$ cycles, using identical 1 in bore specimens to those used by Morrison. Due to the high pressures used specimens were autofrettaged to varying degrees. Although there was least scatter of data when plotted on the basis of maximum hoop stress there was the anomalous situation that the thinner specimens survived longer. Their results tended to show that data could be correlated on a basis of maximum shear stress even in the mortal range if allowance was made for the effect of wall thickness on the propogation phase.

In the work on closed-ended and open-ended cylinders there had been no means of testing specimens where the intermediate, longitudinal, principal stress, $\sigma_2$ , could be varied independently of the major and minor principal stresses, $\sigma_1$ and $\sigma_3$ respectively. Blass and Findley (13) designed a rig to be used with the Bristol machine to

investigate this aspect. Their results show that, although $\sigma_2$ was varied throughout the complete range from $\sigma_1$ to $\sigma_3$, it was found to have no effect on the strength of the 4340 steel used.

Burns and Parry (14) have investigated the effect of mean shear stress. Burns tested duplex cylinders shrunk together to give a mean stress in the liners, which were of En 25. Parry's specimens were En 25 monobloc cylinders subjected to fluctuating internal pressure, giving high mean shear stress. These tests provided mean shear stress data both above and below that for Morrison's monobloc cylinders. They concluded that, between $10^5$ and $10^7$ cycles, the fatigue strength was dependent on maximum range of shear stress and associated mean shear stress, the fatigue strength decreasing with increasing mean stress. They also noted that the range and maximum value of hoop stress may be important. In order to study the effect of pressure medium on fatigue of En 25 in the range $10^6$ to $10^7$ cycles, Frost and Burns (15) subjected thick cylinders to push-pull fatigue and static internal pressures of 15-32 000 lbf/in$^2$, using either Tellus 15 or grade 1 mercury. It was shown that the reductions in fatigue strength which occurred were due, not to the pressure medium, but to the maximum normal stress on planes of maximum range of shear stress. In these two papers useful comparisons of thick cylinder, torsion and push-pull data for En 25 are given, graphs of maximum range of shear stress against other parameters being presented.

Work on low cycle fatigue ($10^3$ to $10^5$ cycles) has been carried out by Austin, Reiner and Davidson (16) using smooth and rifled bore, autofrettaged and non-autofrettaged, cylinders of K ratios 1.2 and 2.0 , made from 4330 steel with yield strengths from 74 to 80 tonf/in$^2$. They found that autofrettage greatly improved fatigue strength, increasing benefit being obtained with thicker specimens also that the benefit was greater to rifled cylinders than smooth cylinders. They referred to similar work

carried out much earlier by Newhall and Kosting (17) showing the beneficial effects of autofrettage.

Work at N.E.L. has lead to the publication, by Marsh and Haslam (18) of initial, repeated pressure tests on cylinders of mild steel and En 26. Haslam (19), using some of the results of Morrison et al, proposed that the apparently low shear stress at the fatigue limit for cylinders is due to the cumulative effect of the high pressure oil and combined stresses.

The catastrophic failures which have resulted from the use of higher yield strength, and lower impact strength, steels led Crossland and Skelton (20) to study the effects of varying hardness on fatigue strength of thick cylinders. They tested cross-bore cylinders made of En 25 with tensile strengths from over 100 down to 60 tonf/in$^2$. Although the long life fatigue strength increased with hardness the lives of the softer specimens were greater in the low endurance region. An important aspect is the mode of failure; catastrophic brittle fracture occurred when testing high tensile strength material at high pressure whereas specimens in the softest state failed in a ductile (safe) manner. Logan and Crossland (21) subsequently obtained fracture toughness data for this steel in the transverse direction. Their experiments revealed that, in spite of the great difference shown in failure mode in the earlier tests, there was a small difference only (from 76 to 88 MN/m$^{3/2}$) in the critical stress intensity factor $K_{IC}$. It was considered that the cylinders might have been too small at the higher tempering temperature for plane strain to be developed.

Shannon and Austin (22) subjected En 26 cylinders, K = 2.0, having a longitudinal notch, to internal pressure in order to study the application of fracture mechanics. Their experimental fracture strengths were about 15% higher than theoretical values based on a linear elastic finite element solution. The difference was thought to be the increase in strength due to crack tip plasticity, crack profile and end effects. Part of the discrepancy could have been due to the fact that the $K_{IC}$ tests were performed in air.

## 1-2 TENSION AND TORSION FATIGUE TESTS

Results of fatigue work on En 25, other than for cylinders, which are relevant to the present research are discussed below.

Crossland (23) studied the effect of hydrostatic pressure on fatigue strength. His specimens were subjected to a uniform triaxial stress superimposed on shear fatigue stress as compared with Morrison's closed-ended cylinders where the triaxial tension cycled in phase with the shear stresses. He tentatively concluded that his results could be correlated on the basis of Mises function modified by maximum volumetric tensile stress. He showed that his pressure medium (castor oil and brake fluid) had a deleterious effect on fatigue strength whether at pressure or not. If, however, the surface was protected (by rubber solution) the fatigue limit was raised by about 25% when a fluid pressure of 20 tonf/in$^2$ was superimposed. Burns and Parry (24) continued Crossland's work. Their results showed the considerable benefit of hydrostatic pressure on protected specimens, there being an increase of between 30 and 40% in fatigue limit for a superimposed pressure of 20 tonf/in$^2$. It seemed that the reason for this was the compressive stress, imposed on planes of maximum alternating shear stress which slowed down or stopped the rate of cracking.

Chodorowski (25) tested solid and hollow specimens under fatigue in torsion and found there to be a small, but measurable, effect of anisotropy, the specimens cut in the oblique direction being stronger than those cut transversely or longitudinally. The difference was attributed to longitudinal inclusions in the 2½ inch diameter bar. He also observed, from tests on thin tubular specimens, that fatigue strength in shear decreased in a linear manner with increasing mean stress. This reduction was not rapid (from $\pm$ 18.3 to $\pm$ 15.3 tonf/in$^2$ as mean shear stress increased from zero to 15.5 tonf/in$^2$). An analysis of results from conventional torsion tests (26)

indicates that mean shear stress has little or no effect on fatigue strength until yield occurs; Chodorowski's data fall within the scatter of these results.

White, Crossland and Morrison (27) tested push-pull specimens with tensile or compressive mean stress at atmospheric pressure and also with the material being subjected to an ambient fluid pressure of 20 tonf/in$^2$. They found that the range of stress to cause failure was reduced by a tensile mean stress and very slightly increased by a compressive mean stress if the tests were carried out at atmospheric pressure. When an ambient pressure of 20 tonf/in$^2$ was used the range of reversed stress was increased slightly; with tensile mean stress the fatigue limit was raised until it coincided with the stress range to cause gross yielding and with a compressive mean stress fatigue failure was eliminated altogether.

Boyd (28) observed the effect of tempering temperature and directional properties using rotating-bending specimens. He hardened and tempered his specimens to give tensile strengths between 60.8 and 128 tonf/in$^2$. His work showed clearly that although the fatigue limit * for specimens cut longitudinally from the rolled bar increased with tensile strength, in the case of those cut transversely there was no increase in fatigue limit above a tensile strength of about 70 tonf/in$^2$; furthermore, above about 102 tonf/in$^2$ there was actually a decrease in fatigue limit. This effect was attributed to the banded structure.

## 1-3 SEMI-CONTINUOUS HYDROSTATIC EXTRUSION

The concept of semi-continuous hydrostatic extrusion, by Alexander and Lengyel (29), lead to a design study by Lengyel, Burns and Prasad (30) on containers for a suitable production machine. Five designs of 4 in diameter bore multi-cylinder containers to withstand the fatigue loading involved were considered, based on a maximum repeated internal pressure of 150 tonf/in$^2$ and a life of

* This term also includes endurance limit values ($10^8$ cycles) for the material in the higher range of tensile strength.

at least $10^5$ cycles. The outer members were subjected to either complex static stress or cyclic stresses kept within the fatigue limit. For this it was assumed that the fatigue life is dependent on maximum range of shear stress and maximum tensile stress with the mean shear stress being relatively unimportant. Available data, for En 25, was extrapolated. The life of the inner member was assumed to be acceptable if the hoop stress was compressive and below yield. Some support for this assumption was available from fatigue data for tungsten carbide liners of cold extrusion containers (31). The design which appeared most attractive consisted of two concentric compound cylinders with high static fluid pressure between them, such that the inner member would always be in compression. This design allows the outside cylinder to be free from fatigue loading under normal operating conditions and easy replacement of liners if failure occurs, but there is the disadvantage that if the interface pressure falls to zero bursting of the inner cylinder would result.

Lengyel et al (30) designed a rig for initial tests on cylinders with static external and cyclic internal pressures in connection with the above. This rig will be referred to as rig E.I.P. 1. It was designed to be used with the Bristol machine and cylinders of K ratio 1.25 were to be subjected to a range of shear stress of 55 tonf/in$^2$ (based on a maximum internal pressure of 20 tonf/in$^2$) and compressive hoop stress. If these tests showed lives of several hundred thousand cycles they could be followed by other, much higher pressure tests. Burns (32) indicated his intention to carry out such work.

In order to increase the extrusion ratio and make the process more attractive it is desirable to use even higher pressures. Lengyel and Alexander (33) subsequently proposed that 220 tonf/in$^2$ should be considered, this being the maximum compressive stress which can be supported by tungsten carbide. Amongst their consideration of various aspects of design the authors showed that the critical stress range in the inner member could be reduced by the use of a "floating liner". In this design there is

dynamic fluid pressure between the two cylinders proportional to the internal pressure. There are, additionally, cyclic tensile stresses introduced in the outer member but these can be made small.

Harvey and Lengyel (34) have designed a fatigue machine to test thick cylinders with cyclic internal pressure up to 55 tonf/in$^2$ and static external or cyclic external (35 tonf/in$^2$ maximum) pressure, using the floating liner principle. Four preliminary results, with range of shear stress approximately constant, suggested that within a limited range there was little, if any, change in life with reduction in maximum hoop stress. The tests showed, however, that the floating liner principle could be put to practical use.

The present project, which followed the design study by Lengyel et al, has been carried out in the High Pressure Fatigue laboratory at Imperial College. Rig E.I.P. 1 had been designed and manufactured, but not tested, at the time the present research was started.

## 2-0 OBJECTS

1. To investigate the effect of various stress parameters on the fatigue life of thick cylinders of En 25 steel by subjecting them to fluctuating internal pressure and static external pressure.

2. In order to achieve the above, to commission rig E.I.P. 1 and to design and develop any further equipment necessary.

During the development period it became desirable that a new rig (E.I.P. 2) be designed to use on the Bristol machine, replacing rig E.I.P. 1. It was also decided, in the interests of machine loading, to consider tests with lives less than $10^7$ cycles.

## 3-0 APPARATUS

### 3-1 BRISTOL FATIGUE MACHINE

The machine used to apply internal pressure was that designed at Bristol by Morrison et al (6). Figures 1 to 4 and photograph 10-1 refer. It is capable of working to pressures of the order of 20 tonf/in$^2$. Although speeds of up to 1 000 rev/min are recorded the usual maximum is about 700 rev/min. Basically, the machine, which is driven by a 3 horsepower d.c. motor, causes a ram to reciprocate in a closed volume of oil which is partly contained in the cylinder; this compression results in a change of pressure.

The lower part of the machine, comprising the reciprocating mechanism, is shown in figure 2. In this two crankshafts drive the ram through connecting rods and a crossbeam. The magnitude of the stroke, and hence the maximum pressure, can be altered in steps by changing the phase of gears attached to the connecting rods.

The high pressure system takes various forms, the arrangement shown in figure 4 being that designed by Parry (11) for testing small specimens; this was used in conjunction with rig E.I.P. 2 for some early tests. The ram and seal body are honed to give very small clearance on their mating surfaces and a lip seal is used between these two parts. Between the seal housing and block sealing is effected by rubber packing. Cone rings are used to seal between the main block and pressure adjusting member and at each end of the specimen. The pressure adjusting member is strain gauged and used for pressure measurement (Section 3-6). There is a slight leakage of oil past the high pressure seal. In the basic machine this is replenished through a connection in the non-return valve block, by oil supplied at 300 lbf/in$^2$. A pressure of 150 lbf/in$^2$ is needed to open the ball valve.

## 3-2 HIGH BASE PRESSURE SYSTEM

In practical situations the base pressure can be a significant proportion of the maximum. In order to simulate such conditions the basic Bristol machine had been modified by Faville (35) so that the make-up oil can be supplied at high pressure. A schematic is given in figure 5.

A Harwood Engineering Company 38 000 lbf/in$^2$ double-acting intensifier is used giving a pressure ratio, neglecting friction, of 31.6:1. The oil on the low pressure side of the piston is driven by an HOA 60 Andrew Fraser Monoradial pump and changeover at the ends of the stroke is achieved by a double solenoid valve controlled by microswitches. The oil to be subjected to increased pressure is supplied by the make-up oil pump of the Bristol machine. The magnitude of the pressure of this oil supplied to the Bristol machine is adjusted by a variable pressure relief valve. It is supplied through a high pressure pipe union replacing part 13 in the non-return valve, in the case of the system shown in figure 4.

The high pressure pipework and components are by Pressure Products Incorporated and rated at 60 000 lbf/in$^2$. Measurement of the high base pressure is by means of a Budenberg 70 000 lbf/in$^2$ gauge. The oil used was either Shell Tellus 15 or 27 or Mobil D.T.E. Extra Heavy.

## 3-3 EXTERNAL AND INTERNAL PRESSURE RIGS

### RIG E.I.P. 1

This rig is shown in figure 6. Although some interesting results were obtained (Section 4-2) the rig was found during testing to be unsatisfactory in some respects.

a) Failures were experienced in the bottom fixing bolts joining the rig to the flange on the main block. These resulted from the high loads imposed on the rig due to the pressure acting on the $\frac{1}{2}$ in diameter area at the

bore of the specimen. Flexible nuts were substituted (36) but failures still occurred.

b) Failures at top and bottom cover plates resulted from sharp corners of the cone ring seating.

c) Difficulties were experienced in aligning the centre line of the rig with the long ram extension. This caused delays in assembly of the apparatus.

d) The core bar was cylindrical with grooves and small holes for oil to pass through; this caused unnecessary restriction on oil flow.

e) The specimens were simple cylinders without strengthened sections at the ends, the shoulder being provided to accomodate the mitre ring backing an O ring (figure 8). Failures at positions other than the gauge length indicated that this design was unsatisfactory.

Section 4-2 refers to modifications made to this rig during test series 1.

RIG E.I.P. 2

This is shown in figure 7.

Advantages of the new rig are:

a) The specimen has the same bore as Morrison's specimens and reduces, by a factor of four, the force for a given pressure.

b) Design of cone ring seatings on inserts shrunk into the cover plates avoids fatigue failures which had occurred in the initial design.

c) The rig is easier to assemble as a short ram extension enters into the transition piece but does not extend into the bore of the specimen. Use of the transition piece gives a rigid base on which to build the rig, which is preferable to using the unit shown in figure 4.

d) Separate core bar segments replace the cylindrical design.

e) The specimen has a definite gauge length.

To replace the Bristol pressure gauges, the transition

piece was strain gauged with two Tokyo Sokki Kenkyujo PLS 10 gauges mounted circumferentially and connected in series. Additionally, a simple cylinder pressure gauge was made to be used above the specimen and was strain gauged in the same way. Both the transition piece (bottom gauge) and top gauge have a K ratio of 3.

A fatigue failure occurred at the cone ring seating in the transition piece (note 5, page 80 ). The replacement part and the top pressure gauge were autofrettaged using a pressure of 66 000 lbf/in$^2$, for greater fatigue strength. PLS 10 strain gauges were attached circumferentially to the new bottom gauge and additional gauges were similarly attached to the top gauge. Apart from the above failure the rig has worked satisfactorily for about 49 million cycles at internal pressures of up to 15.2 tonf/in$^2$ and external pressures of up to 12 tonf/in$^2$.

## 3-4 MATERIAL AND SPECIMENS

### RIG E.I.P. 1

Initially six specimens were made for this rig: three of En 31 and three of Kayser Ellison tool steel (KEA 180). The specimen bore is 2 in diameter and the K ratio 1.25 . Details are given in figure 8.

#### En 31 ball race steel

Chemical composition %: C 1.05, Si 0.32, Mn 0.36, S 0.007, P 0.010, Cr 1.35.

Heat treatment: 1) Austenitised for 30 min at 840-850°C in neutral salts.

2) Quenched to 220-230°C and held at this temperature for 30 min.

3) Air cooled for 2 h.

4) Tempered at 220°C for 9 h.

The material was supplied in the annealed condition and hardening and tempering took place after machining.

#### Kayser Ellison high duty tool steel (KEA 180)

Chemical composition %: C 1.55, Cr 12.00, V 0.20, Mo 0.90 . Heat treated to give 60-63 Rockwell C hardness.

En 25

Six specimens were made of En 25 to the design given in figure 8.

The material was supplied as 4 in diameter bars by Aircraft Materials Ltd.

Chemical composition %: C 0.25, Si 0.28, Mn 0.58, S 0.017, P 0.020, Ni 2.38, Cr 0.60, Mo 0.45 .

Hardened by cooling in oil from 840°C and tempered by cooling in air from 650°C.

0.1% proof stress 43.2 tonf/in$^2$, maximum stress 55.2 tonf/in$^2$, elongation 22%, reduction in area 61.5%, Izod 76-80 ft lbf, Brinell hardness 255-269.

RIG E.I.P. 2

Two specimen designs were used (figure 9), both having 1 in bore and K ratio 1.25.

Seven specimens to part 1(a) were made, six being used for test series 2. For test series 3, 26 specimens were made to design 1 (b). The second design avoids the longitudinal tensile stress which results from external pressure acting on the 1 in radius shoulders. All specimens were made from the En 25 steel described below.

En 25

This was supplied by English Steel Corporation, in the form of 3 ft long 2 5/8 in diameter bars which had been individually hardened by oil quenching from 850°C and tempered at about 620°C.

Chemical composition %: C 0.33, Si 0.26, Mn 0.62, S 0.01, P 0.01, Ni 2.58, Cr 0.67, Mo 0.56, Cu 0.13, Sn 0.02.

Representative mechanical properties: 0.1% proof stress 59.5 tonf/in$^2$, maximum stress 68.1 tonf/in$^2$, elongation ($4\sqrt{A}$) 21.6%, reduction in area 63.6%, Izod 62-66 ft lbf.

Sulphur print examination showed sulphur to be slight and uniformly distributed and the amount of banding in the steel was considered to be normal for the quality.

After machining, the specimens for test series 3 were given a final stress relieving at 600°C in a vacuum furnace.

## 3-5 EXTERNAL PRESSURE SUPPLY

Although in some early work (repeated pressure tests in series 1) external pressure was supplied from the base pressure intensifier, in all remaining tests an airhydropump was used. A schematic of the system normally used, incorporating an airhydropump by C.S.Madan and Co, is given in figure 10; this arrangement is discussed below.

The airhydropump consists of a piston which is operated by compressed air controlled by a diaphragm reducing valve. The piston has a diameter ratio which gives an air/oil pressure ratio of 1:69.4, the oil pressure range being 5 000 to 55 000 lbf/in$^2$. In order to avoid the use of college shop air, which was not continuously provided, an independent supply was made available using an air receiver and an Atlas Copco compressor. The supply pressure was nominally 100 lbf/in$^2$ and the oil used was Shell Tellus 15.

Initially two pressure gauges were fitted in the supply pipe, a 0-80 000 lbf/in$^2$ Aminco pressure control gauge and a 0-70 000 lbf/in$^2$ Budenberg gauge. The Aminco gauge was used to control the pressure between the limits, set by high and low contacts which operated the air solenoid valve via control equipment. It was noticed during test series 3 that this gauge became unreliable in indicating pressure and that it had, in fact, been unnecessary as there was no loss of oil from the system over a period. Consequently it was not used for subsequent tests. The Budenberg gauge was used for indicating pressure and for part of the trip system.

For some tests (note 7, page 80 ) the Madan airhydropump was replaced by one supplied by Olin Mathieson.

Pressure Products Incorporated 60 000 lbf/in$^2$ high pressure pipework was used.

## 3-6 MEASUREMENT OF INTERNAL PRESSURE RANGE

In all tests the magnitude of the cyclic internal pressure was obtained by measuring the dilation of a thicker cylinder acting as a pressure gauge in series with the specimen. Two strain gauges mounted circumferentially on the pressure gauge were connected in series to form the active arm of a Wheatstone bridge. The change in resistance, and hence the change in pressure, being detected electronically by the method described by Roberts (37).

The standard Bristol machine pressure gauge, shown as part 22 in figure 3, was used for tests with rig E.I.P. 1. Other gauges used, for rig E.I.P. 2, are described in section 3-3 and their calibration in section 3-7.

For test series 1 and part of test series 2 a Tecquipment direct reading strain bridge was used and for remaining tests this was replaced by a Peekel 540 DNH strain bridge and Telequipment cathode ray oscilloscope.

### Tecquipment Direct Reading Strain Bridge

A schematic is given in figure 11. The gauges and a decade box form two arms of a Wheatstone bridge external to the Tecquipment bridge. The remaining arms are fixed analogue transformers in series with a slide wire. A 1.7 kHz oscillator energises the bridge network and is connected to the X plates of the cathode ray oscilloscope. The output of the bridge is passed through a high gain amplifier to the Y plates.

The bridge is balanced initially, by the analogue transformers, to give a horizontal line (Y signal zero). When the gauges are dynamically loaded by repeated pressure a "butterfly pattern" appears on the oscilloscope as shown in the figure. The decade box can be used to bring the line AB horizontal, the change of resistance being proportional to the pressure change.

Peekel Strain Bridge and associated equipment

This consisted of three units: a Peekel 4UD extension box, a Peekel 540 DNH strain bridge and a Telequipment cathode ray oscilloscope. A schematic is given in figure 12.

The two active strain gauges in series on a pressure gauge and two identical gauges in series as dummies were connected to the extension box, to form two arms of a Wheatstone bridge. Four such sets of gauges can be connected to the box and can be individually adjusted for resistance and capacitance; they can be switched in turn by a built in selector switch.

The strain bridge can measure by zero or deflection methods and can be used for static or dynamic strains. The principle used is the carrier frequency method. A carrier frequency oscillator supplies the amplitude of the bridge voltage. The carrier frequency amplifier has a bandpass filter to suppress unwanted frequencies. There is also a phase sensitive demodulating circuit, to which a built in moving coil meter is connected. A modulated carrier wave is used for dynamic measurements. The phase relationship between the oscillator supply to the X plates of the CRO and the bridge supply voltage on the strain gauges can be adjusted by a phase shifter.

The trace on the CRO is adjusted to a horizontal line before dynamic testing and after pressure is applied appears as the "butterfly pattern" shown. The slide wire control on the 540 DNH, indicating strain, is used to bring the line AB horizontal. The difference in this strain reading and the reading when CD is horizontal is proportional to the range of pressure.

## 3-7 CALIBRATION OF PRESSURE GAUGES

The E.I.P. 2 top gauge and original bottom gauge were calibrated statically using a dead weight tester. For both gauges a relationship 1 microstrain ≡ 127.5 lbf/in$^2$ was found to exist.

The autofrettaged top gauge and replacement bottom gauge

were calibrated indirectly from a dead weight tester. It was decided that it would be desirable to have a standard for use in the High Pressure laboratory and accordingly a length of 5/16 in diameter Pressure Products Incorporated tubing was strain gauged and calibrated against a dead weight tester. Results of this test are given in figure 13. The tube was then connected into the base pressure supply line and simultaneous readings taken of increasing base pressure, P.P.I. tube microstrain and top and bottom pressure gauge microstrain. Figures 14 and 15 give calibration curves obtained for top and bottom gauges respectively.

Calibration tests carried out with the pressure gauges hot (as in normal use) gave identical results to those obtained with the gauges cold.

P.P.I. tube microstrain and base pressure gauge readings have been plotted in figure 16 and compared with a predicted relationship based on figure 13. Also added for comparison are results of a test performed with the P.P.I. tube connected to the output of the airhydropump.

In all cases the pressure gauge strain values were obtained from the Peekel strain bridge described in 3-6. P.P.I. tube results were obtained from a Budd P350 portable strain indicator.

## 3-8 TRIP SYSTEM

When specimens are tested, with internal pressure only, on the conventional Bristol machine failure is detected by means of a falling in pressure of the make up oil. When oil escapes through the fatigue crack to atmosphere the requirement of make up oil exceeds the pump capacity and the pressure drops. A low electrical contact on the make up oil pressure gauge is arranged to stop the machine. This also operates when there is excessive leaking past the main seal or some other point in the system, for example a failed cone ring. A high contact is used to stop the machine in the event of a non-return valve failure. For early tests in series 1 (section 4-2) this conventional

trip system was used, although inadequate.

It was realised that in tests using external pressure, preventing escape of oil in the usual manner, a different system of detecting failure would have to be used. It was anticipated that when a normal gauge length failure occurred in a specimen the internal oil would be forced into the outer support cylinder area, causing the external pressure to rise whilst the make up oil pressure would remain unaffected. Accordingly, for test series 2 and 3, the Budenberg gauge on the airhydropump, with high and low electrical contacts, was wired to the Bristol machine trip system. Apart from one possible undetected failure this system has proved to be effective.

During testing the electrical contacts were set as close as possible to the needle of the airhydropump gauge. It is considered that pressure rise was rapid and failure was detected quickly. After the machine was found stopped the external pressure was readjusted to the nomimal value and the machine restarted. In cases where the specimen had failed there was almost immediately a considerable rise in pressure, for example from 23 000 to 30 000 lbf/in$^2$, whilst the make up oil pressure was observed to remain at its original value. On two occasions, in test series 3, the rig had been stripped down and the specimen inspected shortly before failure. In the case of specimen 5 an inspection revealed no sign of failure 8 000 cycles before the trips operated. Failure of specimen 7 took place about 1 400 cycles after an inspection.

Operation of the trips stops three motors: on the Bristol machine itself, on the make up oil supply and on the low pressure pump of the base pressure intensifier.

## 3-9 SETTING UP PROCEDURE

The assembly of rig E.I.P. 2 in its final form is straightforward. It had occasionally been found difficult at the end of a test to separate the plate inserts from the specimen but this was obviated by the use of molyslip between the mating surfaces. The Hallprene seal showed virtually no sign of wear but new O rings were used for each test as sometimes wear was evident in these.

Difficulties arose in early tests in obtaining correct combinations of internal and external pressures during setting up. Although the final required combinations of pressures for some tests give elastic conditions, it is obvious that either of the pressures applied individually could cause yielding. A graphical method was devised to make it possible for a single operator to obtain suitable combinations quickly.

On figure 17, which is a graph of internal pressure against external pressure, there are drawn lines representing combinations of pressures which give yielding. These are based on a shear yield stress of 23 tonf/in$^2$, the value given in reference 14 for cyclic yielding of En 25 steel having a tensile strength of 57 tonf/in$^2$. This gives a "safe side" figure for the material used for E.I.P. 2 specimens. By reference to the graph the operator is able to see quickly the allowable range of internal pressure for a given external pressure and adjust his pressures accordingly. A typical sequence of operations is shown on the graph.

## 3-10 COMMENTS ON PRESSURES

Comment is given in this section on some problems which arose in connection with the pressures. To allow for variations in pressures which could occur during tests average values were used in calculations.

The range of internal pressure was developed after a few minutes running, representing a negligible proportion of the total time of a test. It was found that later the

pressure could fall due to the temperature rise produced by the work done on the oil in the specimen. Where possible some adjustment was made to compensate for this. With the apparatus used for most of the present tests, the range of internal pressure is altered mainly in discrete steps by adjusting the tooth setting of the Bristol machine. There is no provision in the top pressure gauge of rig E.I.P. 2 for small adjustments of oil clearance volume whilst the machine is running, as in the standard Bristol machine pressure gauge. However, advantage can be taken of oil bulk modulus by changing from the Tellus oil to D.T.E. Extra Heavy to obtain a greater pressure for a given tooth setting. Seal wear and consequent increased leakage rate can cause a decrease in pressure range.

Difficulties can be experienced with the use of a high base pressure. It is difficult to maintain a base pressure less than, say, 3 500 lbf/in$^2$ since at these "low" pressures friction in the Harwood intensifier becomes significant. This was experienced in test series 3, specimen 13. If there is a high rate of leakage past the main seal of the Bristol machine there will be considerable movement of the intensifier ram to provide the increased supply of the high pressure oil. There is a decrease of pressure during the stroke. For most of the stroke the pressure was observed to be constant and it was this value which was recorded at various times during tests. As the range of pressure is also affected by changes in base pressure it should be noted that the values of range recorded were those corresponding to the constant base pressure.

Although rest periods in themselves would not appear to affect results (7) it was obviously necessary, in the interests of machine loading, to allow tests to run overnight. Any necessary adjustments to compensate for an overnight drop in pressure could be made the following morning. On two occasions in test series 2 (specimens 5 and 6), an electrical fault occurred during overnight running with the solenoid-operated trips being brought into play, removing the base

pressure and consequently reducing the internal pressure range. In the case of specimen 13, already referred to, there was a loss of base pressure during an overnight run.

It would be unreasonable to expect an accuracy greater than, say, 1 000 in 30 000 $lbf/in^2$ with the gauges used for measurement of external and base pressures.

## 4-0 RESULTS AND DISCUSSION

### 4-1 IMPORTANT PARAMETERS AND FURTHER ANALYSIS OF PREVIOUS WORK

Most thick cylinder fatigue data for En 25 are for the material heat treated to about 57 tonf/in$^2$ tensile strength; the following discussion relates to this material except where otherwise stated. Generally, the findings apply to the higher strength material used for most of the present tests.

Maximum range of bore shear stress

There is evidence (6,7,8,14) that the fatigue strength of thick cylinders in the range $10^5$ to $10^7$ cycles is primarily dependent on maximum range of bore shear stress. Although an analysis (18), of results from cylinders with different K ratios, has indicated that correlation at 2 x $10^5$ cycles is better on principal strain, it has shown that, even at this life, the shear stress criterion is reasonable. The shear stress method of presentation shows, at least, a logical trend of results for lives less than $10^5$ cycles (12).

Available results for En 25 of tensile strength 68 tonf/in$^2$ (8) have been correlated on range of shear stress in the life range $10^5$ to $10^7$ cycles. Data on material, similar to En 25, with tensile strength above 70 tonf/in$^2$ (16), for the range $10^3$ to $10^5$ cycles, have shown least K ratio dependency when plotted on basis of maximum hoop stress. Rationalised results for similar tests (10), discussed earlier, had, however, shown that this parameter gave no better correlation than range of shear stress.

Parameters affecting fatigue behaviour of thick cylinders have been discussed by Burns and Parry (14) and Frost and Burns (15). Those considered important, apart from maximum range of bore shear stress, were mean shear stress, maximum tensile stress and maximum normal stress on planes of maximum range of shear stress. Methods of correlating push-pull, rotating bending and cylinder results used by Faupel (38) and Hannon (39), based on energy, were said to be open to criticism. Hannon's work was discussed in some detail.

Mean shear stress

The evidence, by Burns and Parry (14), that fatigue strength of cylinders, in the range $10^5$ to $10^7$ cycles, is also dependent on mean shear stress, is discussed in section 1-1. They plotted range of shear stress against mean shear stress for cylinder, tension and torsion results at a life of $10^7$ cycles. This illustrated that torsion results were higher than push-pull and that cylinder results were the lowest, the difference indicating that other factors were important.

Maximum tensile stress

According to Forsyth (40) cracks are initiated early in fatigue life and propagation is spent in two sequential stages, these being Stage I (shear plane) and Stage II (tensile mode) cracking. The latter occurs normal to the maximum tensile stress and is more significant at high stress. To see if changeover to tensile mode cracking is the important consideration Burns and Parry (14) plotted, for a life of $10^7$ cycles, range of shear stress against maximum tensile stress for torsion, tension and cylinder results. Although there was some agreement, cylinder results were again lower than the others. It was also pointed out that this method of analysis would imply that cylinders with different K ratios should withstand different ranges of shear stress, which is contrary to previous findings (8). Furthermore, Frost and Burns' results are at approximately constant tensile stress but shear stress range decreases with increase in static internal pressure.

Maximum normal stress on planes of maximum range of shear stress

In order to investigate the effect of the normal stress on the critical shear plane (41), assumed to be that on which there exists the maximum range of shear stress, Frost and Burns (15) plotted this parameter against maximum range of shear stress for a life of $10^7$ cycles. Apart from their own results for cylinders with static internal pressure and push-pull, they also considered previous for tension, torsion and cylinders with internal pressure. The analysis revealed

some correlation for all except cylinders with internal pressure, which were still lower. It has been shown (42) that, by making allowance for the mechanical effect of oil penetration into the fatigue crack at the bore of the cylinders, there is better correlation with other results, but there could be uncertainties in the analysis (43). Part of the scatter could perhaps be explained by showing mean shear stress as the third parameter. Anomalies still exist, however, as can be seen by comparing results of torsion tests carried out at zero normal stress and zero mean stress. Ranges of shear stress at $10^7$ cycles for the different series of tests varied between 36 tonf/in$^2$ (25) and 44 tonf/in$^2$ (24) in spite of the constant mean stress.

It is therefore seen that fatigue limit is primarily dependent on maximum range of shear stress. It is further dependent on a tensile stress, either hoop tension or normal stress. Mean shear stress is also shown to affect results.

Further analysis of previous work

To study the effects at lower lives, figures 18 to 23 were prepared for $10^5$ and $10^6$ cycles, results being estimated from available data. The same general situation as for $10^7$ cycles is revealed, results for unprotected cylinders falling below tension results and torsion specimens being the strongest. A slightly better correlation is shown at these lower lives but there is still scatter. As at $10^7$ cycles a reasonable correlation is obtained using normal stress, for all results except cylinders with repeated internal pressure.

The analysis emphasizes the need which existed for much more information on thick cylinder fatigue behaviour in the life range $10^5$ to $10^6$ cycles. It was clearly desirable to include results from tests where the major principal stress was approximately zero.

Expressions have been developed, in terms of pressures and K ratio, for the four parameters: range of shear stress, $\Delta\tau$; hoop tension, $\sigma_\theta$; normal stress, $\sigma_r$; mean shear stress, $\tau_m$. These, and theory for tests based on their use, are given in sections 7-2 to 7-5.

## 4-2 TEST SERIES 1 - RIG E.I.P. 1

This series of tests includes some work on steels other than En 25. Details are given of the practical difficulties which led to the rejection of rig E.I.P. 1.

### En 31 and Kayser Ellison tool steel (KEA 180) specimens

Results for specimens 1 to 3 (En 31) and 4 to 6 (KEA 180) are given in table 1. These cylinders were tested with a repeated internal pressure between 29 800 and 32 800 lbf/in$^2$ together with a supporting external pressure in each case of 38 000 lbf/in$^2$. Points arising from these tests have been reported by Burns (32).

Difficulty was experienced with the apparatus itself; also, where specimens failed the fractures occurred in a brittle manner at the ends (Figure 24 and remarks on table 1 refer). The fractures of specimens 4 and 5 seemed to indicate the effect of cyclic bending stresses due to the built-in ends.

The En 31 cylinders had been heat treated in the same manner as some specimens tested by Parry (11) under repeated internal pressure only. Figure 25 gives a comparison with the results of cylinders 1 and 3 and shows that there is an increase of more than 50 % in the range of shear stress when supporting external pressure is used. It is considered that the increase found from these two results is far too great to fall within normal scatter limits of previous results, particularly bearing in mind the very flat curve obtained by Parry. It is also to be noted that the mean shear stress on plane of maximum range of shear stress for specimens 1 and 3 is 28 tonf/in$^2$, more than double the mean stress in Parry's specimens. This suggested that mean stress is much less important than maximum direct stress, which was confined to compression in the present tests.

The failure of specimen 3 consisted of flaking away of part of the end and could have been caused by unsatisfactory heat treatment after machining.

En 25 specimens

One of these specimens, number 7, was used to obtain the strains which existed when a cyclic internal pressure only was applied. Tokyo Sokki Kenkyujo PL 5 strain gauges were attached to the outside of the test length of the cylinder. The internal pressure was measured by the Tecquipment direct reading strain bridge and the cylinder strains by the Peekel 540 DNH strain bridge. Based on a Young's Modulus value of $29.8 \times 10^6$ lbf/in$^2$ (14) the theoretical hoop strain is 1160 microstrain for the internal pressure of 9 690 lbf/in$^2$ used. The average microstrain reading for four gauges mounted circumferentially midway between the two O ring seals gave an average microstrain reading of 1095 and single gauges mounted circumferentially at each end gave readings of 1048 (near enlarged end of specimen) and 805, these being 4.3 and 26.5 % respectively lower than the average reading at the centre. Some bending effects could be indicated.

It was decided to attempt fluctuating pressure tests (i.e. with base pressure) for the remaining five specimens, numbers 8 to 12. Details are given in table 2 where it can be seen that practical difficulties were experienced.

The test on specimen 8 was intended to be carried out with hoop stress zero or compressive. The limit of internal pressure was set as 20 tonf/in$^2$, the value indicated in the design of the rig (30). The specimen was overpressurised by the external pressure when the base pressure supply failed and the test was abandoned. The same test was attempted with specimen 9 but the $\frac{1}{2}$ inch diameter bolts securing the bottom plate to the flange below failed and the rig left the Bristol machine. This occurred shortly after the required pressures were obtained.

In view of the above the $\frac{1}{2}$ inch diameter bolts at the bottom plate were replaced by 5/8 inch diameter bolts and the next test, on specimen 10, was planned with the maximum internal pressure reduced to 15 tonf/in$^2$. This test was stopped because a second fatigue failure of the bottom

plate occurred (The same trouble had been experienced during the previous test). These failures initiated at a sharp corner at the cone ring seating. It was decided to use a separate insert redesigned to avoid the offending stress concentration. After this, specimen 11 was tested at the same pressures as specimen 10. In spite of fatigue failures in bolts the test was carried on until the specimen failed with a longitudinal crack slightly below centre. It had endured $2.367 \times 10^6$ cycles at a range of shear stress of 19.9 tonf/in$^2$ and a maximum tensile stress of 21 tonf/in$^2$.

The final test, on specimen 12, was discontinued when a 5/8 inch diameter bolt at the bottom cover plate failed. It was decided that rig E.I.P. 1 was inadequate and that rig E.I.P. 2 would be used for future tests.

## 4-3 TEST SERIES 2 - PRELIMINARY TESTS WITH RIG E.I.P. 2

Seven specimens were made, in two batches. The results of numbers 1 to 6 are given in table 3. The design is similar to part 1 (a) figure 9 except for outside diameters of some specimens, as indicated by the K ratios listed in table 3.

Specimen 1 was used for the initial tests on rig E.I.P. 2. This was discontinued after $2.99 \times 10^5$ cycles at a range of shear stress of 20 tonf/in$^2$ when a fatigue failure occurred at the cone ring seating of the bottom cover plate. A separate insert, with cone ring seating redesigned to avoid the stress concentration responsible for the failure, was incorporated. A similar modification was carried out later for the top cover plate.

Inaccuracies of a failing Bristol gauge almost certainly led to specimen 2 being subjected for the last 28 000 cycles to very much higher internal pressure range than indicated. It was decided at this stage to have special pressure gauges for this project. The top and bottom gauges shown in figure 7 were designed, manufactured and commissioned (note 3, remarks on table 3). Average of top and bottom pressure gauge readings were used in calculations (section 4-7).

It is desirable to compare the results of these tests with those obtained in test series 3 at similar $\hat{\sigma}_\theta$ and $\sigma_z$, using specimen 1(b). Hardness tests indicate that the material of specimens 4, 5 and 6 has a tensile strength of the order of 65 tonf/in$^2$; this value has been used as a basis of representing test series 3 results on figure 26 (section 4-6).

A difference between the specimens of test series 2 and those of test series 3 is that the former were not stress relieved. It is known (8) that this leads to higher fatigue strength in the case of En 25 having about 56 tonf/in$^2$ tensile strength; unfortunately insufficient data are available to be certain of the effect in the case of the harder En 25 used in the present tests. The following discussion neglects any possible effects of this difference.

Apart from the result for specimen 2, which is probably low for the reason given above, there would appear to be little, if any, difference between the results obtained with the two designs of specimen. Bearing in mind the practical difficulties and the limited number of results available, any conclusions must necessarily be tentative. It would seem, however, that the longitudinal stress has not significantly affected the results. The maximum range of shear stress is that due to radial and hoop stresses and it appears that the important direct stress is that normal to the plane of this shear stress or that in the hoop direction. This is further indicated by the nature of the fatigue cracks which propagated approximately in radial-longitudinal planes, similar to the usual manner for cylinders with cyclic internal pressure only (section 4-9). It is also known, from reference 13, that (cyclic) longitudinal stresses may be unimportant.

## 4-4 STRAIN GAUGE TESTS - E.I.P. 2 SPECIMEN

### Details of tests

Specimen 7 of the batch referred to in section 4-3 was used to investigate the cylinder strains developed with pressure application. Tables 4 and 5, also figure 27 refer.

For strain gauge tests 1 and 2 the specimen was used in its original form (design 1(a)), first for the determination

of bore strains with application of static external pressure. Subsequently strains at outside diameter were obtained with separate applications of static and repeated internal pressure. The specimen was then machined to design 1(b) and similar tests were carried out (tests 3 and 4).

For all tests the strain gauges used were Tokyo Sokki Kenkyujo PL 3. One hoop gauge and one longitudinal gauge were applied in each case at or near mid gauge length with additional gauges in tests 2 and 4 as indicated. Static pressure application was by means of the Madan airhydropump (external) or base pressure supply from Harwood intensifier (internal). In each case at least six increments were made to a maximum of 16 000 lbf/in$^2$ and repeated. For static pressure measurement Budenberg 0-70 000 lbf/in$^2$ gauge and/or Peekel 540 DNH strain bridge were used. Dynamic pressure measurement was by means of the Peekel strain bridge. Cylinder strains were obtained by a Budd P 350 portable strain indicator and SB 1 switch box or the Peekel strain bridge.

Analysis of results.

Graphs similar to figure 27 were plotted for each of the tests performed and from these the gradients microstrain/pressure were obtained. These were used to obtain experimental values of $\sigma_\theta$ at mid gauge length. Theoretical values are given in table 5 for comparison. The expressions used are developed in section 7-6.

Discussion of results

The significant principal stresses are $\sigma_\theta$ and $\sigma_r$. The most relevant results are therefore those for $\sigma_\theta$, particularly for tests 3 and 4 (specimen 1(b)). It should be emphasized that the elastic constants used have been taken from reference 14 so that an "exact" correlation is, to some extent, fortuitous. The results of (dynamic) test 4 are affected by the fact that there are only four values. It is observed that, in dynamic tests with a given tooth setting, the

pressure was higher for increased speed; this is due to there being less time for oil to escape past the main seal during a stroke.

The ratio of gauge length/bore diameter is small (L/D = 1) compared with ratios normally used, which might have indicated a "stiff" specimen. Available evidence for size effect in cylinder fatigue (11) showed no difference in strength between the original Bristol specimens (L/D = 2.5) and specimens with L/D = 5. The effect of gauge length on ultimate pressure was observed by Crossland and Bones (44). They found that for a short cylinder (L/D = 1) there was a small strengthening effect due to the enlarged ends, but no difference was seen for cylinders with ratios greater than 2. It has been stated (45) that a cylinder would have to be at least four diameters long before the stress system approaches that predicted by Lamé.

The strain gauge tests on E.I.P. 2 specimens indicated that, although experimental stresses obtained statically in test 3 were slightly lower than Lamé stresses (possibly due to some end effect), the results justified proceeding with the main fatigue tests, series 3.

## 4-5 ANCILLARY TESTS - E.I.P. 2 SPECIMENS FOR TEST SERIES 3

The cutting of tension and cylinder specimens from the 3 ft long bars is illustrated in figure 28.

Using the end pieces, longitudinal and transverse tension specimens were cut at $\frac{1}{2}$ inch radius from the bar axis to represent the material at the cylinder bore. Tension tests were carried out in an Instron machine of 10 000 lbf capacity, graphs such as figure 30 being obtained. The diameter of the specimen at the fracture position was measured by means of a Hilger Universal Measuring Projector. Results obtained for longitudinal specimens are shown in table 6 and those for transverse specimens are in table 7. For a given bar the tensile strength in the longitudinal direction was found to be approximately the same as that in the transverse direction;

where an increase occurred it was less than 1%. The ductility, as measured by percentage reduction in area, is, however, considerably greater in the case of longitudinal specimens; the greatest difference was in bar 28 where there was an increase of 65% based on the longitudinal value. Fractures of the longitudinal specimens were of the conventional cup and cone type. In the case of transverse specimens fractures occurred normal to the axis or, for bar 32 and the first result shown for each of bars 28 and 34, at $45^{o}$ to the axis.

V.P.N. hardness tests, using a 30 kgf load, were made on the ends of the tension specimens, and at mid-wall thickness at the 5/16 inch thick ends of the cylinders. The values quoted in tables 6 to 8 are averages for at least three readings. Samples were cut from tension specimens, in cylinder longitudinal and transverse directions, and prepared for metallurgical examination. Polished and unetched specimens were viewed at X 150 magnification and revealed normal distribution and size of impurities. The specimens were then etched in 2% nital and inspected for banding.

The present results may be compared with those obtained for En 25 by Boyd (28). For given values of tensile strength the ductility (reduction in area) of longitudinal specimens is found to be similar; in the case of transverse specimens, however, the present results are much lower. It should be noted that these transverse results are much less consistent in both cases. At about 70 tonf/in$^2$ tensile strength the present tests gave 23 and 27% ; Boyd obtained 35.9 and 41.7%. Crossland and Skelton (figure 15-5, reference 20) plotted values of hardness against tensile strength for En 25 and showed that, in the range 300 to 400 VPN, the ratio VPN/tensile strength (tonf/in$^2$) is approximately 5; this agrees with results for the present tests.

## 4-6 ALLOWANCE FOR VARIATION IN TENSILE STRENGTH

The variation in tensile strength of about 65 to 70 tonf/in$^2$ for the bars used in test series 3 is sufficient to affect fatigue behaviour. Some consideration should therefore be given to means of allowing for its effect when comparing results. The significant tensile strength is that in the transverse direction although, as stated, it is little different from that in the longitudinal direction for the particular material used.

It is known (28) that fatigue limit of transverse (rotating bending) specimens of En 25 is increased when tensile strength is raised between 60 and 70 tonf/in$^2$. Unfortunately, insufficient data are available for the mortal range. The results which are presented suggest that the difference in transverse tensile strength could possibly have rather less effect on fatigue behaviour than is expressed by a simple fatigue ratio (fatigue stress divided by tensile strength).

Investigators have, however, made allowance by using this simple ratio for both fatigue limit and mortal range. For example, in research mainly on fatigue limit, Frost and Burns (15) allowed for variations in tensile strength of En 25 between 55.2 and 62 tonf/in$^2$ by using a fatigue ratio (semi-range of longitudinal stress divided by tensile strength). Marsh and Haslam (18) used maximum range of shear stress divided by longitudinal tensile strength to compare their En 26 (64.6 tonf/in$^2$) and mild steel (35.6 tonf/in$^2$) cylinder results, in the range $5 \times 10^4$ to $10^7$ cycles, with the En 25 (56 tonf/in$^2$) results obtained by Morrison et al (8). The work of Davidson et al (10) on material similar to En 25 gives support for the use of a fatigue ratio in the range $10^3$ to $10^5$ cycles. They concluded, from tests on cylinders with cyclic internal pressure, that fatigue characteristics appeared to be proportional to tensile strength in the range 71.5 to 85 tonf/in$^2$.

It was decided that a fatigue ratio would be the best

way of allowing for variations in tensile strength in test series 3. The ratio used is range of shear stress (semi-difference of principal bore stresses) divided by transverse tensile strength of the bar from which the specimen was cut.

## 4-7 TEST SERIES 3 - MAIN TESTS WITH E.I.P. 2 RIG

Using rig E.I.P. 2 it is possible to obtain the variation in fatigue life with change in $\Delta\tau$, for various constant values of $\hat{\sigma}_\theta$ and $\sigma_z$. (The theory is given in section 7-4). Controlled tests of this type were carried out in series 3, the results of which are given in tables 9 to 12 and figures 31 to 40.

Where different readings of pressure were obtained from gauges above and below the specimen mean values were used in calculations of stresses. In early tests the top gauge often indicated a lower pressure than the bottom gauge. In most cases the effect is small, certainly when comparing the present tests with other cylinder experiments. Checks confirmed that the initial static calibration was correct and it was thought possible that the core bar in the top gauge was responsible for preventing pressure fluctuations being transmitted. On one occasion, at the start of the test on specimen 14, the pressure reading for the top gauge was only about half that for the bottom gauge. From the gear tooth setting it was obvious that the top gauge was at that stage reading incorrectly. The rig was stripped down and reassembled with the result that the trouble was cured. After the first bottom gauge had fatigued, subsequent tests were performed mainly without the top gauge core bar and neither gauge read consistently greater than the other. Analysis based on only bottom gauge readings has been carried out; this does not affect the final conclusions. It is considered that the top gauge would not be required in any future tests.

The results of tests on specimens 1 to 7, from bar 29 of tensile strength 67 tonf/in$^2$, are shown in figure 31.

The test on specimen 6 is the one case, mentioned in section 3-8, where the trip system probably did not function. The horizontal line is drawn to represent the period during which failure must have occurred, the end points representing times when the specimen was removed from the rig and inspected. The results clearly show a general tendency for the life to increase with decrease in tensile stress imposed, for a given range of shear stress. This gave encouragement to proceed with further similar tests.

Figure 32 shows results for specimens 8 to 14 from bar 34 of tensile strength 65.5 tonf/in$^2$. It will be noted that, in some of these tests, tensile stress has been kept low or eliminated. Two specimens were used for "repeat" tests. Specimen 11 was tested at similar stresses to specimen 6 because of the difficulties experienced in the earlier test. The stresses imposed on specimen 12 were approximately as those of specimen 8; this was done because in the case of specimen 8 there was a larger-than-average difference between top and bottom gauge readings.

The results of specimens 15 to 20 (bar 28, tensile strength 69.2 tonf/in$^2$) and specimens 21 to 26 (bar 32, tensile strength 70.1 tonf/in$^2$) are shown together on figure 33. Specimen 14 had experienced a particularly low life (after difficulties with the top pressure gauge); this test was repeated with specimen 15, which gave better correlation.

In order to compare results of specimens from the four bars used the effect of different tensile strengths has been allowed for by using "fatigue ratios", as discussed in section 4-6. Figures 34 to 37 illustrate the results plotted in this way. Each graph represents results at approximately constant $\hat{\sigma}_\theta$ and $\sigma_\tau$ ranging from $-2 \leq \hat{\sigma}_\theta \leq 2.4$, $-8.1 \leq \sigma_\tau \leq -5.8$ to $27 \leq \hat{\sigma}_\theta \leq 28.4$, $6.5 \leq \sigma_\tau \leq 7.1$, all in tonf/in$^2$. The scatter can be attributed mainly to difficulties sometimes experienced in maintaining pressures, also the particular problems mentioned in the case of specimens 6, 8 and 14.

The results of figures 34 to 37 have been summarised on figures 38 and 39; these give fatigue ratio ($\Delta\tau$/tensile strength

against, respectively, $\hat{\sigma}_\theta$ and $\sigma_z$, for lives of $10^5$, $5 \times 10^5$ and $10^6$ cycles. It is seen that, as each of these direct stresses is increased, the range of shear stress for a given life is decreased. Better correlation is experienced at $10^5$ cycles as would be expected if Stage II (tensile mode) cracking is more significant at high stress.

It had been intended to perform tests such as are illustrated in figure 49, where maximum hoop tension and mean shear stress are held constant. Lines AB and CD represent values of $\sigma_z$ varying from 5.5 to 2.5 tonf/in$^2$ only. These tests would, unfortunately, reveal little as this difference in $\sigma_z$ is approximately the same as the degree of scatter obtained in this parameter in figure 36. It can be seen, however, from a plot of all results obtained in this series, figure 40, that mean shear stress appears to be of much less importance than tensile stress. For example, at fatigue ratio 0.52 a specimen with $\tau_m$ equal to 0.5 tonf/in$^2$ lasts for 1.83 x $10^5$ cycles whereas one with a $\tau_m$ of 4.2 tonf/in$^2$ endures 8.05 x $10^5$ cycles. To avoid any controversy over cases where the nominal shear shear stress exceeds 23 tonf/in$^2$ (section 3-9), such results have the value of $\tau_m$ shown in brackets and could be excluded from consideration. Mean shear stress is, however, likely to have some slight effect which could be an additional cause of scatter.

## 4-8 COMPARISON OF RESULTS WITH OTHER INVESTIGATIONS

Figures 41 to 44 have been prepared to compare the results obtained in series 3 with estimated cylinder results from other published work. Attention is confined to the variation of $\hat{\sigma}_\theta$ and $\sigma_z$ with $\Delta\tau$ for lives of $10^5$ and $10^6$ cycles. The graphs are drawn to represent fatigue strength of En 25 heat treated to about 57 tonf/in$^2$ tensile strength. Where work is on significantly stronger material the results have been modified by ratios of tensile strengths; for example, the results of test series 3 are represented by ordinates of figures 34 to 37 multiplied by 57 tonf/in$^2$. Tension and torsion fatigue results have not been included as this would

have necessitated modifications, to cylinder results, to allow for the mechanical effect of oil penetration (42).

The present results are seen to provide useful information in areas where little existed. It is to be noted particularly that new data is provided for compressive normal stress and for low values of tensile hoop stress. Where comparison with other work is possible reasonable correlation obtains, the main differences being discussed below.

The results obtained by Frost and Burns (15) give higher strengths, particularly at $10^6$ cycles. This may be due, in part, to the fact that the plane of failure in these is different from that in the other cylinders considered. The autofrettaged cylinder result (8) is lower than the others and this could be due to fading of residual stresses. One of the preliminary results obtained by Harvey (34) has been shown. His tentative conclusions were contrary to the trend shown in the present tests, but were based on tests confined to a limited range.

Results for En 25 of hardness similar to that used in the present tests, are available in reference 8. These have been included in figures 41 to 44, also the fatigue limit has been shown in figures 34 to 37. These cylinders were not stress relieved after honing; insufficient data are available to be certain of the effect of this. It is known, however, that omitting the final stress relieving leads to higher fatigue strength in the case of softer En 25. Comparison of the results in reference 8, for the material in the two states of hardness, does emphasize a point when comparing results at $10^6$ cycles: in one case results are at fatigue limit and, in the other, they are in the mortal range.

Some results for steel similar in composition to En 25 are included in figures 43 and 44. Horizontal and vertical lines are drawn, respectively, for results by Davidson et al (10) and Austin et al (16). These represent ranges of possible values as far as can be established from available information on tensile strength, since individual cylinder data are not given. Blass and Findley's 4340 steel results (13) compare

well with those for En 25; results for 4340 steel by Davidson et al, and those for 4330 steel by Austin et al, lie much lower. This is partly due to surface finish, which was 16 to 125 μin RMS (10) and 63 μin RMS (16). Other data considered in figures 43 and 44 are for cylinders which were honed and, apart from those of hard En 25 in reference 8, stress relieved.

It can be said that, in figures 41 to 44, there is shown a general tendency for increasing fatigue strength to exist with decreasing direct stress.

## 4-9 FRACTURES OF CYLINDERS

In the early Bristol work (6) the crack path was determined by sectioning specimens in both longitudinal and transverse directions. There was found to be a straight, radial-longitudinal crack which started at the bore and spread normally to the hoop stress. The form of the crack was roughly semicircular and failure occurred when this reached the outside of the cylinder. The same, or similar (semi-elliptic), cracks have been reported in subsequent work on monobloc cylinders with repeated internal pressure (12,16), including some tests with additional repeated external pressure (34). In contrast to this, failure under static internal pressure of monobloc (44), and compound (46), cylinders usually consists predominantly of fracture along 45 degree spiral planes of maximum shear stress.

Specimens used in test series 2, and some of those used in test series 3, of the current work were sectioned longitudinally. As seen in this view, fractures appear to be of conventional fatigue type. An example is given in 10-3.

Thirteen of the specimens of test series 3 were sectioned transversely and ground, to determine the fracture path at mid crack length. This path was not normally visible to the naked eye. Fortunately, it was found that, if polished with wet and dry paper, some powder would collect at the crack and identify it so that photographs could be taken.

The views in the transverse direction are of particular interest. Seven of the thirteen specimens investigated had cracks which propagated entirely in a non-radial direction.*

* It is emphasized that the crack path referred to here is that seen in the photographs and neglects Stage I propagation.

These cracks were inclined to the radial direction, initially, by angles of up to 27 degrees. In three of the seven, and in some cylinders in which the cracks started radially, there was seen to be a change in direction after some distance through the wall; this final path was always nearer to the $45^{o}$ maximum shear direction. Examples of non-radial cracks are given in 10-4 and a summary of all observations is given in table 13. The thirteen cylinders included some from each bar used and it is noted that the non-radial effect is not restricted to any one bar.

The radial cracks observed in the earlier work quoted represent Stage II propagation normal to the hoop stress, which was always tensile. Hence it could be argued that the significantly different hoop stresses, imposed in the present tests, are responsible for crack paths in directions between those usually associated with Stage I (shear) and Stage II propagation. Some support for this is given in figures 50 to 52, discussed below. In each case $\phi$ is the angle measured between crack and radial direction at cylinder bore, any subsequent change in direction being ignored. The nominal stresses quoted are therefore those at the bore.

Angle $\phi$ is shown against range of hoop stress in figure 50 and this gives some correlation of results. To take account of the compressive nature of the hoop stress, figure 51 shows $\phi$ plotted against mean hoop stress. There is scatter, but the graph shows the probability for cracks to be inclined to the radial direction when the mean compressive hoop stress exceeded about 9. tonf/in$^2$.

The ratio of hoop stress to shear stress affects changeover from Stage I to Stage II propagation. A graph of $\sigma_\theta/\tau$ against $\phi$ shed no light on the reason for the non-radial fractures and was excluded. Figure 52 was plotted to investigate the effect of the ratio $\sigma_\theta/\Delta\tau$. The figure shows, approximately, that non-radial propagation is associated with the lower values of $\sigma_\theta/\Delta\tau$. The probable demarcation, and the higher values of $\sigma_\theta/\Delta\tau$ used in the earlier work, are shown on the figure.

## 5-0 CONCLUSIONS

5-1 Existing results for cylinder, torsion and push-pull fatigue tests on En 25 steel have been re-analysed to study the variation of $\Delta\tau$ with $\hat{\sigma}_\theta$, $\sigma_z$ and $\tau_m$, for lives of $10^5$ and $10^6$ cycles. Best correlation is obtained when $\Delta\tau$ is plotted against $\sigma_z$. In all cases, however, cylinders with cyclic internal pressure have lower fatigue strengths than the others.

5-2 A new rig was designed for testing open-end cylinders with fluctuating internal, and static external, pressures; this was commissioned for use in the main tests. An existing rig (30) was found to be unsuitable for the present purposes, several failures being experienced in the rig itself during initial tests.

5-3 The main tests were carried out with controlled, approximately constant, values of maximum direct stress ($\hat{\sigma}_\theta$ and $\sigma_z$). Results were analysed using a fatigue ratio ($\Delta\tau$ divided by tensile strength) to take account of variations in tensile strength of cylinder material between 65.5 and 70 tonf/in$^2$. These tests show:

a) For a given life, there is a non-linear relationship between fatigue ratio and the direct stresses, fatigue strength increasing as direct stresses decrease. At $10^5$ cycles the fatigue ratio was increased from 0.53 to 0.63 when the direct stress (tonf/in$^2$) was reduced from $\hat{\sigma}_\theta = 28$, $\sigma_z = 7$ to $\hat{\sigma}_\theta = 0$, $\sigma_z = -7$. At $10^6$ cycles the fatigue ratio was increased from 0.37 to 0.525 for a reduction in direct stress (tonf/in$^2$) from $\hat{\sigma}_\theta = 21$, $\sigma_z = 4$ to $\hat{\sigma}_\theta = 0$, $\sigma_z = -7$.

b) $\tau_m$ is much less important, in its effect on $\Delta\tau$, than direct stress.

5-4 Transverse cross-sections of a selection of specimens used in the main tests revealed that, in some cases, the crack path was inclined to the radial direction. The difference between this propagation, and that in the radial direction as found in other cylinder research (6, 12, 16, 34), was investigated considering stresses at the bore. Non-radial propagation appears to be encouraged by a sufficiently high mean compressive hoop stress and/or low ratio $\sigma_\theta/\Delta\tau$ . Approximate demarcation values found were, respectively, 9 tonf/in$^2$, and 0.65 at maximum internal pressure.

## 6-0 RECOMMENDATIONS FOR FUTURE WORK

The results show sufficient of the effect of the parameters to justify carrying out further tests. Additional results for zero hoop stress, and results for compressive hoop stress, would be particularly useful. Further consideration could be given to the possibility of separating the effects of $\hat{\sigma}_\theta$ and $\sigma_r$. With more time available the work could be extended to cover fatigue limit.

Material should be selected so that there is as small as possible variation in tensile strength between bars. It would be of interest to obtain some results for the softer En 25 used by Morrison et al. These could be compared with results from the present tests, investigating further the use of a fatigue ratio in the mortal range.

More closely controlled tests would require the frequent attention of an operator and this should be borne in mind when planning any future programme.

## 7-0 THEORY - THICK CYLINDERS WITH INTERNAL AND EXTERNAL PRESSURES - ELASTIC STRESSES

### 7-1 SYMBOLS USED

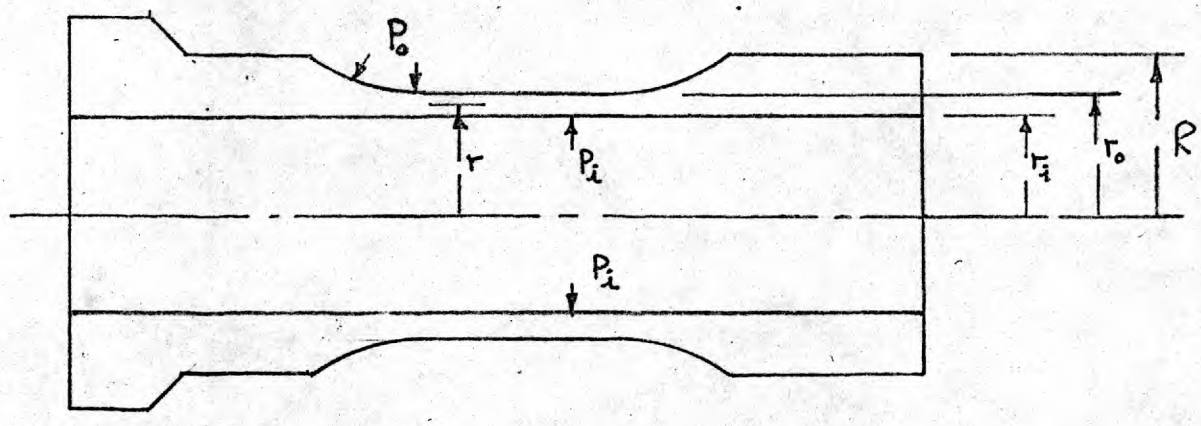
| | |
|---|---|
| $E$ | Young's modulus |
| $K$ | Ratio of external/internal diameters |
| $P_o$ | External pressure |
| $P_i$ | Internal pressure |
| $\Delta P_i$ | Range of internal pressure |
| $\epsilon_\theta$ | Hoop strain |
| $\epsilon_z$ | Longitudinal strain |
| $\nu$ | Poisson's ratio |
| $\sigma_z$ | Longitudinal stress |
| $\sigma_\theta$ | Hoop stress |
| $\sigma_r$ | Radial stress |
| $\sigma_1, \sigma_2, \sigma_3,$ | Principal stresses $\sigma_1 > \sigma_2 > \sigma_3$ algebraically |
| $\sigma_\tau$ | Maximum normal stress on plane of maximum range of shear stress |
| $\tau_{\theta r}$ | Maximum shear stress, hoop-radial plane |
| $\tau_{zr}$ | Maximum shear stress, longitudinal-radial plane |
| $\tau_{\theta z}$ | Maximum shear stress, hoop-longitudinal plane |
| $\Delta\tau_{\theta r} = \Delta\tau$ | Maximum range of shear stress, hoop-radial plane |
| $\Delta\tau_{\theta z}$ | Maximum range of shear stress, hoop-longitudinal plane |
| $\Delta\tau_{rz}$ | Maximum range of shear stress, radial-longitudinal plane |
| $\tau_m$ | Mean shear stress on plane of maximum range of shear stress |

Other maximum values are denoted by $\hat{}$ and minimum values by $\check{}$.

See also diagrams in sections 7-2 and 7-3.

Sign convention: tensile stresses and strains positive.

## 7-2 CYLINDER WITH LONGITUDINAL STRESS




In the first specimen design for rig E.I.P. 2 (figure 9, part 1a) longitudinal stresses are induced due to the external pressure acting on the shoulders of the specimen, the magnitude being

$$\sigma_z = P_o \left( \frac{R^2 - r_o^2}{r_o^2 - r_i^2} \right) \qquad (1)$$

The stress system is axi-symmetric, the hoop, radial and longitudinal stresses being the principal stresses.

Using the Lamé equations, the hoop stress is found to be

$$\sigma_\theta = \frac{(P_i - P_o)(r_i^2 + \frac{r_i^2 r_o^2}{r^2})}{(r_o^2 - r_i^2)} - P_o \qquad (2)$$

The maximum value of this occurs at the bore and is given by

$$\hat{\sigma}_\theta = (P_i - P_o)\left(\frac{K^2 + 1}{K^2 - 1}\right) - P_o \qquad (3)$$

The radial stress at the bore is

$$\sigma_r = -P_i \qquad (4)$$

The three maximum shear stresses, found by taking half the difference of pairs of principal stresses, are

$$\tau_{\theta r} = \frac{K^2}{(K^2 - 1)} (P_i - P_o) \qquad (5)$$

$$\tau_{\theta z} = \tfrac{1}{2}\left[ (P_i - P_o)\left(\frac{K^2 + 1}{K^2 - 1}\right) - P_o - \sigma_z \right] \qquad (6)$$

$$\tau_{rz} = \tfrac{1}{2}(\sigma_z + P_i) \qquad (7)$$

With constant external pressure and fluctuating internal pressure the maximum ranges of these shear stresses are

$$\Delta\tau_{\theta r} = \frac{K^2}{(K^2 - 1)} \left( \hat{P}_i - \check{P}_i \right) \qquad (8)$$

$$\Delta\tau_{\theta z} = \frac{(K^2 + 1)}{2 (K^2 - 1)} (\hat{P}_i - \check{P}_i) \qquad (9)$$

$$\Delta\tau_{rz} = \tfrac{1}{2} (\hat{P}_i - \check{P}_i) \qquad (10)$$

The absolute maximum of these three is $\Delta\tau_{\theta r}$, which will be referred to as $\Delta\tau$.

$$\Delta\tau = \frac{K^2}{(K^2 - 1)} \Delta P_i \qquad (11)$$

The mean shear stress on this plane is

$$\tau_m = \frac{K^2}{2 (K^2 - 1)} (\hat{P}_i + \check{P}_i - 2P_o) \qquad (12)$$

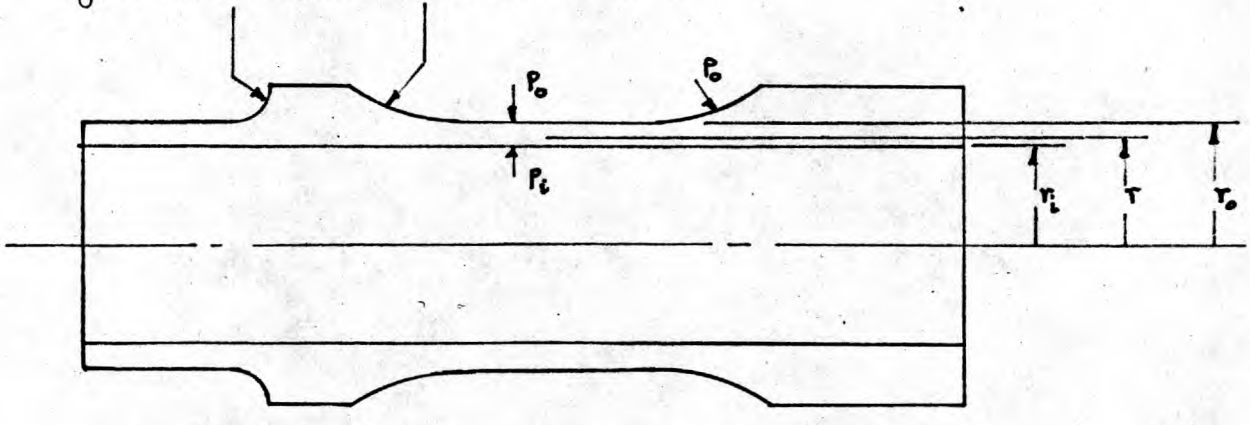
and the maximum direct stress on this plane is

$$\sigma_t = \tfrac{1}{2} \left\{ \left[ \frac{(K^2 + 1)}{(K^2 - 1)} - 1 \right] \hat{P}_i - \left[ \frac{(K^2 + 1)}{(K^2 - 1)} + 1 \right] P_o \right\} \qquad (13)$$

These expressions for elastic stresses have been used for all calculations connected with test series 2.

## 7-3 CYLINDER WITHOUT LONGITUDINAL STRESS

$P_o$ acts on equal annular areas .




In this design the external pressure acting on the equal annular areas shown gives equal and opposite forces and hence zero longitudinal stress in the gauge length of the specimen.

The expressions for stress are identical to equations 2 to 13 with the exception of equations 6 and 7; these are

replaced by

$$\tau_{\theta z} = \tfrac{1}{2}\left[(P_i - P_o)\frac{(K^2+1)}{(K^2-1)} - P_o\right] \qquad (14)$$

$$\tau_{rz} = \tfrac{1}{2} P_i \qquad (15)$$

Cylinder with K=1.25

Considering a cylinder of the above design with K=1.25 and being subjected to fluctuating internal pressure and constant external pressure, the important stress expressions become:

$$\hat{\sigma}_\theta = \sigma_1 = 4.555\,(\hat{P}_i - P_o) - P_o \qquad (3a)$$

$$\tau_{\theta r} = 2.777\,(\hat{P}_i - P_o) \qquad (5a)$$

$$\Delta\tau = 2.777\,\Delta P_i \qquad (11a)$$

$$\tau_m = 2.777\left[\frac{(\hat{P}_i + \check{P}_i)}{2} - P_o\right] \qquad (12a)$$

$$\sigma_r = 1.778\,\hat{P}_i - 2.778\,P_o \qquad (13a)$$

$$\tau_{\theta z} = 2.777\,(\hat{P}_i - P_o) - 0.5\,P_o \qquad (14a)$$

$$\tau_{rz} = 0.5\,\hat{P}_i \qquad (15a)$$

These expressions for elastic stresses have been used for all calculations connected with test series 1 and 3. All pressures and stresses above are in tonf/in$^2$.

## 7-4 TESTS WITH CONSTANT $\hat{\sigma}_\theta$ AND CONSTANT $\sigma_z$

This will be described in detail for the case where $\sigma_z$ is zero (main series of tests).

Important parameters

Some stress parameters which are considered in the fatigue of thick cylinders are $\Delta\tau$, $\hat{\sigma}_\theta$, $\sigma_r$ and $\tau_m$ (section 4-1). Equations 3a, 11a, 12a and 13a show that $\hat{\sigma}_\theta$ and $\sigma_r$ depend on $\hat{P}_i$ and $P_o$,
$\tau_m$ on $\hat{P}_i$, $\check{P}_i$ and $P_o$
and $\Delta\tau$ on $\hat{P}_i$ and $\check{P}_i$.

It is therefore possible to carry out a series of tests under conditions of constant $\hat{\sigma}_\theta$ and $\sigma_r$ (by having constant $\hat{P}_i$ and $P_o$) and at the same time vary $\Delta\tau$ (by changing the value of $P_i^{\vee}$).

Figure 48

On figure 48, which is a plot of $P_i$ against $P_o$, equation 3a is expressed for four constant values of $\hat{\sigma}_\theta$ : zero, 10, 20 and 30 tonf/in$^2$ tensile. Similar lines, but at different gradients, would express lines of constant $\sigma_r$. Tests carried out at $\hat{P}_i$ = 15 tonf/in$^2$ and $P_o$ = 10.5 tonf/in$^2$ (point B) would have constant $\hat{\sigma}_\theta$ = 10 tonf/in$^2$ and constant $\sigma_r$ = -2.6 tonf/in$^2$. The series of tests which could be carried out are represented by the line AB, a typical test having a base pressure 5 tonf/in$^2$ and range of pressure 10 tonf/in$^2$.

Using equations 5a and 14a lines have been drawn representing each of these maximum shear stresses equal to 23 tonf/in$^2$. Two lines are drawn for $\tau_{\theta r}$ and two for $\tau_{\theta z}$, the upper one in each case representing conditions at maximum internal pressure and the lower one conditions at minimum internal pressure. Thus at high pressure $\tau_{\theta r}$ is significant and at low pressure $\tau_{\theta z}$ is important; a cylinder tested at pressures represented on the graph by the area between these two lines would remain elastic if the cyclic yield stress of the material is at least 23 tonf/in$^2$. A third boundary would theoretically be given by the third maximum shear stress, $\tau_{rz}$ ; this would be represented by a horizontal line at $P_i$ = 46 tonf/in$^2$ and therefore lies outside the pressures which could be obtained in practice.

Tests with specimen part 1a, figure 9

The theory for this specimen is represented on figure 47. This is different from figure 48 in the following respects.

i) $\tau_{\theta z}$ and $\tau_{rz}$ lines are affected by $\sigma_z$ and give a smaller "elastic zone" on the graph.

ii) $\sigma_z$ becomes significant as the greatest tensile stress when a given pressure is exceeded. Two examples are shown,

those for maximum tensile stress equal to 10 and 20 tonf/in$^2$. In the first case line AB represents $\hat{\sigma}_\theta$, the greatest tensile stress up to an external pressure of 5.2 tonf/in$^2$; at higher external pressures $\sigma_z$ would be greater than 10 tonf/in$^2$.

## 7-5 TESTS WITH CONSTANT $\hat{\sigma}_\theta$ AND CONSTANT $\tau_m$

Theoretically it is possible to perform a series of tests with constant $\hat{\sigma}_\theta$ and $\tau_m$ and with varying $\Delta\tau$ and $\sigma_\tau$, in order to compare the results with those obtained in the tests described in section 7-4.

Equation 12a rearranged gives

$$\hat{P}_i = 2P_o - \check{P}_i + \frac{\tau_m}{1.39} \qquad (16)$$

For constant $\hat{\sigma}_\theta$,

$$= 4.555\ (\hat{P}_i - P_o) - P_o\ , \qquad (3a)$$

is given

$$\hat{P}_i = 1.22\ P_o + \frac{\hat{\sigma}_\theta}{4.55} \qquad (17)$$

Eliminating $P_i$ between equations 16 and 17 gives

$$\check{P}_i = 0.78\ P_o + \frac{\tau_m}{1.39} - \frac{\hat{\sigma}_\theta}{4.55} \qquad (18)$$

The desired constant values of $\tau_m$ and $\hat{\sigma}_\theta$ can be substituted in equation 18 and the relationship found between $\check{P}_i$ and $P_o$.

Figure 49

This has been drawn to represent equations 3a and 18 for $\tau_m$ = 2 tonf/in$^2$ and $\hat{\sigma}_\theta$ = 20 tonf/in$^2$. Two typical tests are illustrated by AB ($\Delta P_i$ = 9 tonf/in$^2$, $\check{P}_i$ = zero) and CD ($\Delta P_i$ = 15 tonf/in$^2$, $\check{P}_i$ = 3.8 tonf/in$^2$). Specimen design figure 9 part 1b is considered and the elastic zone is defined between the lines $\tau_{\theta r}$ = 23 tonf/in$^2$ (EF) and $\tau_{\theta z}$ = 23 tonf/in$^2$ (GH).

## 7-6 STRAIN GAUGE TESTS

The following expressions have been used in calculations connected with the strain gauge tests on specimens 1(a) and 1(b), figure 9.

### Stress and strain at bore with application of $P_o$ only

### Theoretical (Lamé prediction) value of hoop stress

Equation 3, $$\sigma_\theta = -P_o \frac{(K^2 + 1)}{(K^2 - 1)} - P_o$$

becomes $$\sigma_\theta = -5.555\ P_o \qquad (19)$$

### Hoop stress obtained from strain measurement

$$\epsilon_\theta = \frac{1}{E}(\sigma_\theta - \nu(\sigma_r + \sigma_z))$$

and $$\epsilon_z = \frac{1}{E}(\sigma_z - \nu(\sigma_r + \sigma_\theta))$$ in general, but $\sigma_r$ = zero

therefore $$\sigma_\theta = \frac{E}{(1 - \nu^2)}(\epsilon_\theta + \nu\epsilon_z)$$

and using $E = 29.8 \times 10^6$ lbf/in$^2$ and $\nu = 0.283$ (reference 14)

$$\sigma_\theta = 32.4\ (\epsilon_\theta + 0.283\epsilon_z) \qquad (20)$$

where $\sigma_\theta$ is in lbf/in$^2$, $\epsilon_\theta$ and $\epsilon_z$ in microstrain.

### Stress and strain at outside diameter with application of $P_i$ only

### Theoretical (Lamé prediction) value of hoop stress

Equation 2, $$\sigma_\theta = \frac{2r_i^2 P_i}{(r_o^2 - r_i^2)}$$

becomes $$\sigma_\theta = 3.56\ P_i \qquad (21)$$

### Hoop stress obtained from strain measurement

Equation 20 applies.

## 8-0 REFERENCES


1. Lamé, G., Clapeyron, B.P.E. Mémoire sur l'équilibre intérieur des corps solides homogènes. Mem. Acad. Sci. Paris 1833, 4, 465. From ref. 47.

2. Manning, W.R.D. High pressure engineering. Bullied memorial lectures. Vol 2. Univ. of Nottingham. 1963.

3. Googin, J.M., Greene, H.T., Guinn, G.R., Neeley, A.C. Tungsten powder metallurgy in the production of large crucibles and susceptors. International Powder Metallurgy Conference. New York. 1965.

4. Pugh, H.Ll.D. Recent developments in cold forming. Bullied memorial lectures. Vol IIIA and IIIB. Univ. of Nottingham. 1965.

5. Morrison, J.L.M., Cook, G. Report on the effect on an autofrettaged gun tube of 2 000 repetitions of the autofrettage pressure. Declassified paper of Gun Design Committee. 1943. From ref. 12.

6. Morrison, J.L.M., Crossland, B., Parry, J.S.C. Fatigue under triaxial stress: development of a testing machine and preliminary results. Proc. I. Mech. E. Vol 170, p. 697. 1956.

7. Parry, J.S.C. Further results of fatigue under triaxial stress. Proc. Int. Conf. on Fatigue of Metals. I. Mech. E. p. 132. 1956.

8. Morrison, J.L.M., Crossland, B., Parry, J.S.C. Strength of thick cylinders subjected to repeated internal pressure. Proc. I. Mech. E. Vol 174, No 2, p 95. 1960.

9. Morrison, J.L.M., Crossland, B., Parry, J.S.C. Fatigue strength of cylinders with cross-bores. J.Mech. Eng. Sci. Vol 1, No 3. 1959.

10. Davidson, T.E., Eisenstadt, R., Reiner, A.N. Fatigue characteristics of open-end thick-walled cylinders under cyclic internal pressure. J. Basic Engineering. A.S.M.E. Series D, Vol 85, p 555. 1963.

11. Parry, J.S.C. Fatigue of thick cylinders: further practical information. Proc. I. Mech. E. Vol 180, Pt 1, p 387. 1965-66.

12. Austin, B.A., Crossland, B. Low-endurance fatigue strength of thick-walled cylinders: development of a testing machine and preliminary results. Proc. I. Mech. E. Vol 180, Pt 1. 1965-66.

13. Blass, J.J., Findley, W.N. The influence of the intermediate principal stress on fatigue under triaxial stress. Materials Research and Standards. Vol 7, No 6. 1967.

14. Burns, D.J., Parry, J.S.C. Effect of mean shear stress on the fatigue behaviour of thick-walled cylinders. High Pressure Eng. Proc. I. Mech. E. Vol 182. Pt 3C. Paper 28. 1967-68.

15. Frost, W.J., Burns, D.J. Effect of oil and mercury at high pressure on the fatigue behaviour of thick-walled cylinders of En 25 steel. Ibid. Paper 29.

16. Austin, B.A., Reiner, A.N., Davidson, T.E. Low cycle fatigue strength of thick-walled pressure vessels. Ibid. Paper 35.

17. Newhall,D.H., Kosting, P.R. Progressive stress damage and strength of centrifugally cast CW gun tubes. Watertown Arsenal Lab. 731/281. 1949. Details from ref. 16.

18. Marsh, K.J., Haslam, G.H. Fatigue of cylinders subjected to pulsating internal oil pressure. NEL Report 381. 1969.

19. Haslam, G.H. The fatigue strength of thick-walled steel cylinders subjected to pulsating internal pressures. NEL Report 444. 1970.

20. Crossland, B., Skelton, W.J. Effect of varying hardness on the fatigue strength of thick-walled cross-bore cylinders of En 25. High Pressure Eng. Proc. I. Mech. E. Vol 182. Pt 3C. Paper 15. 1967-68.

21. Logan, J.G., Crossland, B. The fracture toughness of En 25 and a 3% Ni-Cr-Mo-V steel at various strength levels together with Charpy impact data. Paper 40. Conf. on Practical Application of Fracture Mechanics to Pressure Vessel Technology. I. Mech. E. 1971.

22. Shannon R.W.E., Austin, B.A. The application of fracture mechanics to failure of thick-walled cylinders. Ibid. Paper 32.

23. Crossland, B. Effect of large hydrostatic pressures on the torsional fatigue strength of an alloy steel. Proc. Int. Conf. on Fatigue of Metals. I. Mech. E. p. 138. 1956.

24. Burns, D.J., Parry, J.S.C. Effect of large hydrostatic pressures on the torsional fatigue strength of two steels. J. Mech. Eng. Sci. Vol 6, No 3. 1964.

25. Chodorowski, W.T. Fatigue strength in shear of an alloy steel, with particular reference to the effect of mean stress and directional properties. Proc. Int. Conf. on Fatigue of Metals. I. Mech. E. p. 122. 1956.

26. Smith, J.O. Effect of range of stress on fatigue strength. Univ. Illinois Eng. Exptl. Stn. Bulletin 334. 1942.

27. White, D.J., Crossland, B., Morrison, J.L.M. Effect of hydrostatic pressure on the direct-stress fatigue strength of an alloy steel. J. Mech. Eng. Sci. Vol 1, p.39. 1959.

28. Boyd, R.K. Fatigue strength of an alloy steel. Effect of tempering temperature and directional properties. Proc. I. Mech. E. Vol 179. Pt 1. No 23. 1964-65.

29. Alexander, J.M., Lengyel, B. Semi-continuous hydrostatic extrusion of wire. Paper 7. Appl. Mech. Conv. 1966. Proc. I. Mech. E. Vol 180. Pt 31. 1965-66.

30. Lengyel, B., Burns, D.J., Prasad, L.V. Design of containers for a semi-continuous hydrostatic extrusion production machine. 7th Int. Conf. of Machine Tool Design and Research. Birmingham University. 1966.

31. Seiber, K. Tooling design for cold forging. Sh. Metal Inds. Vol 44, p. 111. 1966.

32. Burns, D.J. Discussion, p. 298. High Pressure Eng. Proc. I. Mech. E. Vol 182. Pt 3C. 1967-68.

33. Lengyel, B., Alexander, J.M. Design of a production machine for semi-continuous hydrostatic extrusion. Ibid. Paper 9.

34. Harvey, D.C., Lengyel, B. Pressure vessels under cyclic loading: test rig and initial results. 9th international M.T.D.R. Conf. held at University of Manchester. 16-20 Sept 1968. Pergamon.

35. Faville, W.S. Repeated pressure fatigue testing of thick walled cylinders. M.Sc. Thesis. Imperial College. 1966.

36. Heywood, R.B. Designing against fatigue. Chapman and Hall. 1962.

37. Roberts, M.H. Precise measurement of fatigue test load. Laboratory Methods. Vol XLVI No 274. 1952.

38. Faupel, J.H. Engineering design. A synthesis of stress analysis and materials engineering. 647-651. John Wiley New York. 1964.

39. Hannon, B.M. Correlation of fatigue tests on thick-walled cylinders subjected to repeated internal pressure. J. Basic Eng. Trans. A.S.M.E. Vol 87. Series D. p. 405. 1965.

40. Forsyth, P.J.E. The physical basis of metal fatigue. Blackie. 1969.

41. Findley, W.N. A theory for the effect of mean stress on fatigue of metals under combined torsion and axial load or bending. Journal of Engineering for Industry. p. 301. Nov 1959.

42. Jones, P.M., Tomkins, B. Discussion, p. 309. High Pressure Eng. Proc. I. Mech. E. Vol 182. Pt 3C. 1967-68.

43. Frost, W.J., Burns, D.J. Authors' replies. Ibid. p.334.

44. Crossland, B., Bones, J.A. Behaviour of thick-walled steel cylinders subjected to internal pressure. Proc. I. Mech. E. Vol 172, No 25. 1958.

45. Comstock, C.W. Some considerations in the design of thick-wall pressure cylinders. Trans. Am. Inst. Chem. Engrs. 39, 299. 1943. Contribution by Jasper and Scudder.

46. Crossland, B., Burns, D.J. Behaviour of compound steel cylinders subjected to internal pressure. Proc. I. Mech. E. Vol 175, No 27. 1961.

47. Wilson, W.R.D., Skelton, W.J. Design of high pressure cylinders. High Pressure Eng. Proc. I. Mech. E. Vol 182. Pt 3C. Paper 5. 1967-68.

RESULTS - TEST SERIES 1 E.I.P. 1 RIG
En 31 AND KEA 180 SPECIMENS

OBSERVED RESULTS

| Specimen number | Material | Pressures (Lbf/in$^2$) | | | Cycles |
|---|---|---|---|---|---|
| | | Pi range = Pi max | Pi min | Po | |
| 1 | En 31 | 29 800 | Zero | 38 000 | 133 600 U |
| 2 | En 31 | - | Zero | - | - |
| 3 | En 31 | 30 400 | Zero | 38 000 | 36 400 |
| 4 | KEA 180 | 32 000 | Zero | 38 000 | 59 400 |
| 5 | KEA 180 | 32 000 | Zero | 38 000 | 139 500 |
| 6 | KEA 180 | 32 800 | Zero | 38 000 | 6 500 U |

Notes: 1. U denotes unbroken specimen.
2. For remarks on these tests see following page.

DERIVED RESULTS

| Specimen number | Stresses (Tonf/in$^2$) | | | |
|---|---|---|---|---|
| | $\Delta\tau$ | $\sigma_\theta$ | $\tau_m$ | $\sigma_\tau$ |
| 1 | 37 | -34 | 28.7 | -24 |
| 3 | 37.8 | -32 | 28.3 | -23 |
| 4 and 5 | 39.7 | -29 | 27.3 | -22 |
| 6 | 40.7 | -28 | 26.8 | -21 |

TABLE 1

## RESULTS - TEST SERIES 1 E.I.P. 1 RIG REMARKS

Specimen 1

Specimen was removed unbroken. Evidence of fretting on specimen and core bar. Fatigue cracks between small holes in cylindrical core bar.

Specimen 2

Three bolts failed at the bottom of the rig after a few cycles. No reading of pressures taken. Specimen damaged but not broken.

Specimen 3

Oil leak from outer support cylinder. No normal gauge length type failure but brittle fracture at bottom face of specimen.

Specimen 4

Trips operated. Oil leak at outer support cylinder. Failure occurred at change in cross section of specimen to carry bottom external seal. Some holes in core bar closed by metal flow.

Specimen 5

Trips operated. Oil leak at bottom cone ring joint. Brittle fracture near end of parallel portion.

Specimen 6

Trips operated. Oil leak at cone ring joint. Specimen damaged.

Positions of fractures in specimens 3,4 and 5 are shown in figure 24.

## RESULTS - TEST SERIES 1 E.I.P. 1 RIG En 25 SPECIMENS

### OBSERVED RESULTS

| Specimen number | Pressures (Lbf/in$^2$) | | | | Cycles |
|---|---|---|---|---|---|
| | Pi min | Pi range | Pi max | Po | |
| 8 | up to 7 500*<br><br>Intended 21 000 | up to 24 000 average 20 300*<br><br>pressures 24 000 | up to 31 000*<br><br>were: 45 000 | 16 000*<br><br>37 000 | 20 000 U |
| 9 | up to 21 000<br><br>average 20 000* | up to 23 800<br><br>average 21 100* | up to 44 800<br><br>average 41 400* | up to 30 000<br><br>average 27 700* | 85 100 U |
| 10 | 17 500 | 16 000 | 33 500 | 19 000 | 340 600 U |
| 11 | 17 500 | 16 000 | 33 500 | 19 000 | 2 367 200 |
| 12 | 5 500 | 28 000 | 33 500 | 19 000 | 159 000 U |

Notes: 1. U denotes unbroken specimen.
2. For specimens 8 and 9 pressures marked * were used to calculate stresses below.
3. For remarks on these tests see following page.

### DERIVED RESULTS

| Specimen number | Stresses (Tonf/in$^2$) | | | |
|---|---|---|---|---|
| | $\Delta\tau$ | $\hat{\sigma}_0$ | $\tau_m$ | $\sigma_\tau$ |
| 8 | 25.2<br><br>Intended 29.8 | 16.8<br><br>stresses 0 | 2.1<br><br>were: -10.1 | 2<br><br>5 |
| 9 | 26.2 | 4.8 | -1.7 | 3.5 |
| 10 and 11 | 19.9 | 21 | 3 | 8.1 |
| 12 | 34.7 | 21 | 3 | 0.6 |

TABLE 2

## RESULTS - TEST SERIES 1 E.I.P.1 RIG REMARKS

Specimen 8

Fatigue crack of cone ring, pressure gauge, high base pressure supply pipe. The latter caused specimen to be overpressurised on outside, deformed too badly to get core bar in. Intended pressures not reached.

Specimen 9

Intended pressures and stresses as for specimen 8. Fatigue crack of cone ring seating of bottom cover plate, nuts and $\frac{1}{2}$" diameter bolts securing this plate to flange. Final pressures (design limit) obtained for few cycles only due to complete failure of the $\frac{1}{2}$" diameter bolts. Specimen damaged.

Specimen 10

Smaller maximum pressures used because of previous failures. Half inch diameter bolts at bottom replaced by 5/8" diameter before test. Fatigue crack in replacement bottom plate. Specimen damaged.

Specimen 11

Bottom plate modified before test (separate insert without severe stress concentration). Test conditions as for specimen 10. Fatigue of three 5/8" diameter bolts joining pressure gauge to top cover plate, three bolts joining cover plate to flange and later more bolts at top. Longitudinal fatigue crack slightly below centre line of specimen.

Specimen 12

5/8" diameter bolt failed on bottom plate. Rig E.I.P.1 not used after this.

RESULTS TEST SERIES 2 E.I.P.2 RIG

| Specimen number | K ratio | Pressures (Lbf/in$^2$) | | | | |
|---|---|---|---|---|---|---|
| | | $P_i$ min | $P_i$ range (Bottom gauge) | $P_i$ range (Average of top and bottom gauges) | $P_i$ max | $P_o$ |
| 1 | 1.4 | 12 000 | 22 000 | 22 000 | 34 000 | 14 000 |
| 2 | 1.25 | 5 600 | 27 400 | 27 400 | 33 000 | 21 200 |
| 3 | 1.22 | 5 000 | 25 800 | 25 200 | 30 200 | 20 000 |
| 4 | 1.25 | - | 34 300 | 33 700 | 33 700 | 22 500 |
| 5 | 1.25 | 8 300 | 25 700 | 25 300 | 33 600 | 23 000 |
| 6 | 1.25 | 7 000 | 25 100 | 25 100 | 32 100 | 22 500 |

| Specimen number | VPN | Stresses (Tonf/in$^2$) | | | | | Cycles |
|---|---|---|---|---|---|---|---|
| | | $\Delta\tau$ | $\hat{\sigma}_\theta$ | $\tau_m$ | $\sigma_r$ | $\sigma_z$ | |
| 1 | 348 | 20 | 12 | 12.2 | 3 | 4.5 | $2.99 \times 10^5$ unbroken |
| 2 | 373 | 34 | 14.3 | 2.5 | -0.2 | 18.2 | $1.16 \times 10^5$ |
| 3 | 356 | 34.2 | 14.2 | 3.3 | -0.7 | 21 | $5.2 \times 10^5$ |
| 4 | 308 | 41.9 | 13 | 6.7 | -0.9 | 19.2 | $7.2 \times 10^4$ |
| 5 | 308 | 31.5 | 11.6 | 2.5 | -1.8 | 19.6 | $1.62 \times 10^6$ |
| 6 | 319 | 31.2 | 9.6 | 3.5 | -2.3 | 19.2 | $1.11 \times 10^6$ |

For remarks on these tests see following page.

TABLE 3

RESULTS - TEST SERIES 2 E.I.P. 2 RIG REMARKS

Specimen 1

Details shown are for first test on this specimen with K= 1.4 . Specimen later tested to failure with K = 1.25 .

Specimen 2

Inaccuracies of Bristol pressure gauge caused internal pressure range to be underestimated. Circumferential mark where failure initiated.

Specimen 3

Trips on Bristol machine unreliable at this stage and failure estimated. Final reading corresponded to 736 500 cycles. Circumferential mark where failure initiated.

Notes

1. Gauge length failures of all specimens. Longitudinal crack propagated approximately in radial direction. (See also section 4-10).
2. Lives of specimens 4, 5 and 6 estimated from product of speed and time interval because of inaccuracies of rev counter.
3. E.I.P. 2 rig used in conjunction with Parry's Bristol machine head, figure 4, for tests on specimen 1 ( K = 1.4 ) and specimen 2. For specimen 1 ( K = 1.25 ) and specimens 3 to 6 E.I.P. 2 top and bottom pressure gauges, figure 7, used.

STRAIN GAUGE TESTS - E.I.P. 2 SPECIMENS

| Test no | Specimen design | Pressure Intl/extl | For static pressure tests Supply | Measurement |
|---|---|---|---|---|
| 1 | 1a | External | Airhydropump | Budenberg |
| 2 | 1a | Internal | Base pressure intensifier | Peekel (i) / Budenberg (ii) |
| 3 | 1b | External | Airhydropump | Budenberg |
| 4 | 1b | Internal | Base pressure intensifier | Peekel (i) / Budenberg (ii) |

CYLINDER STRAINS - STATIC

| Test no | Measure-ment | Observed strains Microstrain for 10 000 lbf/in$^2$ | | | |
|---|---|---|---|---|---|
| | | longitudinal Gauge 1 | Hoop Gauge 2 | Gauge 3 | Gauge 4 |
| 1 | Budd | 1 170 | -2 050 | | |
| 2i | Budd | -350 | 1 200 | 1 180 | 1 080 |
| ii | | -330 | 1 180 | 1 060 | 1 050 |
| 3 | Peekel | 560 | -1 810 | | |
| 4i | Budd | -340 | 1 195 | 1 195 | 1 200 |
| ii | | -333 | 1 195 | 1 180 | 1 180 |

Note: 1. Gauge 1 at cylinder mid length.
Gauge 2 at cylinder mid length (tests 2 and 4).
Gauge 2 at 3/16" from cylinder mid length (tests 1 and 3).
Gauges 3 and 4 at ends of gauge length.

2. See also table 5.

TABLE 4.

STRAIN GAUGE TESTS - E.I.P. 2 SPECIMENS

Continued from table 4.

CYLINDER STRAINS - DYNAMIC

| Test no | Machine tooth setting | Pressure Lbf/in$^2$ | Observed microstrain (Peekel) Gauge 1 | Gauge 2 | Gauge 3 | Gauge 4 |
|---|---|---|---|---|---|---|
| 2 | 27 | 4 850 | -161 | 570 | 519 | 514 |
| | 25 | 8 670 | - 279 | 924 | 910 | 920 |
| 4 | 27 | 2 550 at 230 rev/min | -58 | 276 | 270 | 289 |
| | 27 | 3 570 at 350 rev/min | -104 | 383 | 388 | 347 |
| | 24 | 8 690 at 250 rev/min | -278 | 1 070 | 1 050 | 1 050 |
| | 24 | 9 050 at 350 rev/min | -282 | 1 091 | 1 070 | 1 078 |

Gradient of specimen microstrain - pressure graph equal to:
-340 microstrain for 10 000 lbf/in$^2$ pressure - gauge 1
1 270 - gauge 2

MID GAUGE LENGTH HOOP STRESS

Lbf/in$^2$ for 10 000 lbf/in$^2$ pressure

| Test no | Theoretical | Experimental | % Difference |
|---|---|---|---|
| 1 static | -55 700 | - 55 700 | |
| 2 static | 35 600 | 35 700 | 0.3 |
| static | 35 600 | 35 200 | 1.4 |
| dynamic - two results only | | | |
| 3 static | -55 550 | -53 600 | 3.4 |
| 4 static | 35 600 | 35 600 | |
| static | 35 600 | 35 600 | |
| dynamic | 35 600 | 38 000 | 6.7 |

TABLE 5

## ANCILLARY TESTS - E.I.P. 2 SPECIMENS FOR TEST SERIES 3

### LONGITUDINAL TENSION SPECIMENS

| VPN | Diameter (in) Initial | Final | % RA | Load (lbf) Max | Tensile strength Tonf/in$^2$ | VPN/TS |
|---|---|---|---|---|---|---|
| Bar 29 | | | | | | |
| 332 | 0.2524 | 0.146 | 66.4 | 7 580 | 67.4 | 4.94 |
| 330 | 0.2521 | 0.153 | 63 | 7 580 | 67.8 | 4.87 |
| 331 | | | 64.7 | | 67.6 | Average |
| Bar 34 | | | | | | |
| 328 | 0.2528 | 0.146 | 66.7 | 7 350 | 65.2 | 5.02 |
| 331 | 0.2528 | 0.146 | 66.7 | 7 320 | 65.2 | 5.08 |
| 329 | 0.253 | 0.147 | 66.3 | 7 450 | 66.1 | 4.97 |
| 329 | | | 66.6 | | 65.5 | Average |
| Bar 28 | | | | | | |
| 345 | 0.2525 | 0.148 | 65.8 | 7 800 | 69.5 | 4.96 |
| 345 | 0.2528 | 0.148 | 65.8 | 7 800 | 69.5 | 4.96 |
| 346 | 0.2525 | 0.148 | 65.8 | 7 850 | 70 | 4.95 |
| 345 | | | 65.8 | | 69.7 | Average |
| Bar 32 | | | | | | |
| 358 | 0.253 | 0.148 | 65.7 | 7 980 | 70.6 | 5.06 |
| 357 | 0.2525 | 0.148 | 65.8 | 7 950 | 70.6 | 5.05 |
| 355 | 0.2525 | 0.148 | 65.8 | 7 900 | 70.1 | 5.06 |
| 357 | | | 65.8 | | 70.4 | Average |

TABLE 6

## ANCILLARY TESTS - E.I.P. 2 SPECIMENS FOR TEST SERIES 3

### TRANSVERSE TENSION SPECIMENS

| VPN | Diameter (in) Initial | Final | % RA | Load (lbf) Max | Tensile strength Tonf/in$^2$ | VPN/TS |
|---|---|---|---|---|---|---|
| Bar 29 | | | | | | |
| 336 | 0.253 | 0.202 | 36.2 | 7 520 | 67 | 5.01 |
| 334 | 0.2528 | 0.205 | 34.3 | 7 500 | 66.9 | 5 |
| 335 | | | 35.2 | | 67 | Average |
| Bar 34 | | | | | | |
| 327 | 0.2528 | 0.213 | 29 | 7 380 | 65.8 | 4.98 |
| 329 | 0.2523 | 0.206 | 33.1 | 7 320 | 65.2 | 5.05 |
| 328 | | | 31 | | 65.5 | Average |
| Bar 28 | | | | | | |
| 352 | 0.2525 | 0.225 | 20.5 | 7 800 | 69.4 | 5.08 |
| 348 | 0.2527 | 0.224 | 21.3 | 7 750 | 69 | 5.04 |
| 354 | 0.2525 | 0.219 | 24.7 | 7 800 | 69.3 | 5.11 |
| 351 | | | 22.2 | | 69.2 | Average |
| Bar 32 | | | | | | |
| 355 | 0.253 | 0.222 | 23 | 7 900 | 70 | 5.07 |
| 364 | 0.2522 | 0.215 | 27 | 7 900 | 70.2 | 5.18 |
| 360 | | | 25 | | 70.1 | Average |

TABLE 7

## ANCILLARY TESTS - E.I.P. 2 SPECIMENS FOR TEST SERIES 3

### HARDNESS TESTS ON CYLINDER SPECIMENS

Cylinders from bar 29

| Specimen no | 1 | 2 | 3 | 4 | 5 | 6 | 7 |
|---|---|---|---|---|---|---|---|
| VPN | 338 | 339 | 345 | 340 | 343 | 345 | 335 |
| VPN/Bar tensile strength | 5.05 | 5.06 | 5.15 | 5.08 | 5.14 | 5.15 | 5 |

Cylinders from bar 34

| Specimen no | 8 | 9 | 10 | 11 | 12 | 13 | 14 |
|---|---|---|---|---|---|---|---|
| VPN | 328 | 325 | 320 | 319 | 318 | 307 | 318 |
| VPN/Bar tensile strength | 5 | 4.97 | 4.88 | 4.87 | 4.86 | 4.7 | 4.86 |

Cylinders from bar 28

| Specimen no | 15 | 16 | 17 | 18 | 19 | 20 |
|---|---|---|---|---|---|---|
| VPN | 338 | 347 | 348 | 348 | 346 | 347 |
| VPN/Bar tensile strength | 4.89 | 5.02 | 5.04 | 5.04 | 5 | 5.02 |

Cylinders from bar 32

| Specimen no | 21 | 22 | 23 | 24 | 25 | 26 |
|---|---|---|---|---|---|---|
| VPN | 346 | 347 | 346 | 345 | 348 | 345 |
| VPN/Bar tensile strength | 4.93 | 4.95 | 4.93 | 4.92 | 4.96 | 4.92 |

Bar tensile strength values used in the above table are those obtained from transverse tension specimens.

TABLE 8

RESULTS TEST SERIES 3 E.I.P.2 RIG

Specimens 1 to 7 from bar 29 (67 tonf/in$^2$)

| Specimen number | Pressures (Lbf/in$^2$) | | | | |
|---|---|---|---|---|---|
| | $P_i$ min | $P_i$ range (Bottom gauge) | $P_i$ range (Average of top and bottom gauges) | $P_i$ max | $P_o$ |
| 1 | - | - | 28 200 | 28 200 | 22 700 |
| 2 | - | - | 33 900 | 33 900 | 18 000 |
| 3 | 5 900 | 28 600 | 27 400 | 33 300 | 18 200 |
| 4 | 10 400 | 22 800 | 22 500 | 32 900 | 17 900 |
| 5 | - | 34 300 | 33 300 | 33 300 | 22 400 |
| 6 | 5 600 | 28 000 | 27 700 | 33 300 | 22 700 |
| 7 | 10 000 | 23 800 | 23 300 | 33 300 | 22 900 |

| Specimen number | Stresses (Tonf/in$^2$) | | | | $\Delta\tau$ / Tensile strength | Cycles |
|---|---|---|---|---|---|---|
| | $\Delta\tau$ | $\hat{\sigma}_\theta$ | $\tau_m$ | $\sigma_\tau$ | | |
| 1 | 35 | 1 | 10.7 | -5.8 | 0.523 | $7.75 \times 10^5$ |
| 2 | 42 | 24.6 | 1.2 | 4.7 | 0.627 | $2.7 \times 10^4$ |
| 3 | 34 | 22.7 | 1.6 | 3.9 | 0.509 | $1.6 \times 10^5$ |
| 4 | 28 | 22.5 | 4.6 | 3.9 | 0.418 | $7.5 \times 10^5$ |
| 5 | 41.4 | 12.3 | 7.0 | -1.3 | 0.618 | $8.3 \times 10^4$ |
| 6 | 34.4 | 11.7 | 3.9 | -1.5 | 0.514 | $6.4 \times 10^5$ U |
| 7 | 28.9 | 11.4 | 1.4 | -1.8 | 0.432 | $5.6 \times 10^6$ |

For remarks on these tests see pages 79 and 80.

TABLE 9

RESULTS TEST SERIES 3 E.I.P.2 RIG

Specimens 8 to 14 from bar 34 (65.5 tonf/in$^2$)

| Specimen number | Pressures (Lbf/in$^2$) | | | | |
|---|---|---|---|---|---|
| | $P_i$ min | $P_i$ range (Bottom gauge) | $P_i$ range (Average of top and bottom gauges) | $P_i$ max | $P_o$ |
| 8 | - | 34 400 | 32 700 | 32 700 | 26 300 |
| 9 | 5 500 | 27 400 | 27 400 | 32 900 | 26 600 |
| 10 | 8 400 | 24 400 | 24 200 | 32 600 | 26 700 |
| 11 | 5 500 | 27 500 | 27 300 | 32 800 | 22 600 |
| 12 | - | 34 000 | 33 600 | 33 600 | 26 600 |
| 13 | 3 200 | 28 900 | 28 600 | 31 800 | 26 900 |
| 14 | 11 600 | 22 900 | 21 700 | 33 300 | 19 000 |

| Specimen number | Stresses (Tonf/in$^2$) | | | | $\frac{\Delta\tau}{\text{Tensile strength}}$ | Cycles |
|---|---|---|---|---|---|---|
| | $\Delta\tau$ | $\hat{\sigma}_\theta$ | $\tau_m$ | $\sigma_r$ | | |
| 8 | 40.7 | 1.3 | 12.4 | -6.6 | 0.621 | $7.95 \times 10^4$ |
| 9 | 34 | 1.1 | 9.1 | -6.8 | 0.520 | $1.35 \times 10^6$ U |
| 10 | 30.1 | 0.2 | 9.1 | -7.2 | 0.46 | $8.7 \times 10^6$ U |
| 11 | 33.9 | 10.7 | 4.2 | -2 | 0.518 | $8.05 \times 10^5$ |
| 12 | 41.8 | 2.4 | 12.1 | -6.2 | 0.638 | $1.41 \times 10^5$ |
| 13 | 35.6 | -2 | 11.7 | -8.1 | 0.544 | $5.55 \times 10^5$ |
| 14 | 27 | 20.7 | 4.3 | 2.9 | 0.413 | $2.5 \times 10^5$ |

For remarks on these tests see pages 79 and 80.

TABLE 10

RESULTS TEST SERIES 3 E.I.P.2 RIG
Specimens 15 to 20 from bar 28 (69.2 tonf/in$^2$)

| Specimen number | Pressures (Lbf/in$^2$) | | | | |
|---|---|---|---|---|---|
| | $P_i$ min | $P_i$ range (Bottom gauge) | $P_i$ range (Average of top and bottom gauges) | $P_i$ max | $P_o$ |
| 15 | 12 500 | 20 800 | 20 600 | 33 100 | 19 200 |
| 16 | - | 19 800 | 19 400 | 19 400 | 8 500 |
| 17 | 7 200 | 18 800 | 18 100 | 25 300 | 17 900 |
| 18 | 7 200 | 20 200 | 20 100 | 27 300 | 17 700 |
| 19 | 5 000 | 24 500 | 23 300 | 28 300 | 14 900 |
| 20 | 7 200 | 19 600 | 18 900 | 26 100 | 17 700 |

| Specimen number | Stresses (Tonf/in$^2$) | | | | $\Delta\tau$ / Tensile strength | Cycles |
|---|---|---|---|---|---|---|
| | $\Delta\tau$ | $\hat{\sigma}_\theta$ | $\tau_m$ | $\sigma_\tau$ | | |
| 15 | 25.6 | 19.3 | 4.5 | 2.5 | 0.37 | $6.76 \times 10^5$ |
| 16 | 24.1 | 18.4 | 1.5 | 5.0 | 0.348 | $1.6 \times 10^6$ |
| 17 | 22.5 | 7.1 | 2.1 | -2.1 | 0.325 | $3.48 \times 10^6$ U |
| 18 | 25 | 11.7 | 0.5 | -0.2 | 0.362 | $5.94 \times 10^6$ U |
| 19 | 29 | 20.7 | 2.2 | 4.1 | 0.42 | $3.94 \times 10^5$ |
| 20 | 23.5 | 9.2 | 1.3 | -1.3 | 0.34 | $2.44 \times 10^6$ |

For remarks on these tests see pages 79 and 80.

TABLE 11

RESULTS TEST SERIES 3 E.I.P.2 RIC

Specimens 21 to 26 from bar 32 (70.1 tonf/in$^2$)

| Specimen number | Pressures (Lbf/in$^2$) | | | | |
|---|---|---|---|---|---|
| | $P_i$ min | $P_i$ range (Bottom gauge) | $P_i$ range (Average of top and bottom gauges) | $P_i$ max | $P_o$ |
| 21 | - | 28 800 | 29 400 | 29 400 | 15 100 |
| 22 | - | 30 200 | 31 800 | 31 800 | 15 100 |
| 23 | 10 000 | 21 500 | 22 300 | 32 300 | 15 000 |
| 24 | 5 000 | 26 200 | 27 100 | 32 100 | 14 800 |
| 25 | 10 000 | 22 200 | 22 600 | 32 600 | 18 500 |
| 26 | - | 30 500 | 31 300 | 31 300 | 18 700 |

| Specimen number | Stresses (Tonf/in$^2$) | | | | $\Delta\tau$ / Tensile strength | Cycles |
|---|---|---|---|---|---|---|
| | $\Delta\tau$ | $\hat{\sigma}_\theta$ | $\tau_m$ | $\sigma_\tau$ | | |
| 21 | 36.5 | 22.5 | 0.5 | 4.7 | 0.52 | $1.83 \times 10^5$ |
| 22 | 39.5 | 27.0 | 0.9 | 6.5 | 0.564 | $7.34 \times 10^4$ |
| 23 | 27.7 | 28.3 | 7.6 | 7.0 | 0.395 | $5.88 \times 10^5$ |
| 24 | 33.6 | 28.4 | 5.2 | 7.1 | 0.479 | $1.87 \times 10^5$ |
| 25 | 28.1 | 20.3 | 3.5 | 3 | 0.401 | $6.7 \times 10^6$ U |
| 26 | 38.9 | 17.4 | 3.8 | 1.7 | 0.556 | $1.21 \times 10^5$ |

For remarks on these tests see pages 79 and 80.

TABLE 12

RESULTS - TEST SERIES 3 E.I.P. 2 RIG REMARKS

Specimens 1 and 2

Top gauge readings only taken; average top and bottom gauge reading estimated at 2 % higher.

Specimen 8

Larger than average difference in top and bottom gauge readings. Conditions of stresses repeated in test on specimen 12.

Specimen 6

Inspected for failure at $6.4 \times 10^5$ cycles - had not failed. Readings of pressures taken at $1.7 \times 10^6$ cycles. Specimen inspected, after trips operated due to lack of make-up oil at $2.85 \times 10^6$ cycles, and found to have failed. Repeated by specimen 11.

Specimen 11

Noted that variation in base pressure from 5 000 to 6 000 $lbf/in^2$ increased internal pressure range by 1 000 $lbf/in^2$.

Specimen 13

Low pressure insufficient to drive intensifier for base pressure of 3 000 $lbf/in^2$.

Specimen 14

Difficulties experienced during the first 39 000 cycles with low reading of top gauge, this being about half only of the bottom gauge reading for some of the time. Later sensible readings were obtained and the test was continued, the original cycles being discounted. Repeated approximately by specimen 15.

RESULTS - TEST SERIES 3 E.I.P. 2 RIG REMARKS CONTINUED

Notes:

1. Before these tests the last specimen made for test series 2 ( specimen no 7 ) was machined to design 1b and tested. It endured $5.5 \times 10^6$ cycles at $\Delta\tau = 34.2$, $\hat{\sigma}_\theta = 8.2$, $\tau_m = 5.6$ and $\sigma_\tau = -3.3$ tonf/in$^2$. Fatigue failure of bottom plate insert occurred ( it had endured $3.5 \times 10^6$ cycles ). Replaced by insert without high stress concentration.

2. Zero base pressure is actually 150 lbf/in$^2$, which is negligible compared with the other pressures involved.

3. U denotes unbroken specimen.

4. Some difficulties experienced with failure of rev counters and on these occasions cycles were calculated from speed and time readings.

5. During test on specimen 20 fatigue of bottom pressure gauge occurred at top cone ring seating. Replacement bottom gauge and existing top gauge were autofrettaged before use on remaining tests ( specimens 17, 18 and 21 to 26)

6. Top core bar removed and lower core bar quadrants drilled to give 3/8" diameter vertical hole on centre line of rig for tests 17, 18 and 21 to 25.

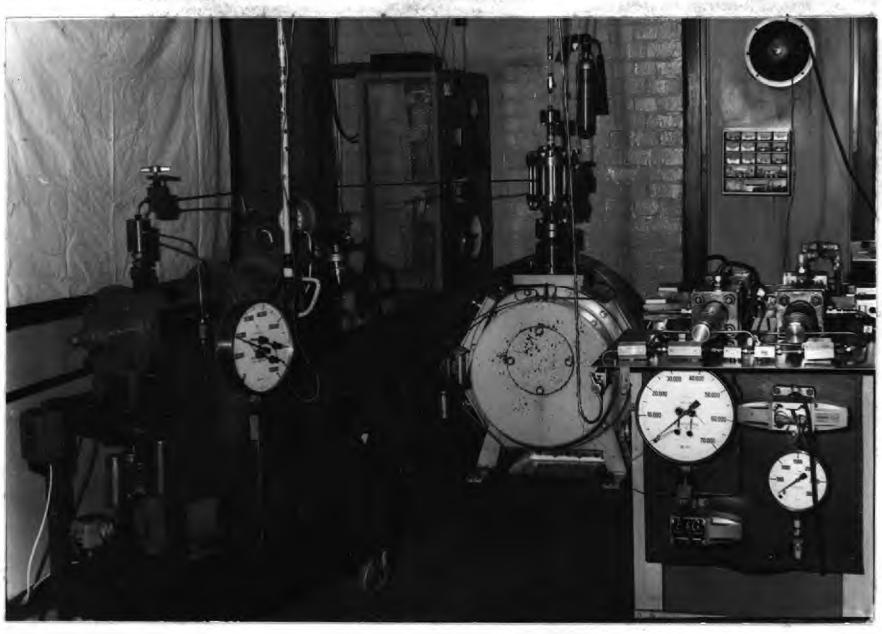
7. For tests on specimens 12 to 16, 19 and start of test on specimen 20 the Madan airhydropump was replaced by an Olin Mathieson unit.

## FRACTURES OF SPECIMENS

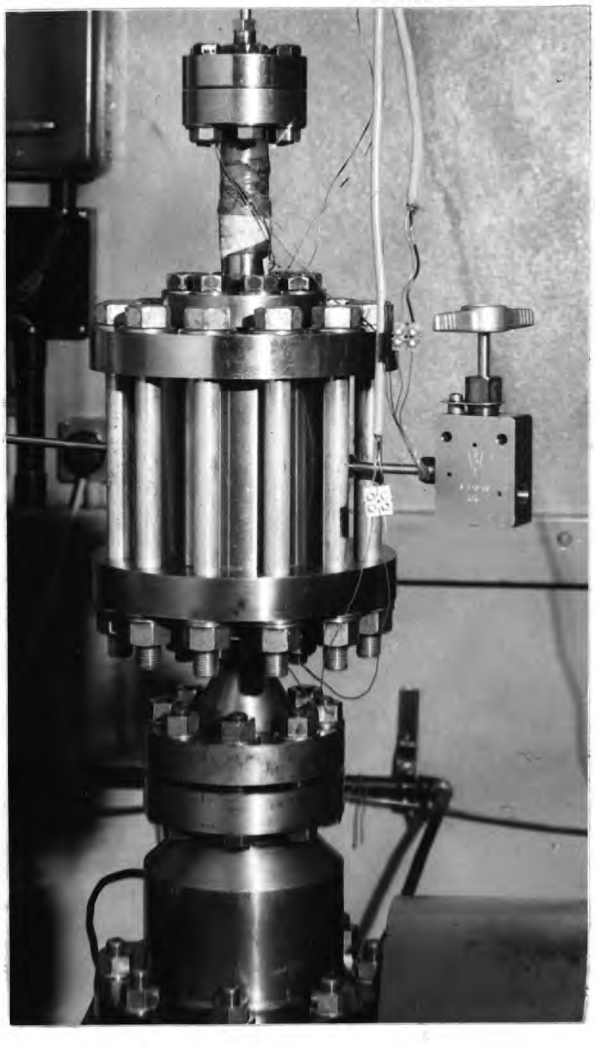
TEST SERIES 3
Specimens sectioned transversely

| Specimen | Initial direction of crack - angle to radial (degrees) | Change of direction of crack - angle to radial (degrees) |
|---|---|---|
| 1 | 5 | 22, after half way through wall. |
| 2 | 19 | - |
| 3 | Radial | 17, after quarter way through wall. |
| 5 | 20 | - |
| 6 | 7 | - |
| 7 | Radial | - |
| 8 | 27 | - |
| 13 | Radial | 11½, after half way through wall. |
| 15 | Radial | 27, after half way through wall. |
| 16 | Radial | - |
| 19 | Radial | - |
| 23 | 8 | 27, after half way through wall. |
| 26 | 13 | 35, after three quarters way through wall. |

TABLE 13



10-1 LAYOUT OF APPARATUS

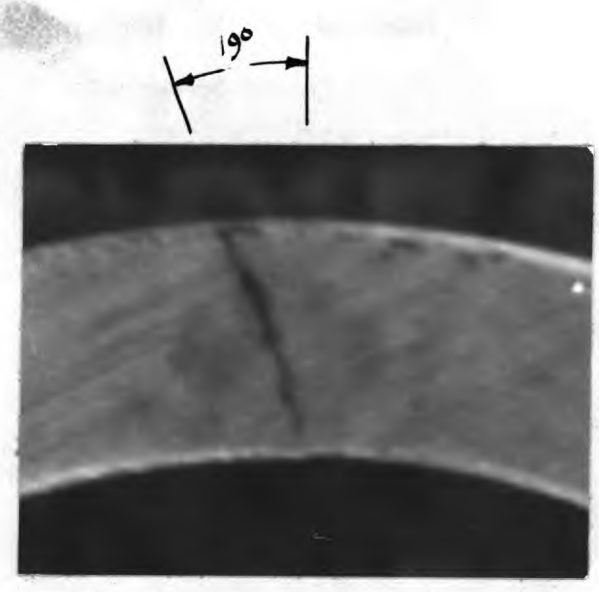


10-2 RIG E.I.P.2

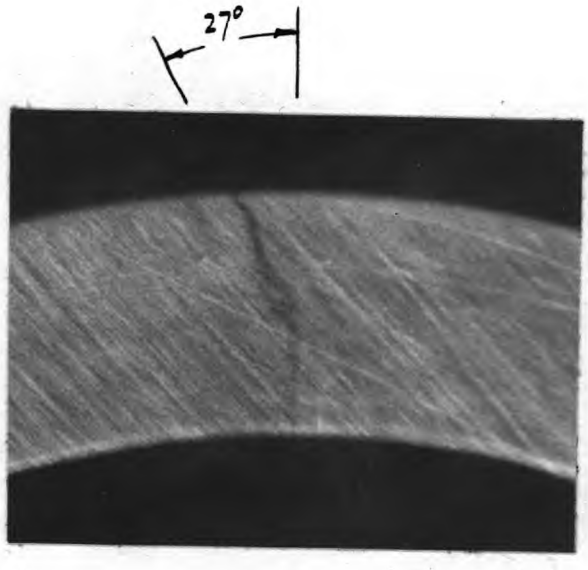


10-3 LONGITUDINAL CROSS-SECTION OF CYLINDER

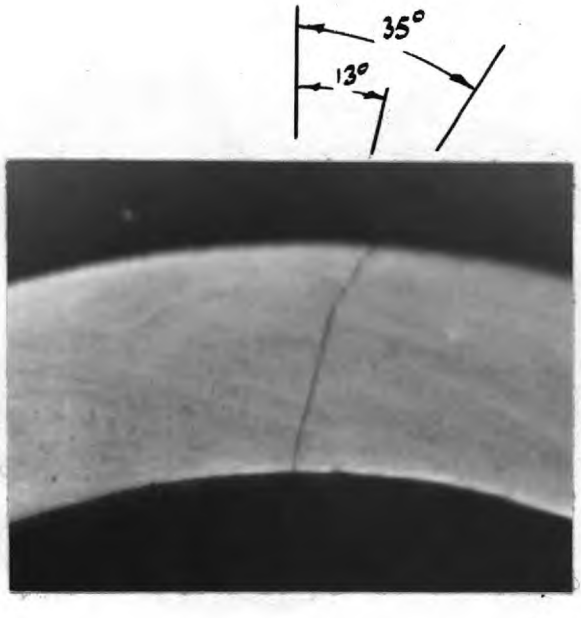
Specimen 24 of test series 3




Specimen 2




Specimen 15




Specimen 26

10-4 TRANSVERSE CROSS-SECTIONS OF CYLINDERS

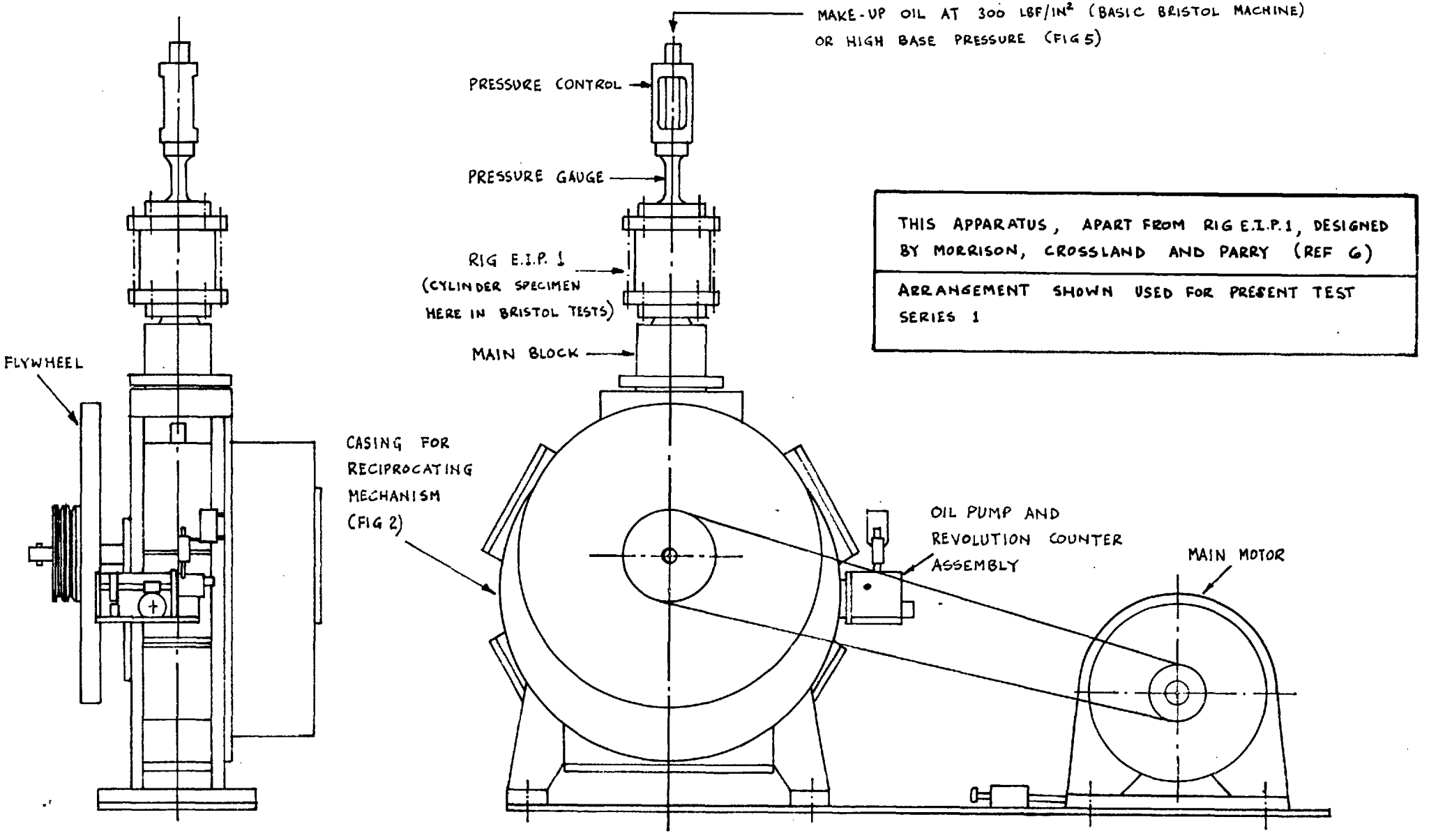



FIG 1 GENERAL ARRANGEMENT OF BRISTOL FATIGUE TESTING MACHINE

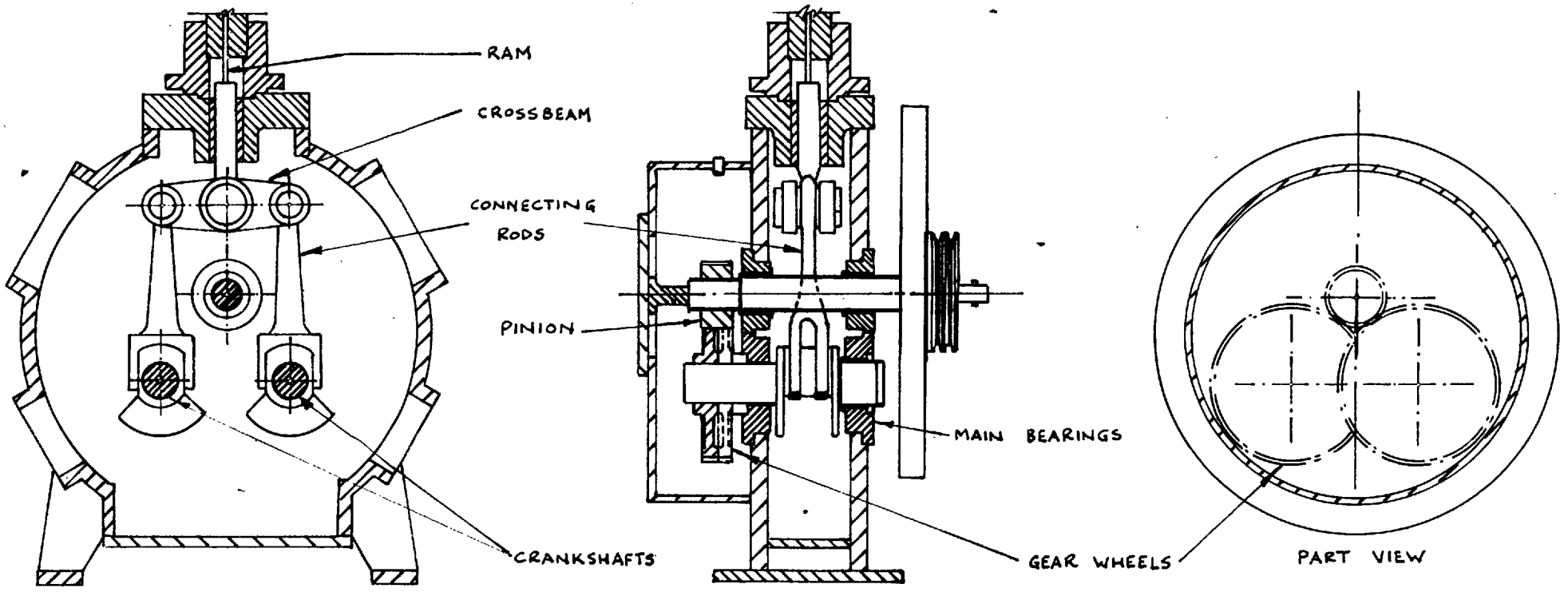
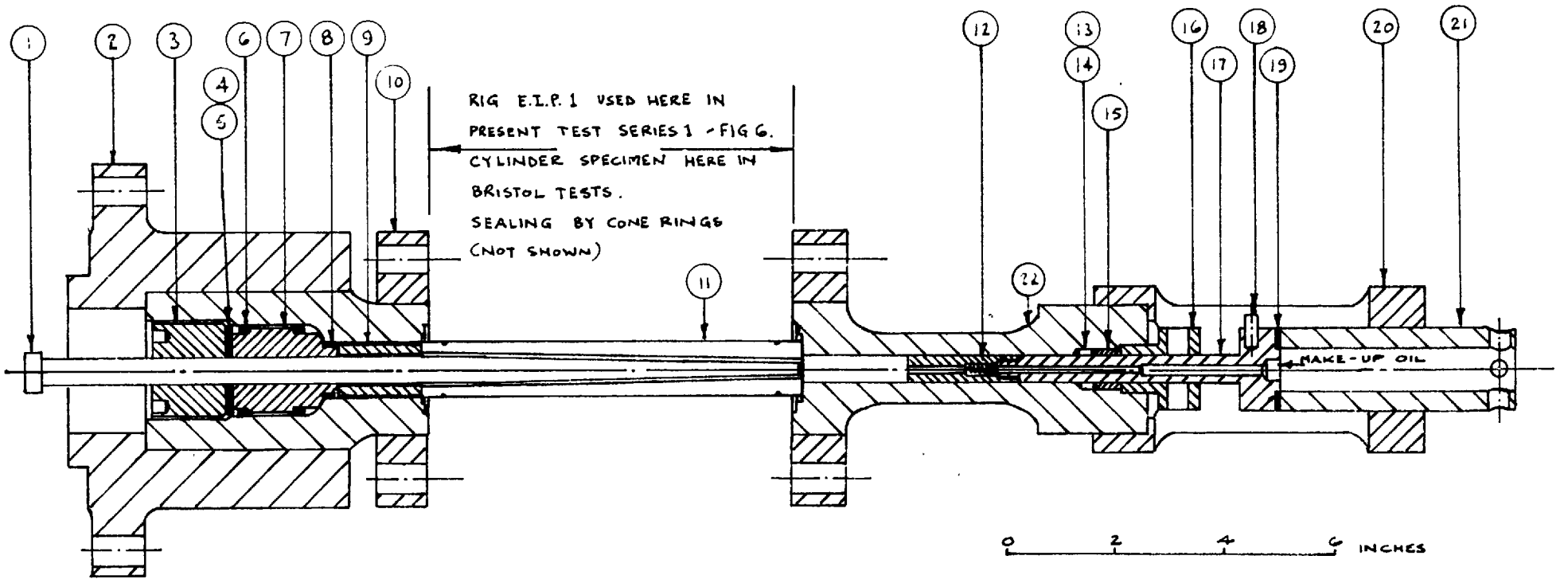



FIG 2 LAYOUT OF BRISTOL FATIGUE TESTING MACHINE RECIPROCATING MECHANISM

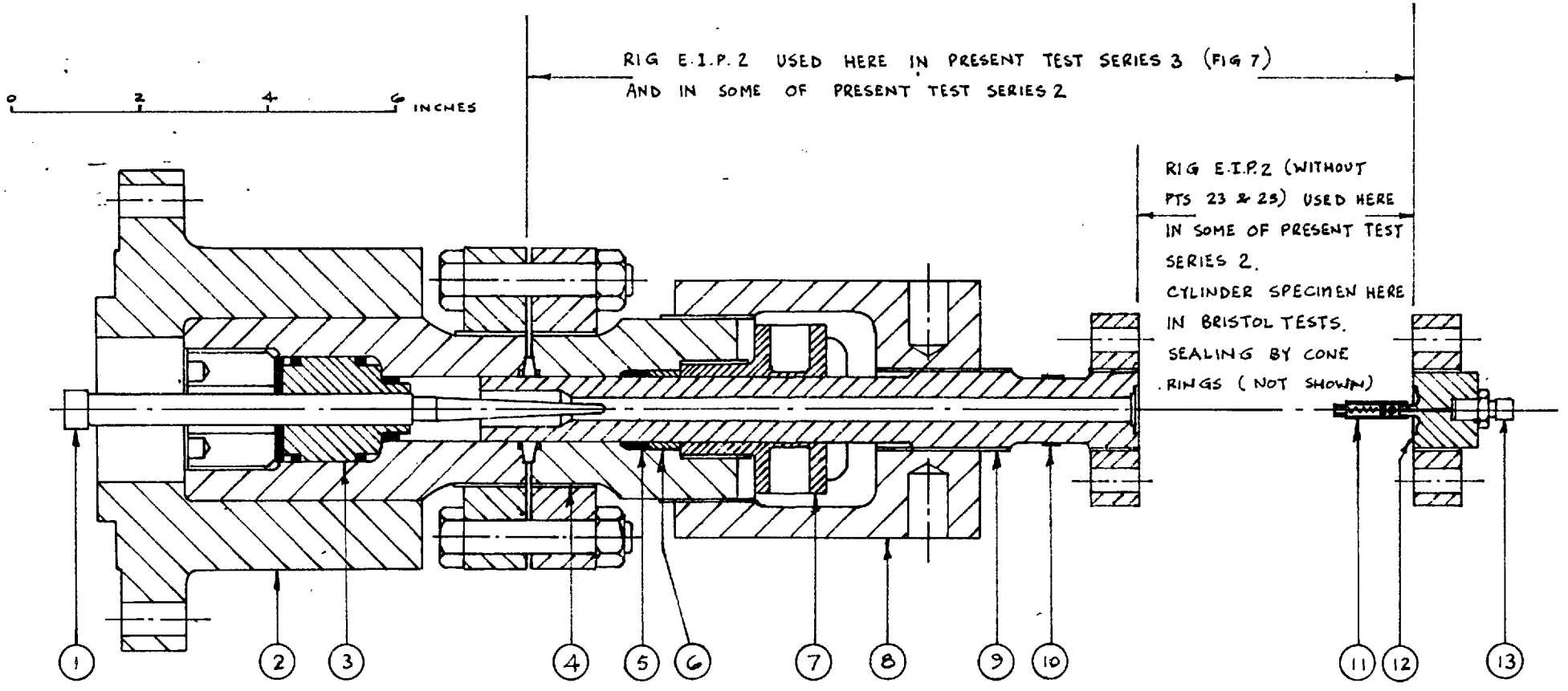
MACHINE DESIGNED BY MORRISON, CROSSLAND AND PARRY (REF 6)




1 RAM (SHOWN AT B.D.C.)
2 MAIN BLOCK WITH SHRUNK IN SLEEVE
3 RETAINING SCREW
4 RUBBER WASHER
5 BACKING RING
6 'HYDURAX' RINGS
7 LIP SEAL
8 RUBBER SEAL
9 CORE BAR
10 FLANGE
11 SEGMENTED CORE BAR
12 NON-RETURN VALVE
13 RUBBER GLAND RING
14 CHAMFER RINGS
15 GLAND BUSH
16 GLAND NUT
17 PRESSURE-ADJUSTING RAM
18 GUIDE PIN
19 'HYDURAX' PRESSURE PAD
20 SCREW FRAME
21 ADJUSTING SCREW
22 PRESSURE GAUGE

FIG 3 SECTIONAL VIEW OF HIGH PRESSURE SYSTEM - BRISTOL FATIGUE TESTING MACHINE

DESIGNED BY MORRISON, CROSSLAND AND PARRY (REF 6)




1 RAM
2 MAIN SEAL BLOCK
3 LIP SEAL
4 GLAND HOUSING
5 GLAND
6 GLAND BUSH
7 GLAND NUT
8 PRESSURE ADJUSTING NUT
9 PRESSURE ADJUSTING MEMBER
10 STRAIN GAUGES FOR PRESSURE MEASUREMENT
11 NON-RETURN VALVE
12 NON-RETURN VALVE BLOCK
13 CONNECTION FOR MAKE-UP OIL

FIG 4 SECTIONAL VIEW OF HIGH PRESSURE SYSTEM - BRISTOL FATIGUE TESTING MACHINE

DESIGNED BY PARRY (REF 11) FOR 0.375 IN BORE CYLINDER SPECIMENS

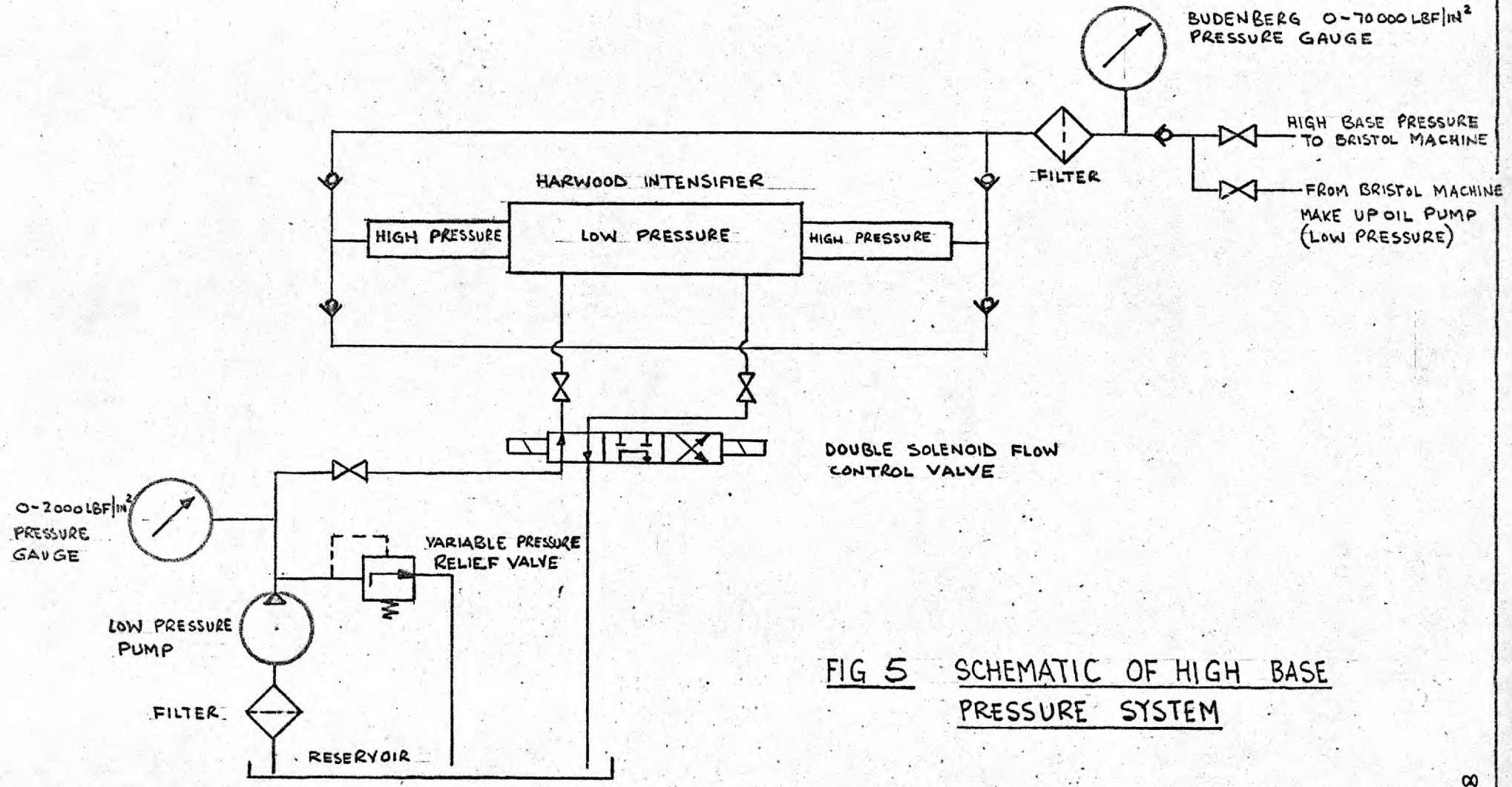



FIG 5 SCHEMATIC OF HIGH BASE PRESSURE SYSTEM

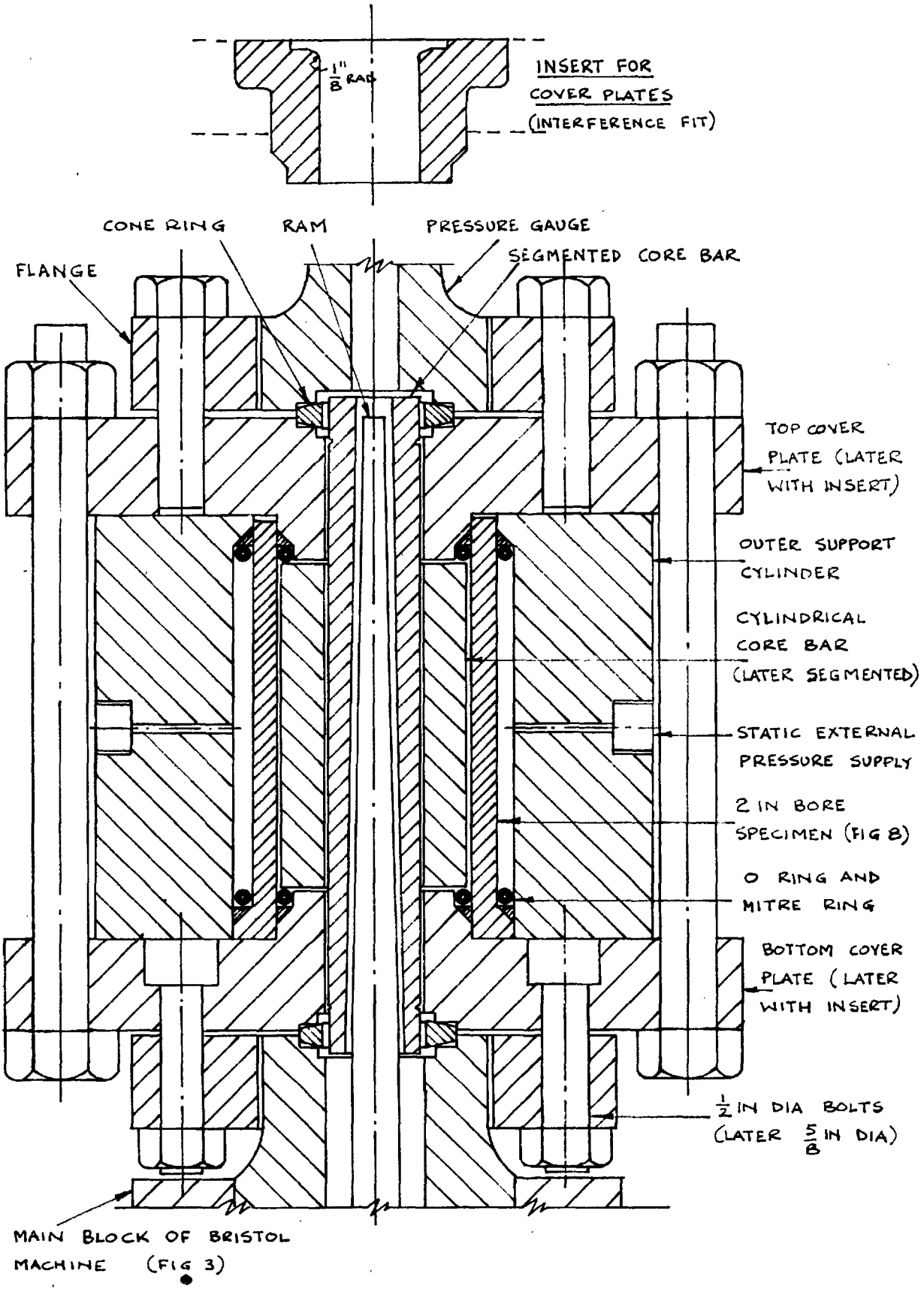
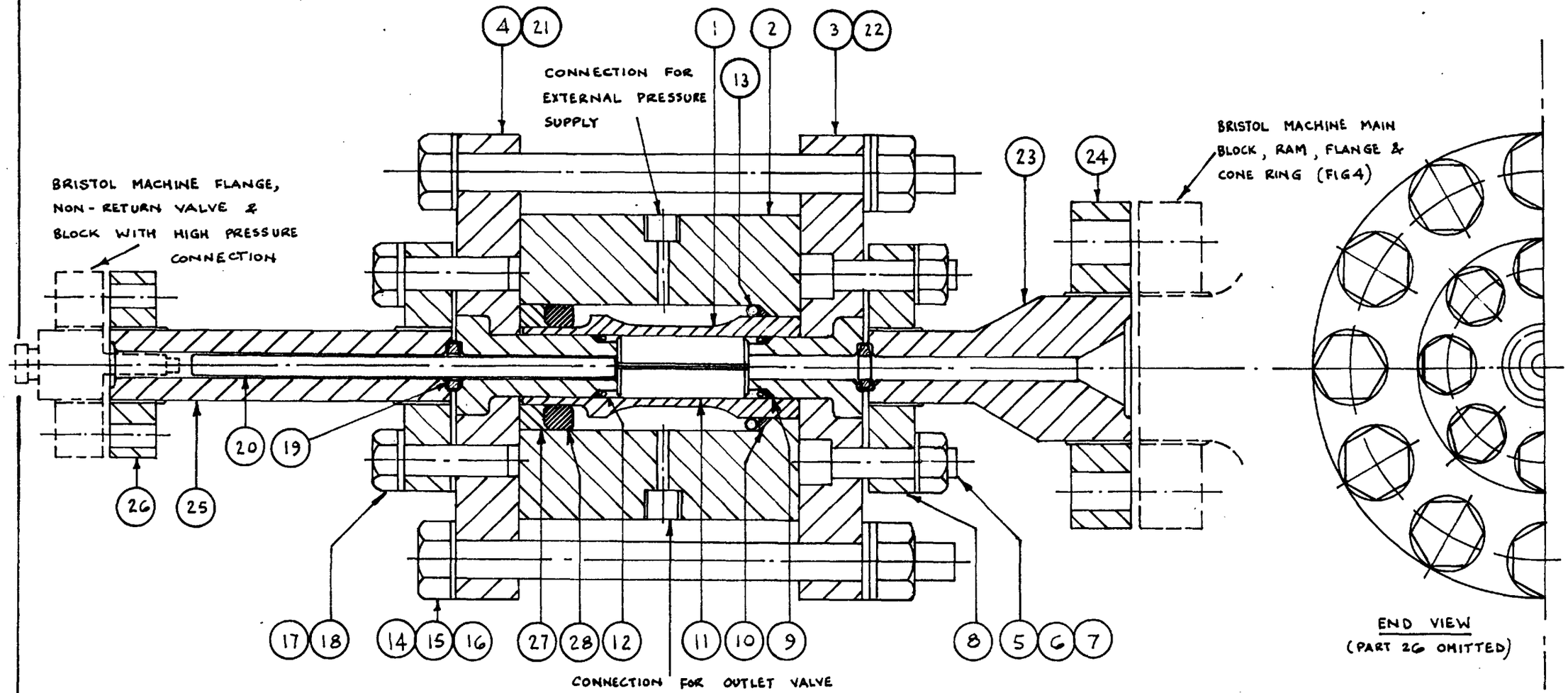



FIG 6 RIG E.I.P. 1

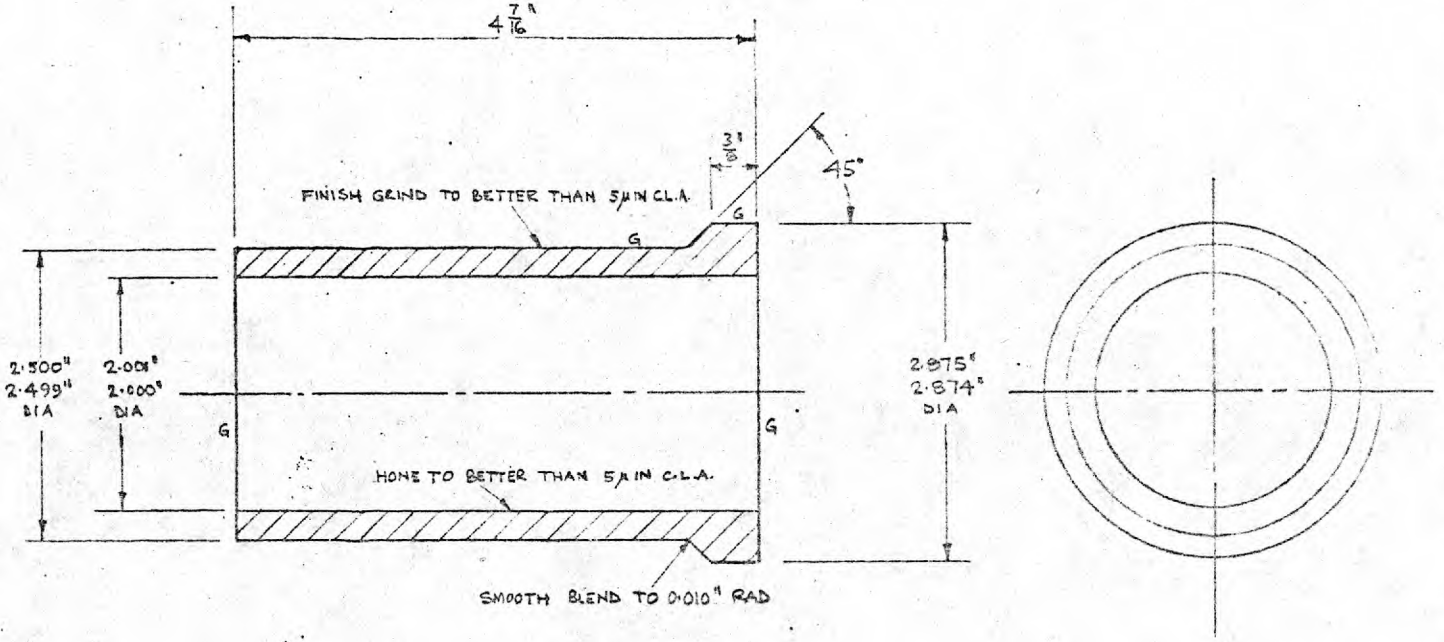
DESIGNED BY LENGYEL, BURNS AND PRASAD (REF. 30)
MODIFIED DURING PRESENT TEST SERIES 1




| PART NO | NO REQD | DESCRIPTION | MATERIAL |
|---|---|---|---|
| 1 | | SPECIMEN - FIG 9 | EN 25 |
| 2 | 1 | SUPPORT CYLINDER | EN 30 B |
| 3 | 1 | BOTTOM COVER PLATE | EN 30B or EN24 or EN 25 |
| 4 | 1 | TOP COVER PLATE | EN 30B or EN 24 or EN25 |
| 5 | 8 | SOCKET HD CAP SC $\frac{1}{2}$" BSF 2" LG | UNBRAKO |
| 6 | 8 | NUT $\frac{1}{2}$" B.S.F. | M.S. |
| 7 | 8 | PLAIN WASHER $\frac{1}{2}$" | M.S. |
| 8 | 2 | FLANGE | EN 30 B or EN24 or EN25 |
| 9 | 2 | MITRE RING | BER. COPPER |
| 10 | 1 | MITRE RING | BER. COPPER |
| 11 | 4 | CORE BAR QUADRANTS | AL. ALLOY |
| 12 | 2 | O RING SEAL | GACO R4075 GRADE P90 |
| 13 | 1 | O RING SEAL | GACO R G162 GRADE P90 |
| 14 | 12 | BOLT $\frac{5}{8}$" B.S.F. 8" LONG $1\frac{1}{2}$" THR | HIGH TENSILE |
| 15 | 12 | NUT $\frac{5}{8}$" B.S.F. | M.S. |
| 16 | 36 | PLAIN WASHER $\frac{5}{8}$" | M.S. |
| 17 | 8 | BOLT $\frac{1}{2}$" B.S.F. $1\frac{3}{4}$" LONG | HIGH TENSILE |
| 18 | 8 | PLAIN WASHER $\frac{1}{2}$" | M.S. |
| 19 | 2 | CONE RING | |
| 20 | 1 | CORE BAR | M.S. |
| 21 | 1 | TOP PLATE INSERT | EN 31 |
| 22 | 1 | BOTTOM PLATE INSERT | EN 31 |
| 23 | 1 | BOTTOM PRESSURE GAUGE - TRANSITION PIECE | EN 25 |
| 24 | 1 | FLANGE | EN 25 |
| 25 | 1 | TOP PRESSURE GAUGE | EN 25 |
| 26 | 1 | FLANGE | EN 25 |
| 27 | 1 | SEAL BACKING RING | M.S. |
| 28 | 1 | SEAL | HALLPRENE |

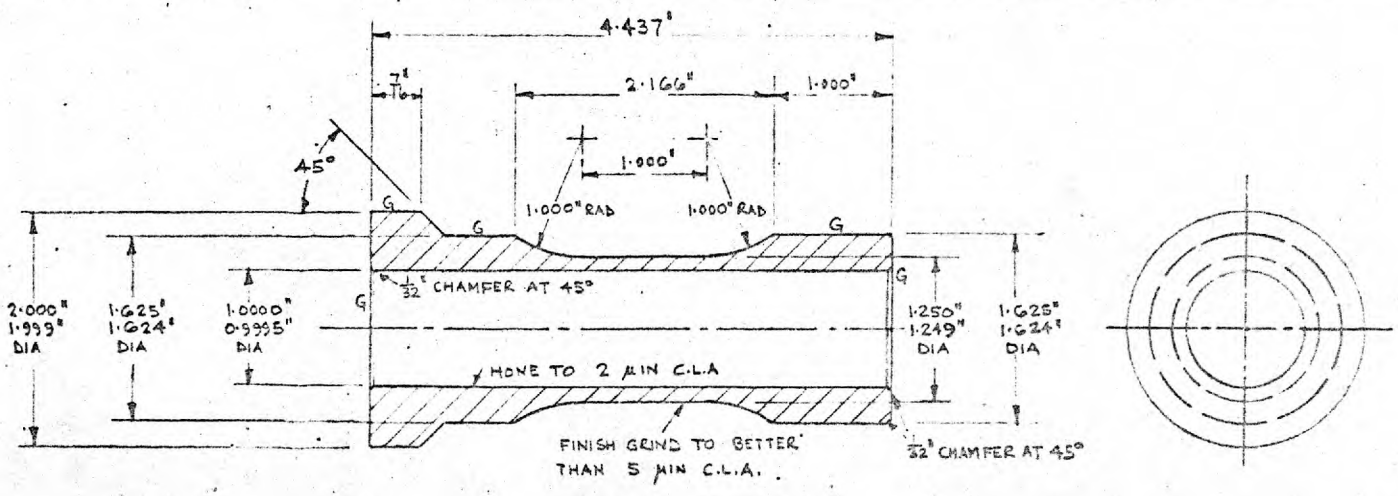
FIG 7 RIG FOR TESTING CYLINDER WITH FLUCTUATING INTERNAL AND SUPPORTING EXTERNAL PRESSURES - RIG E.I.P. 2

SCALE: HALF FULL SIZE
JAN 1969
C.T. Kendall

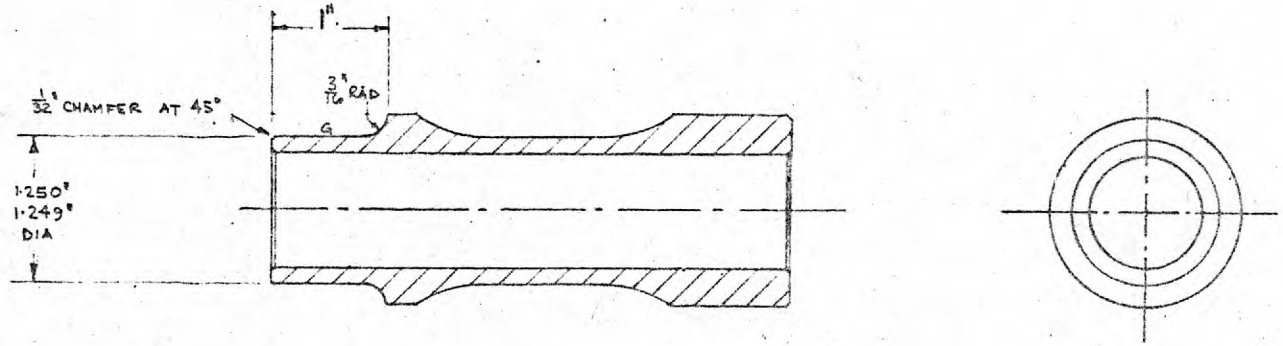



| | | | |
|---|---|---|---|
| MATERIAL | EN 31 | AUSTENITISED FOR 30 MIN AT 840–850°C IN NEUTRAL SALTS<br>QUENCHED TO 220–230°C AND HELD FOR 30 MIN<br>AIR COOLED FOR 2 HOURS<br>TEMPERED AT 220°C FOR 9 HOURS | DESIGN AS SHOWN |
| | KE 4180 | HEAT TREATED TO GIVE 60 – 63 ROCKWELL C HARDNESS | |
| | EN 25 | HARDENED (OIL COOL FROM 840°C) TEMPERED (AIR COOL FROM 650°C)<br>DESIGN SIMILAR TO ABOVE BUT SMOOTH BLEND TO 0·1875" RAD | |

FIG 8 SPECIMENS FOR RIG E.I.P. 1




PART 1 (a)

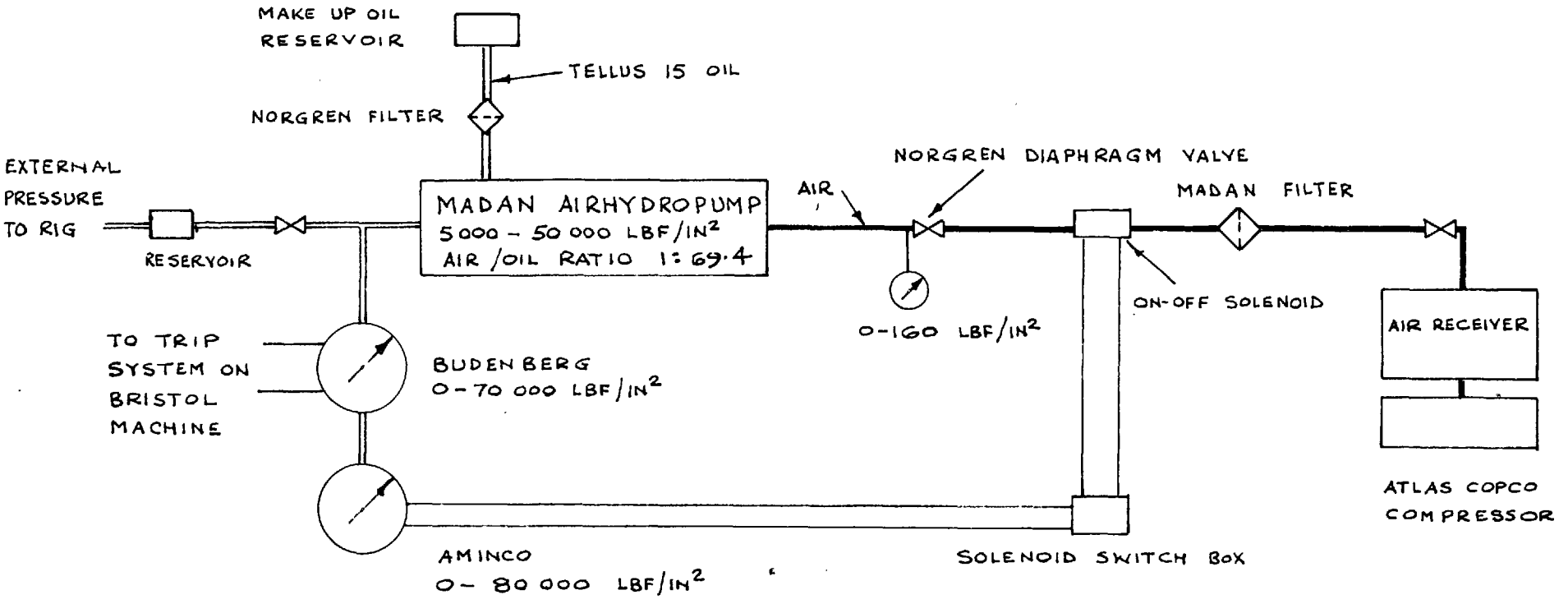



PART 1 (b)

OTHER DETAILS AS FOR PART 1(a)

FIG 9 SPECIMENS FOR RIG E.I.P.2.

MATL: EN 25
STRESS RELIEVE AT 600°C FOR 1 HOUR
IN VACUUM FURNACE AFTER FINAL MACHINING




ORIGINAL SYSTEM SHOWN
IN FINAL SYSTEM SOLENOID, SWITCH BOX AND AMINCO GAUGE OMITTED

FIG 10 SCHEMATIC OF EXTERNAL PRESSURE SYSTEM

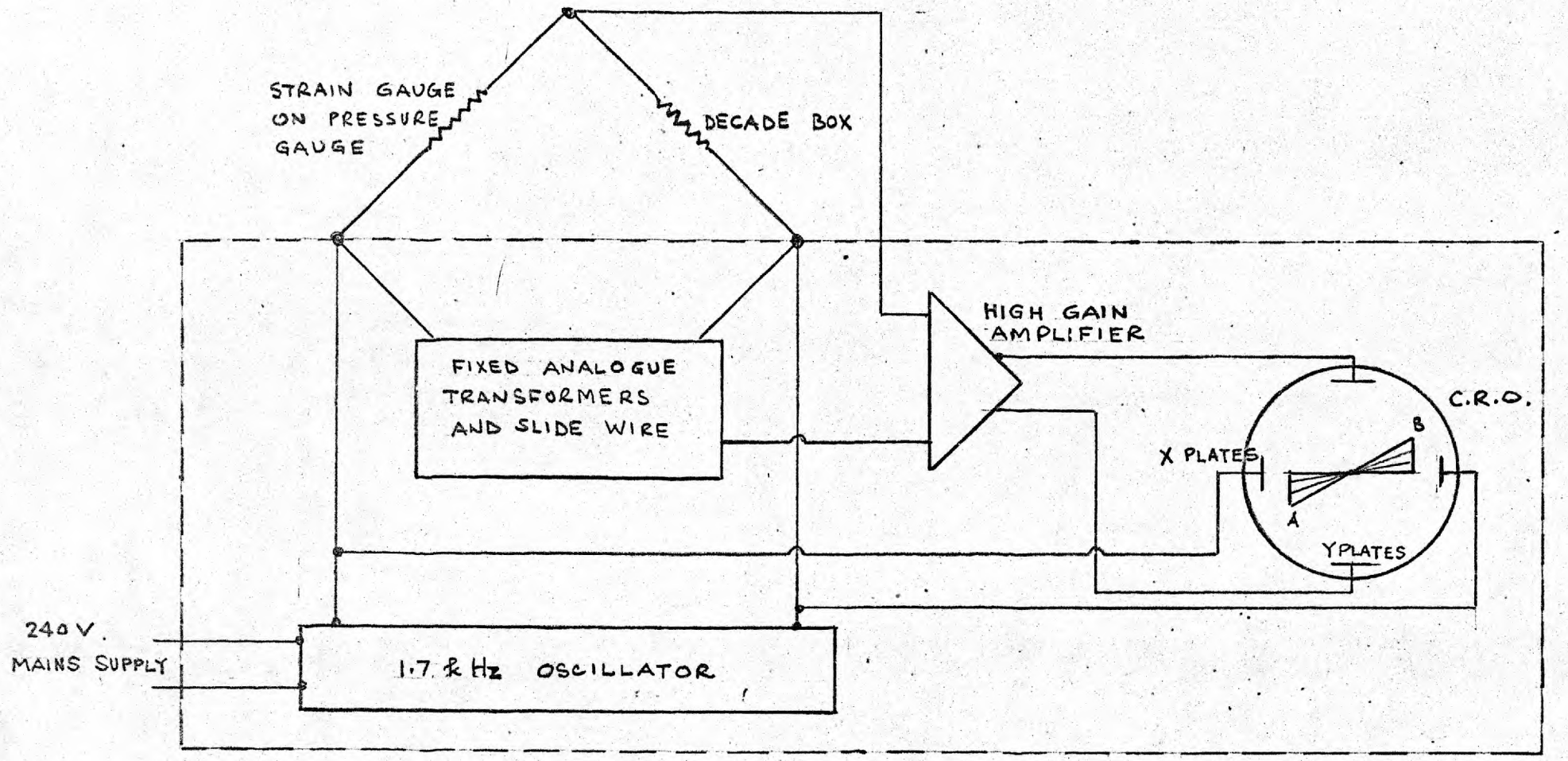



FIG 11 SCHEMATIC OF TECQUIPMENT DIRECT READING STRAIN BRIDGE

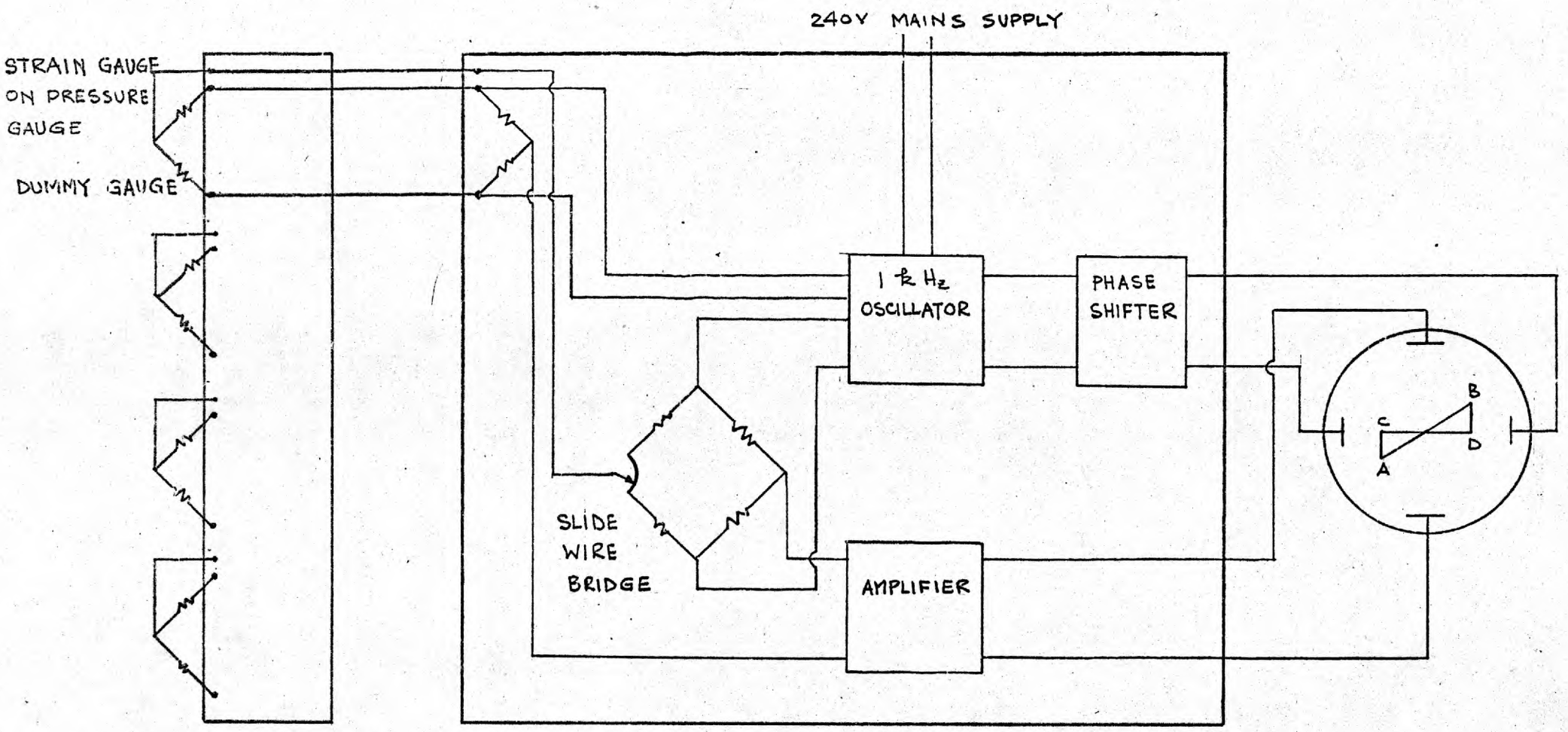



FIG 12 SCHEMATIC OF PEEKEL STRAIN BRIDGE AND ASSOCIATED EQUIPMENT

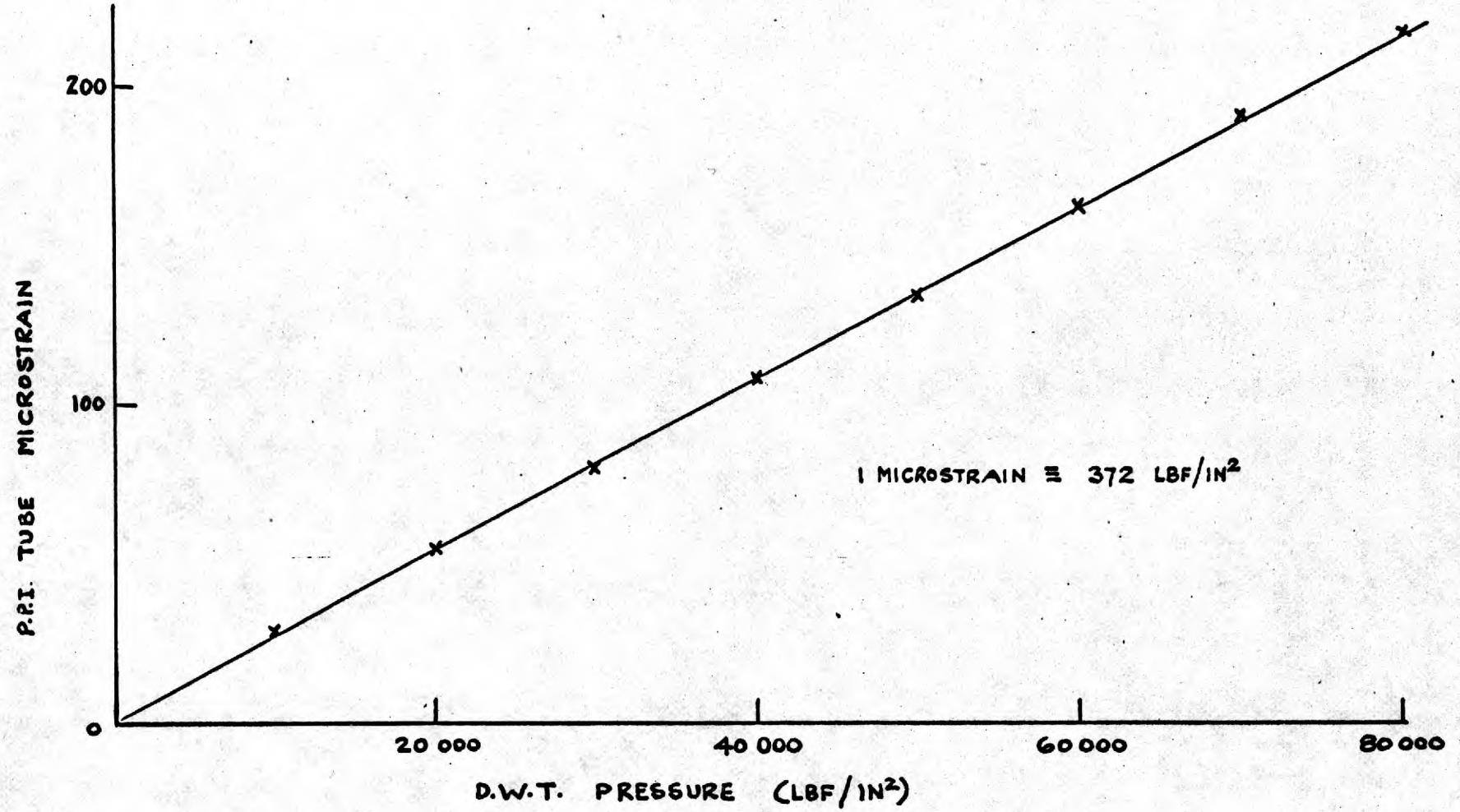



FIG 13 - CALIBRATION OF P.P.I. TUBE

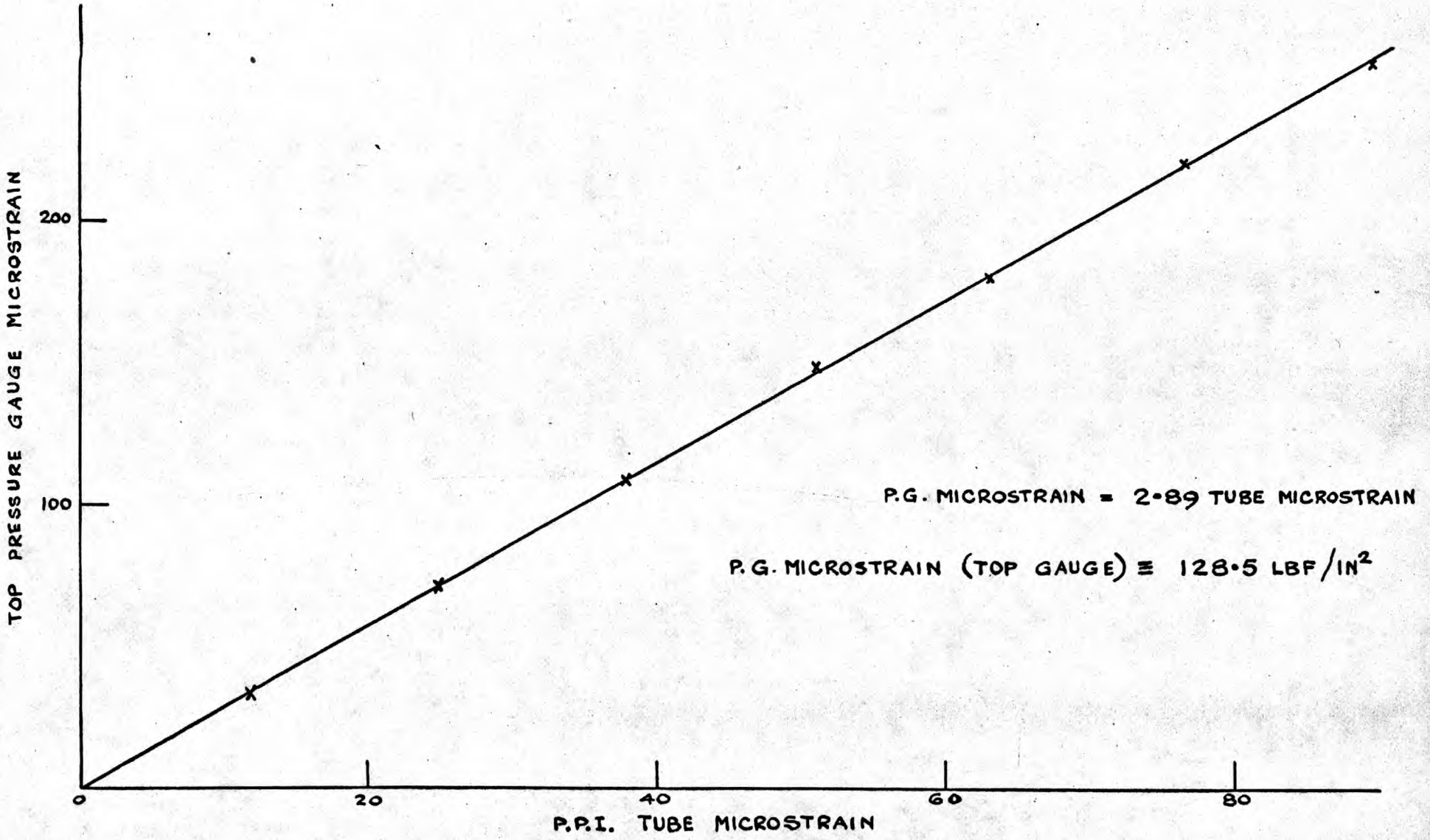



FIG 14 - CALIBRATION OF TOP PRESSURE GAUGE

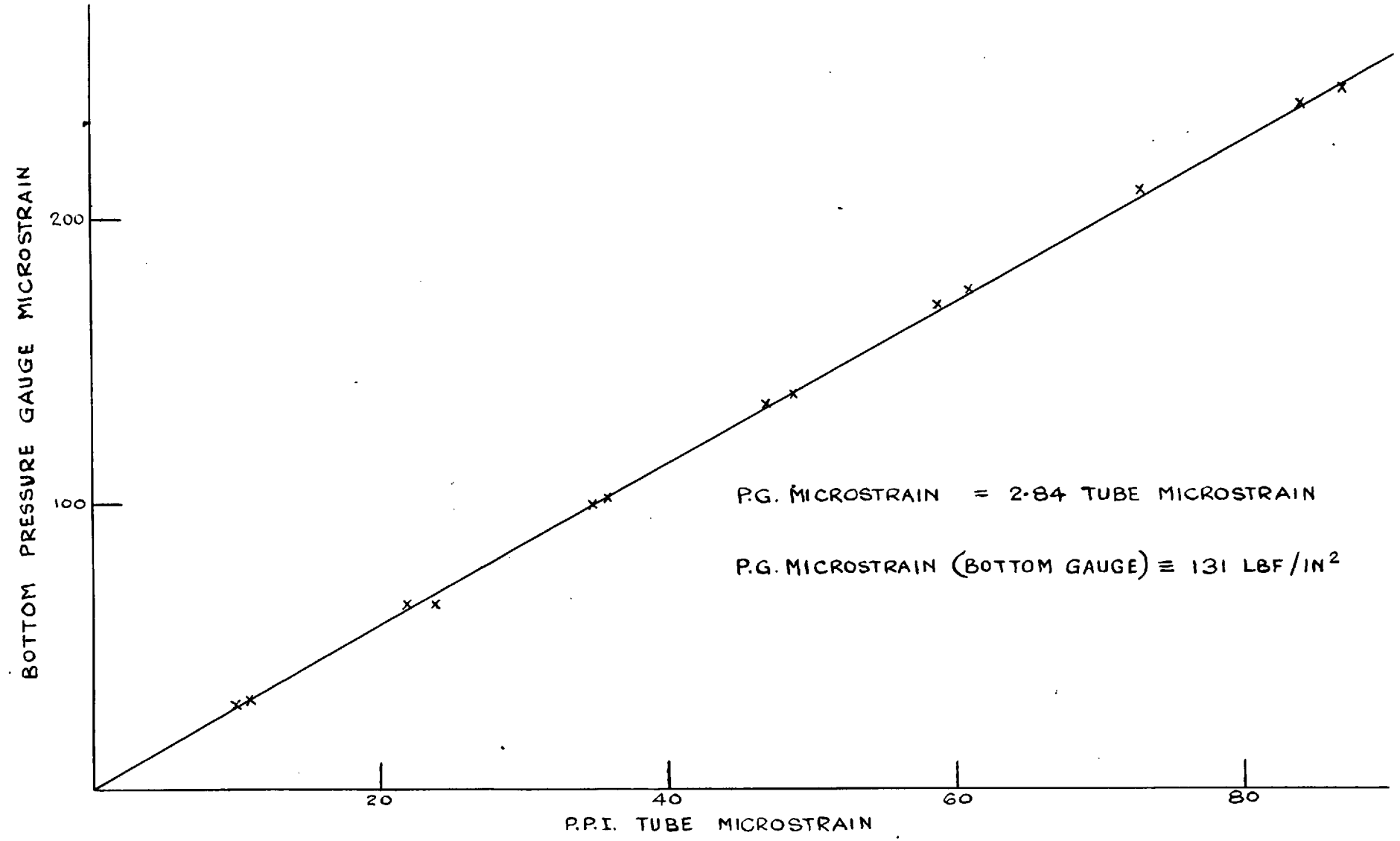



FIG 15 - CALIBRATION OF BOTTOM PRESSURE GAUGE

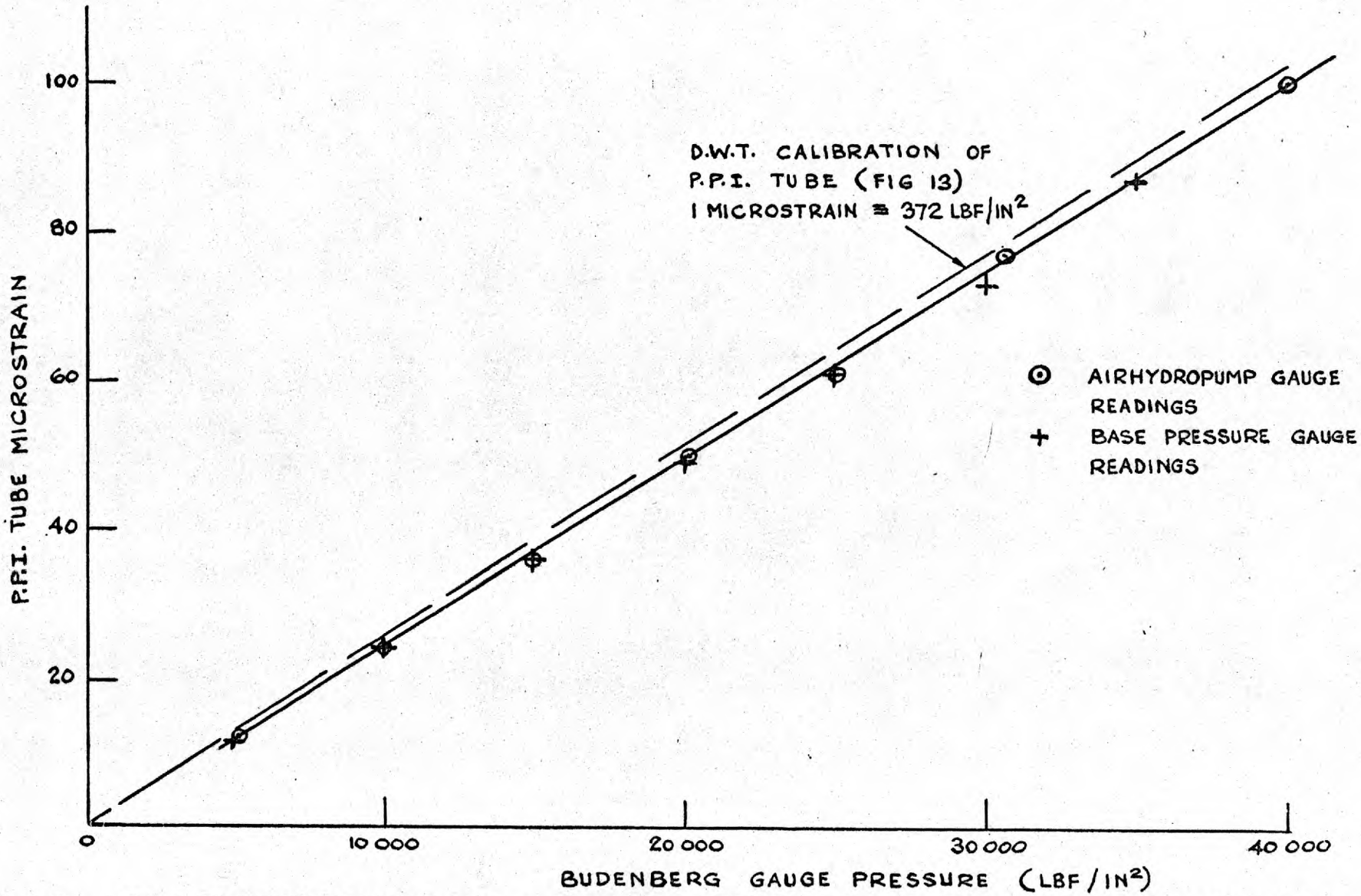
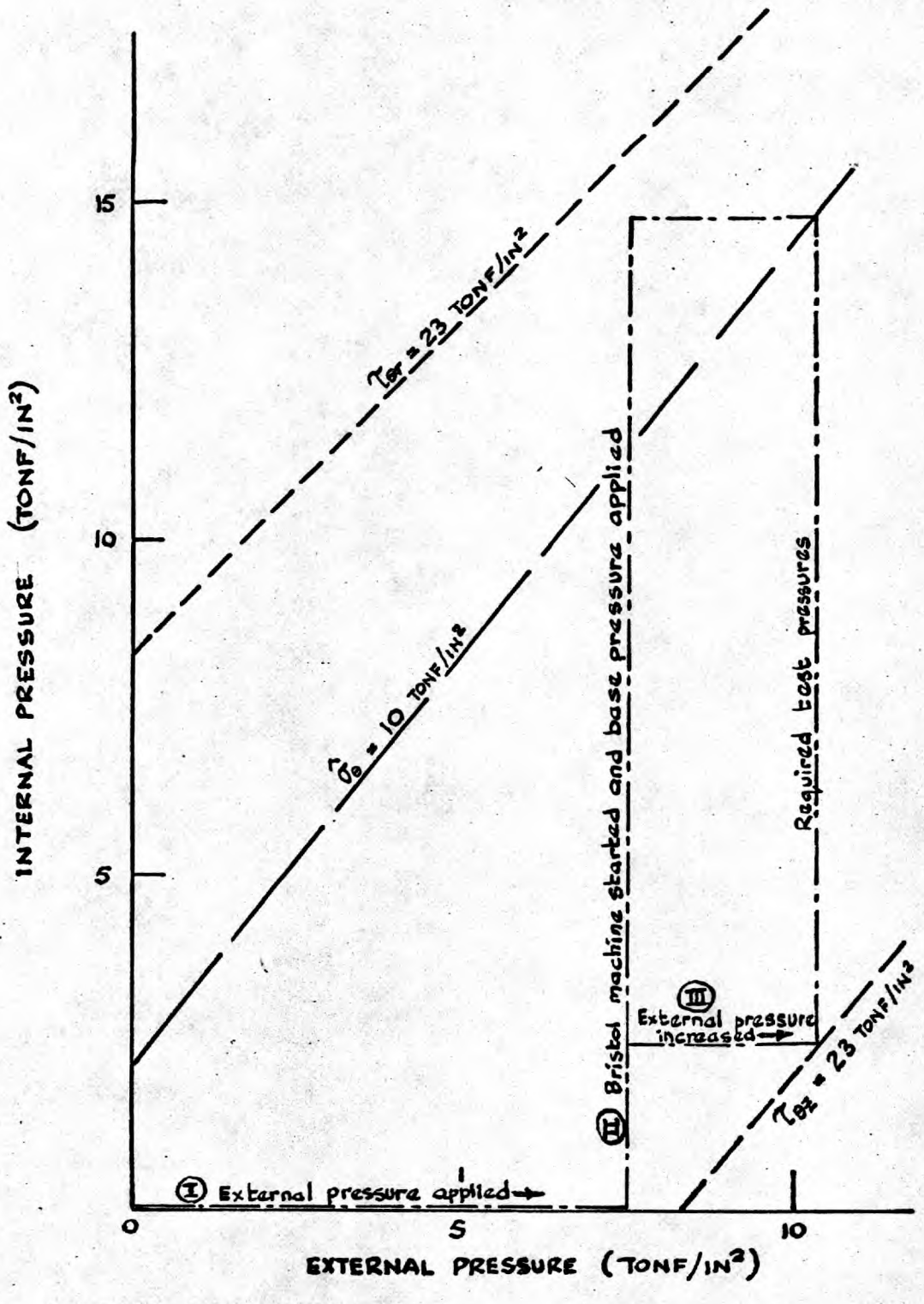



FIG 16 - P.P.I. TUBE MICROSTRAIN AGAINST AIRHYDROPUMP AND BASE PRESSURE GAUGE READINGS




LOADING PROCEDURE

I EXTERNAL PRESSURE OF 7·5 TONF/IN² APPLIED

II BRISTOL MACHINE STARTED AND REQUIRED BASE PRESSURE APPLIED

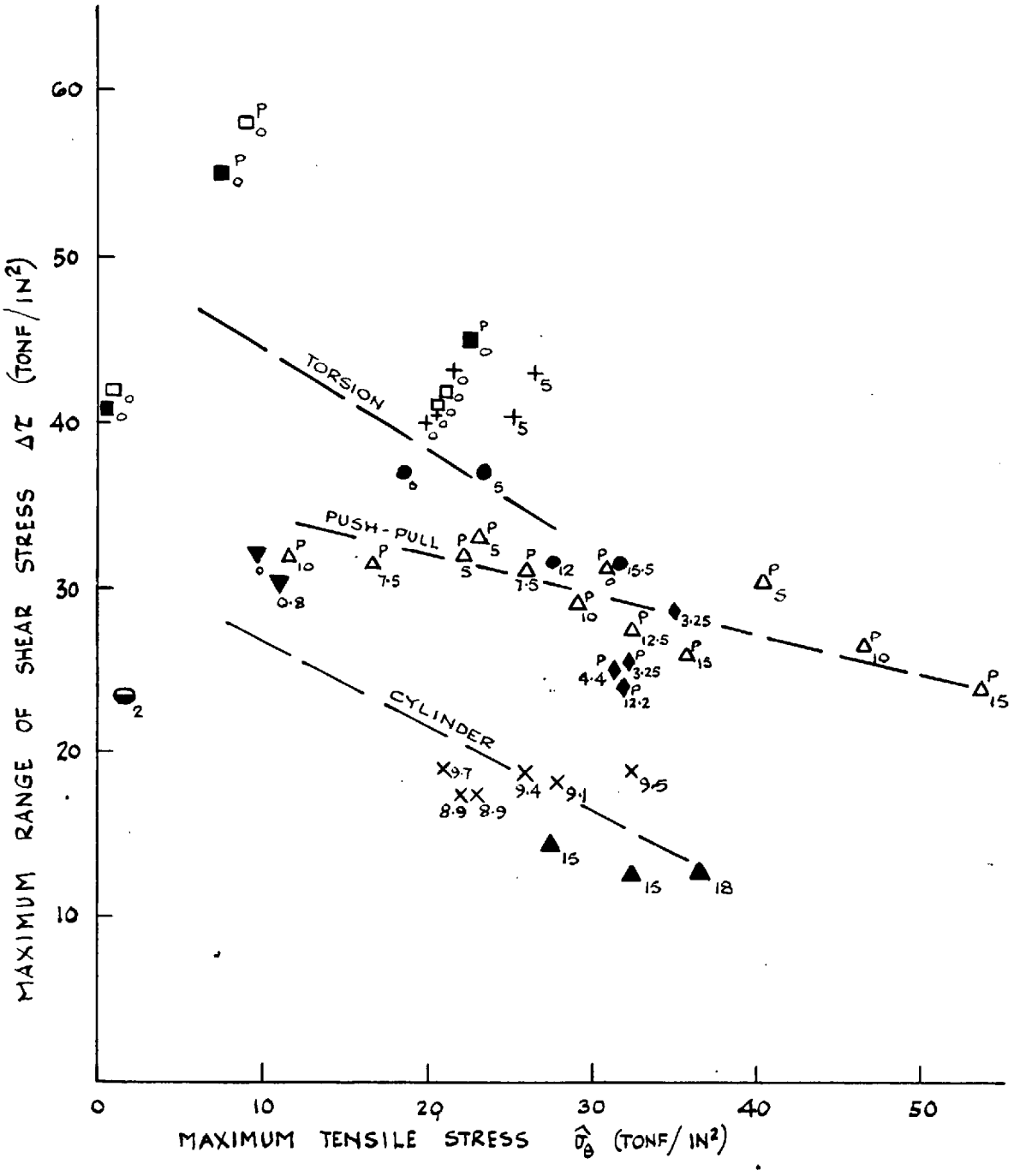
III EXTERNAL PRESSURE INCREASED TO REQUIRED VALUE

CYLINDER ELASTIC BETWEEN $\tau_{\theta r}$ = 23 TONF/IN² AND $\tau_{\theta z}$ = 23 TONF/IN² LINES

EN 25

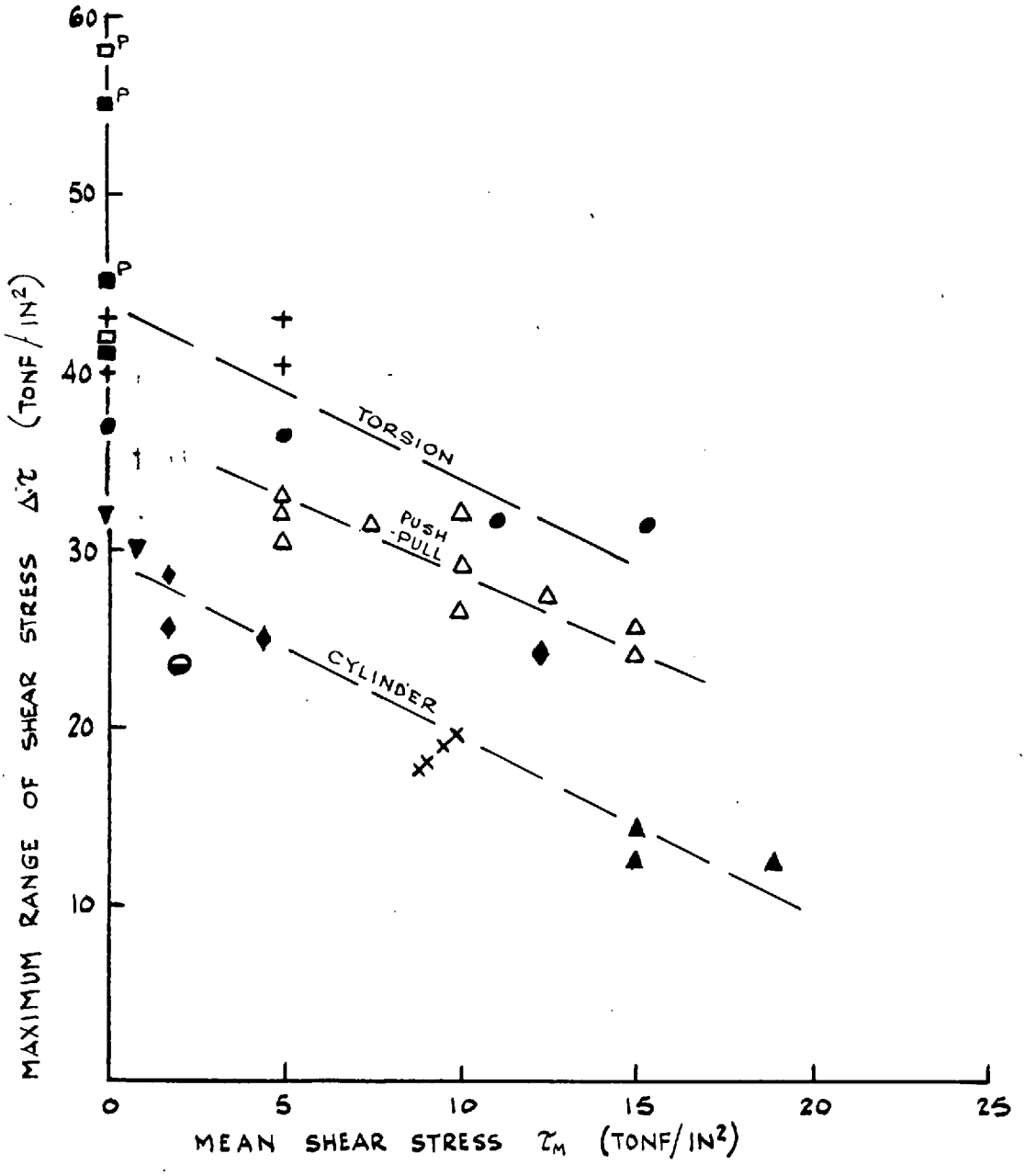
K = 1·25

FIG 17 LOADING PROCEDURE



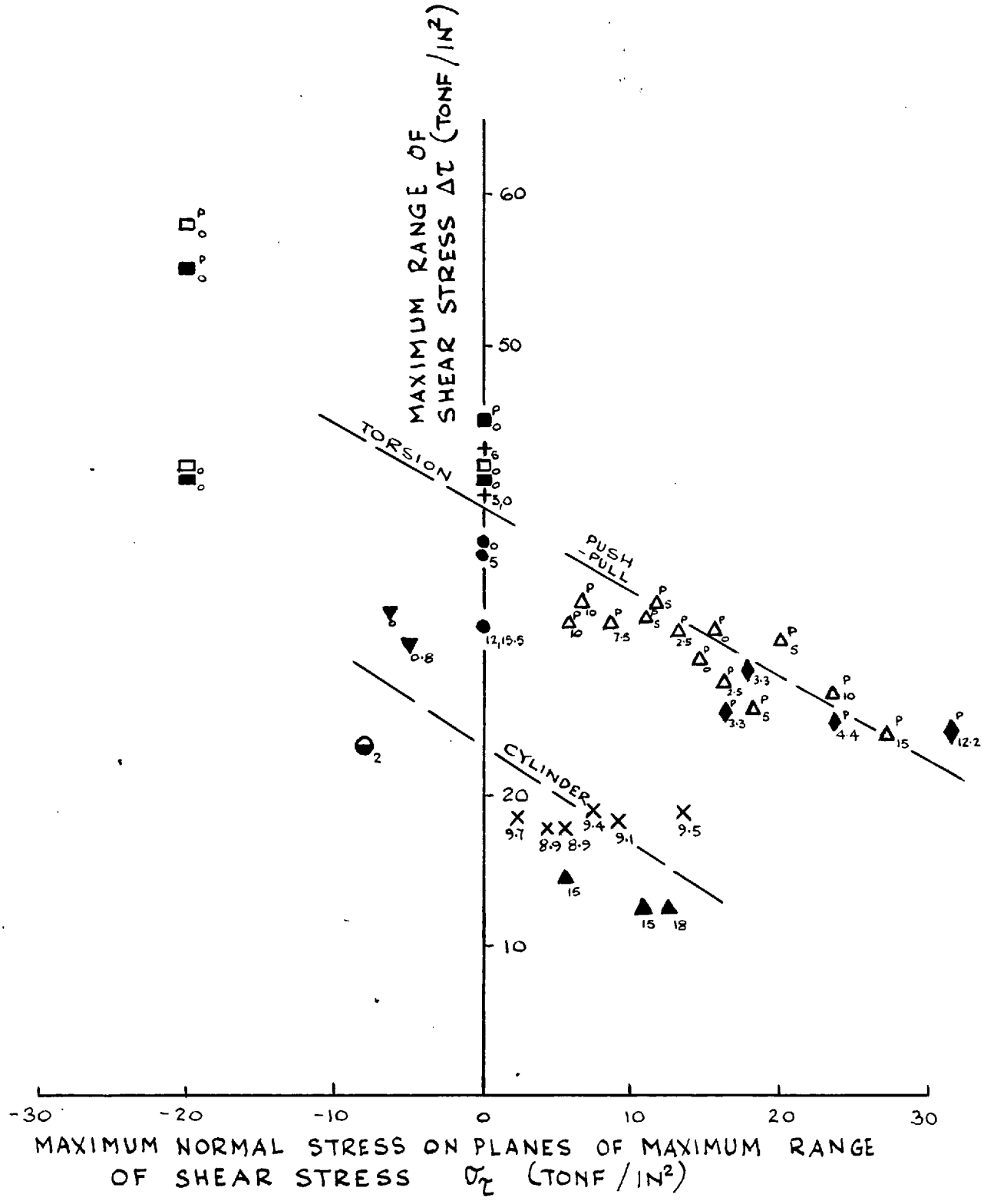

SEE FIGS 45 AND 46 FOR NOTATION

FIG 18 EFFECT OF TENSILE STRESS ON FATIGUE STRENGTH OF EN 25 STEEL FOR LIFE OF $10^6$ CYCLES



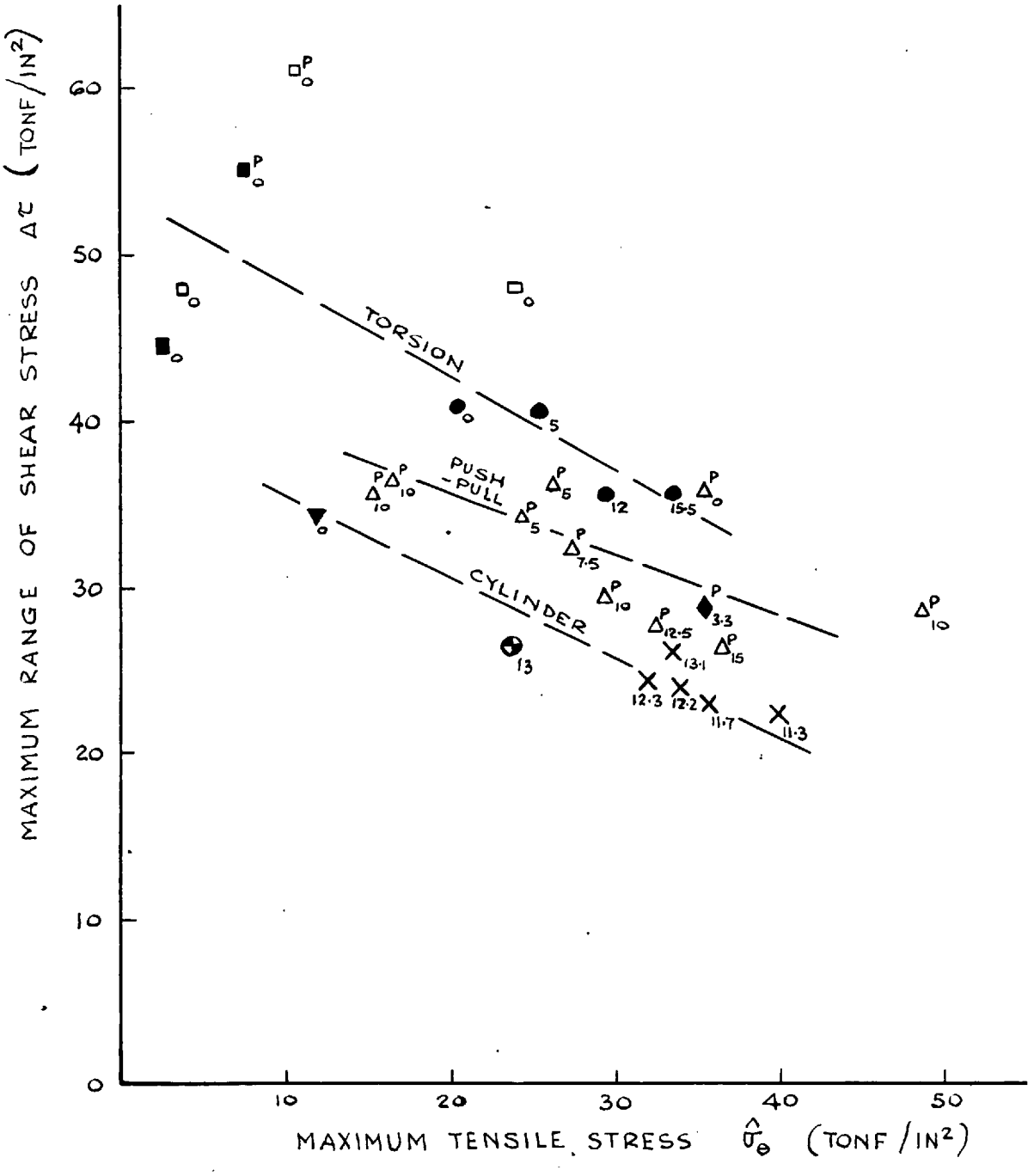

SEE FIGS 45 AND 46 FOR NOTATION

FIG 19 EFFECT OF MEAN SHEAR STRESS ON FATIGUE STRENGTH OF EN25 STEEL FOR LIFE OF $10^6$ CYCLES



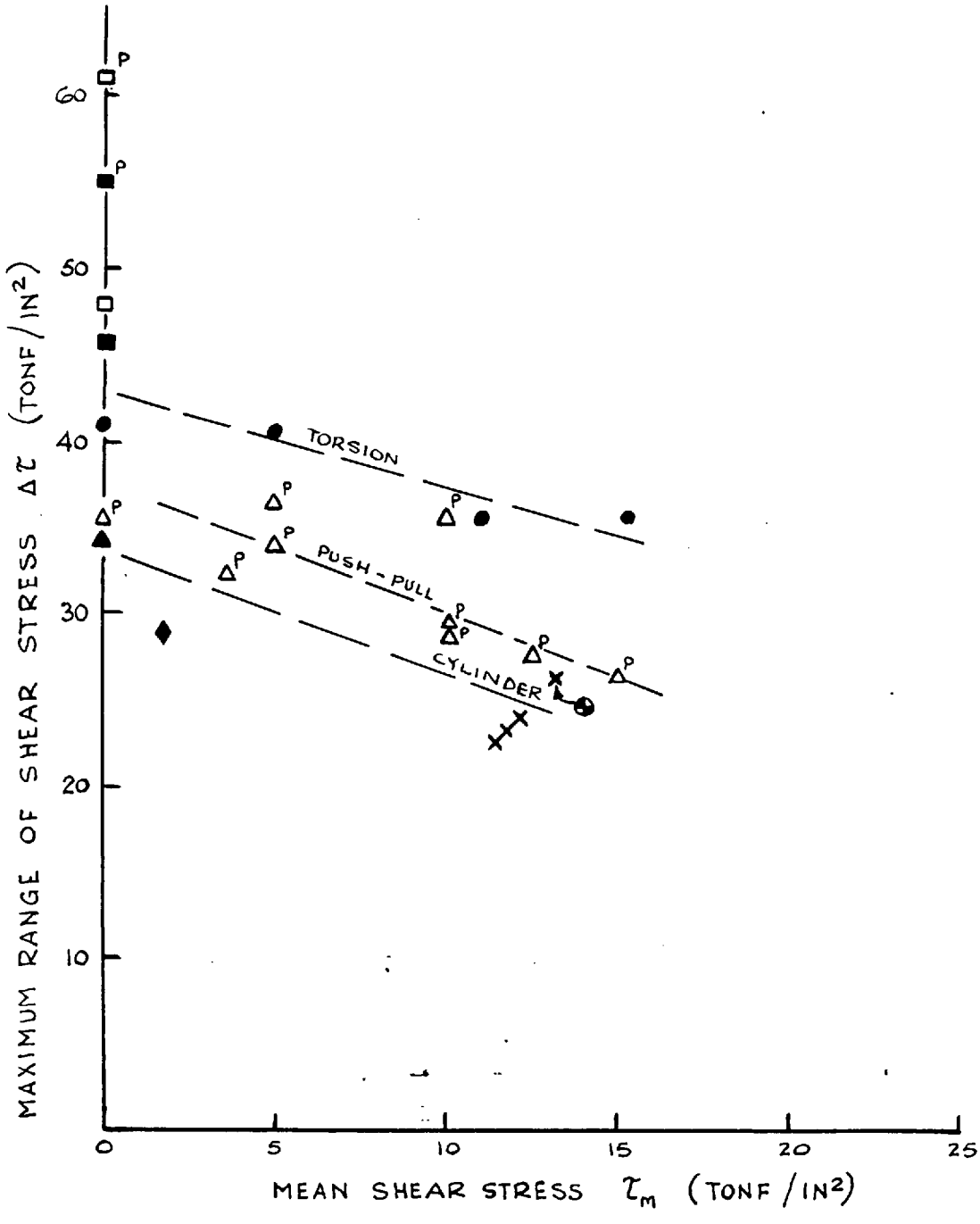

SEE FIGS 45 AND 46 FOR NOTATION

FIG 20 EFFECT OF NORMAL STRESS ON FATIGUE STRENGTH OF EN25 STEEL FOR LIFE OF $10^6$ CYCLES



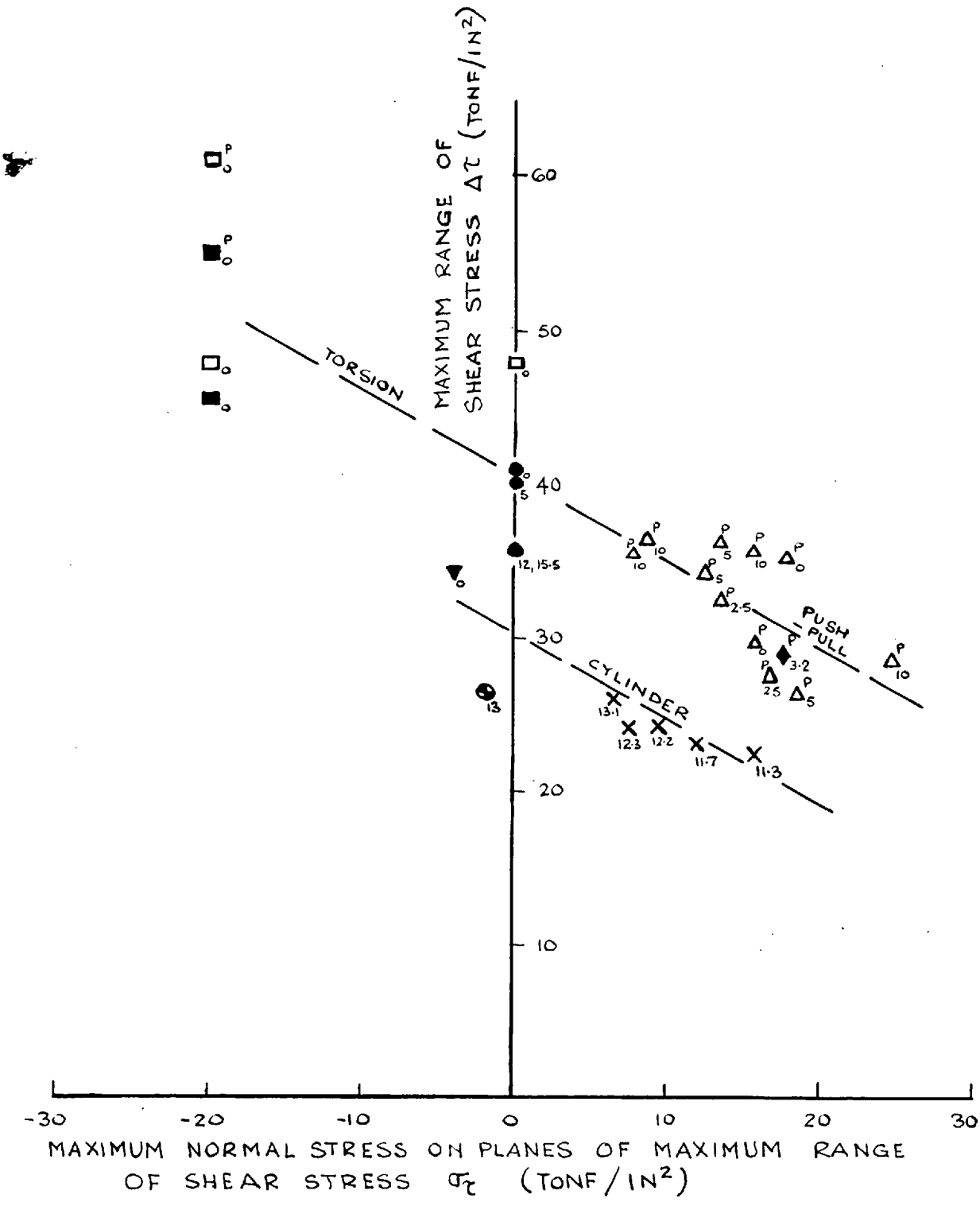

SEE FIGS 45 AND 46 FOR NOTATION

FIG 21 EFFECT OF TENSILE STRESS ON FATIGUE STRENGTH OF EN 25 STEEL FOR LIFE OF $10^5$ CYCLES




SEE FIGS 45 AND 46 FOR NOTATION

FIG 22 EFFECT OF MEAN SHEAR STRESS ON FATIGUE STRENGTH OF EN 25 STEEL FOR LIFE OF $10^5$ CYCLES




SEE FIGS 45 AND 46 FOR NOTATION

FIG 23 EFFECT OF NORMAL STRESS ON FATIGUE STRENGTH OF EN 25 STEEL FOR LIFE OF $10^5$ CYCLES

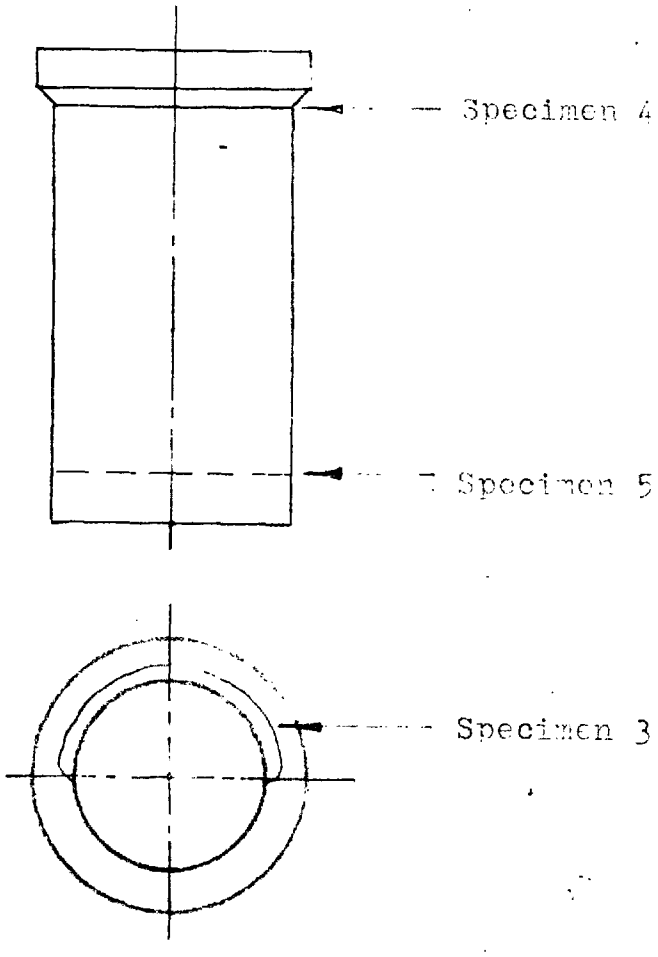



FIGURE 24 POSITIONS OF FRACTURES
Specimens 3,4 and 5.
Test series 1.

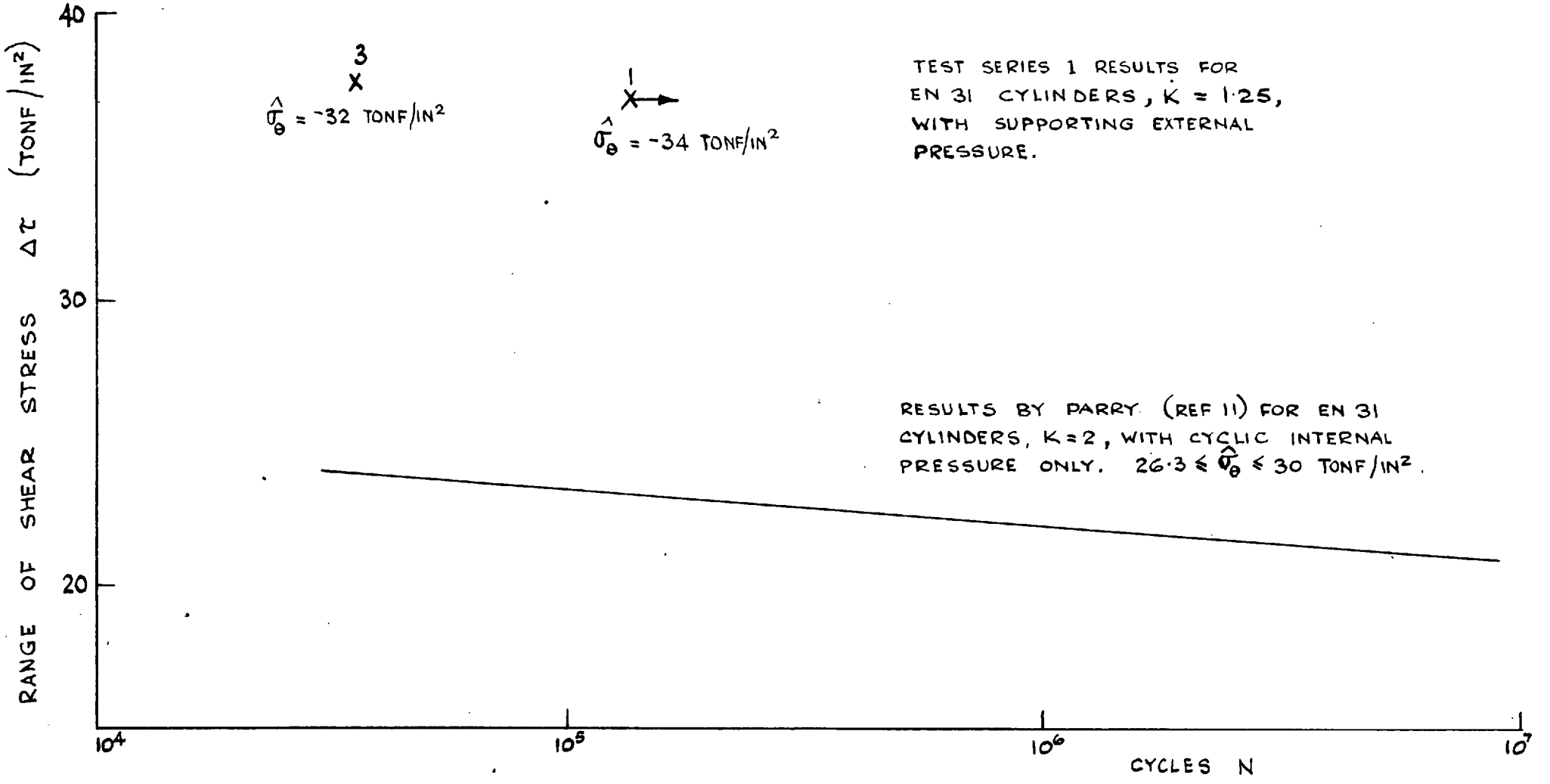



FIG 25 REPEATED PRESSURE TESTS ON EN 31 CYLINDERS

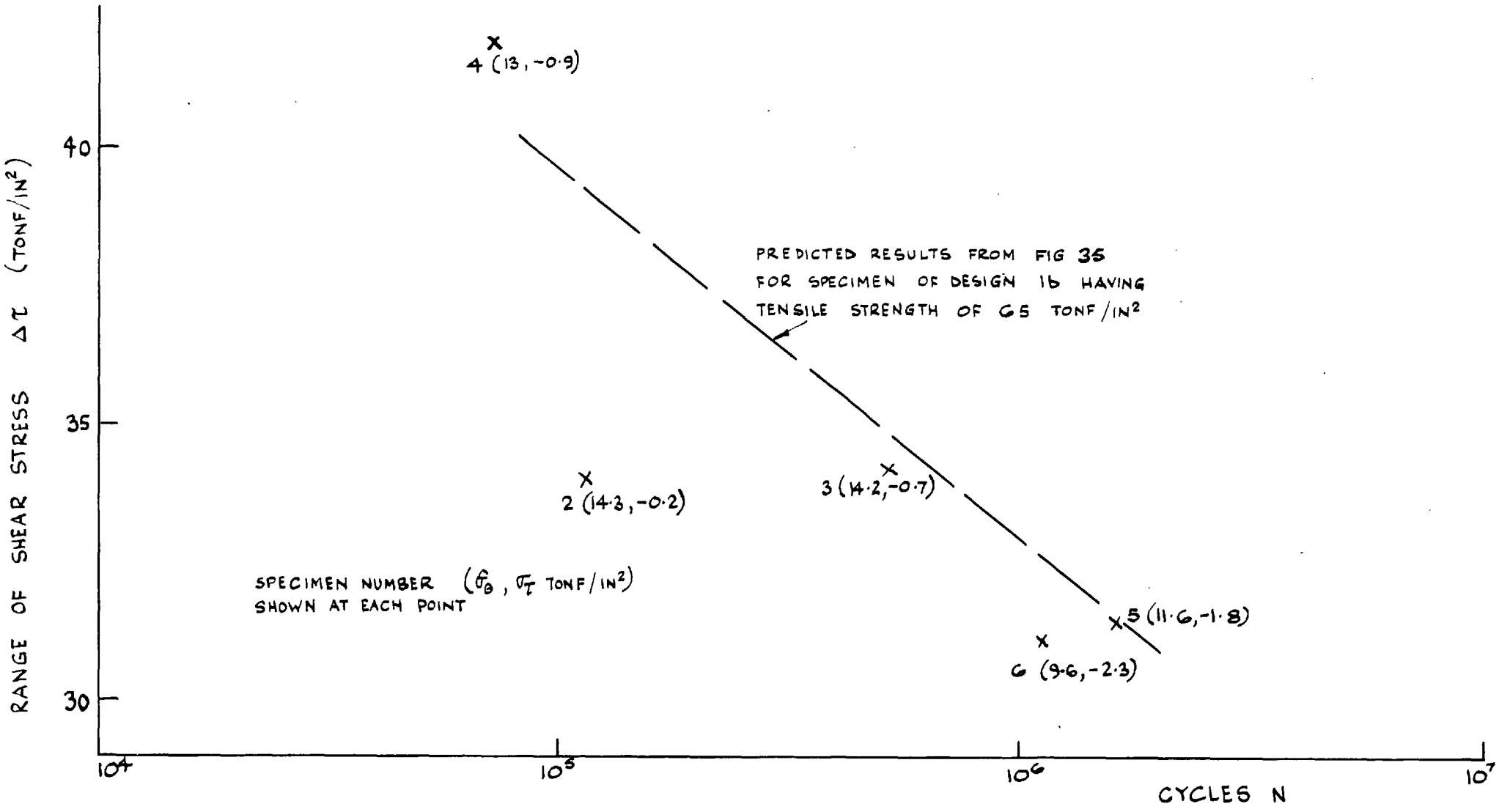



FIG 26 RESULTS OF TEST SERIES 2

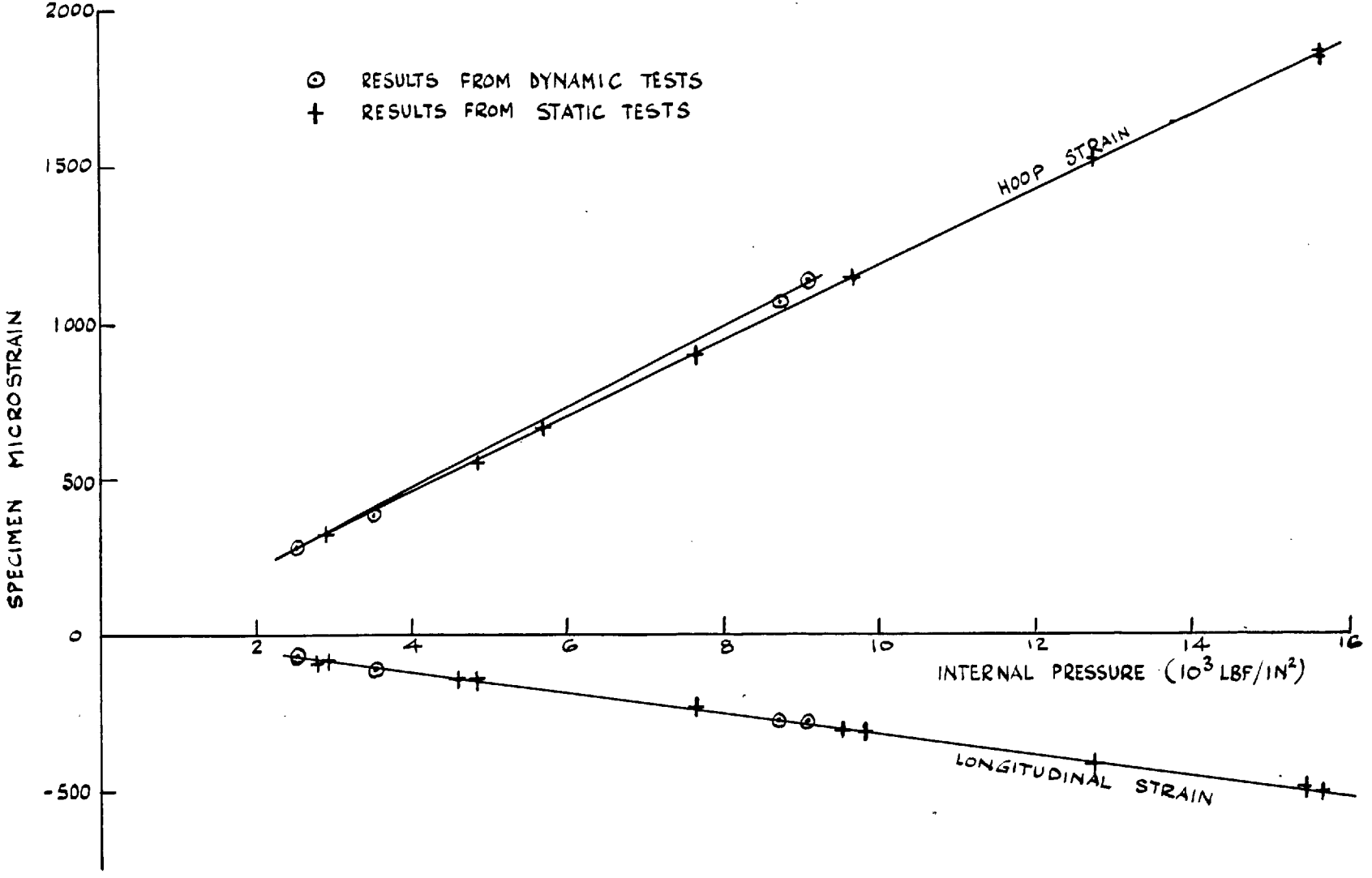



FIG 27 STRAIN GAUGE TEST 4 - E.I.P.2 CYLINDER WITH INTERNAL PRESSURE

STRAINS AT MID GAUGE LENGTH OF CYLINDER SHOWN

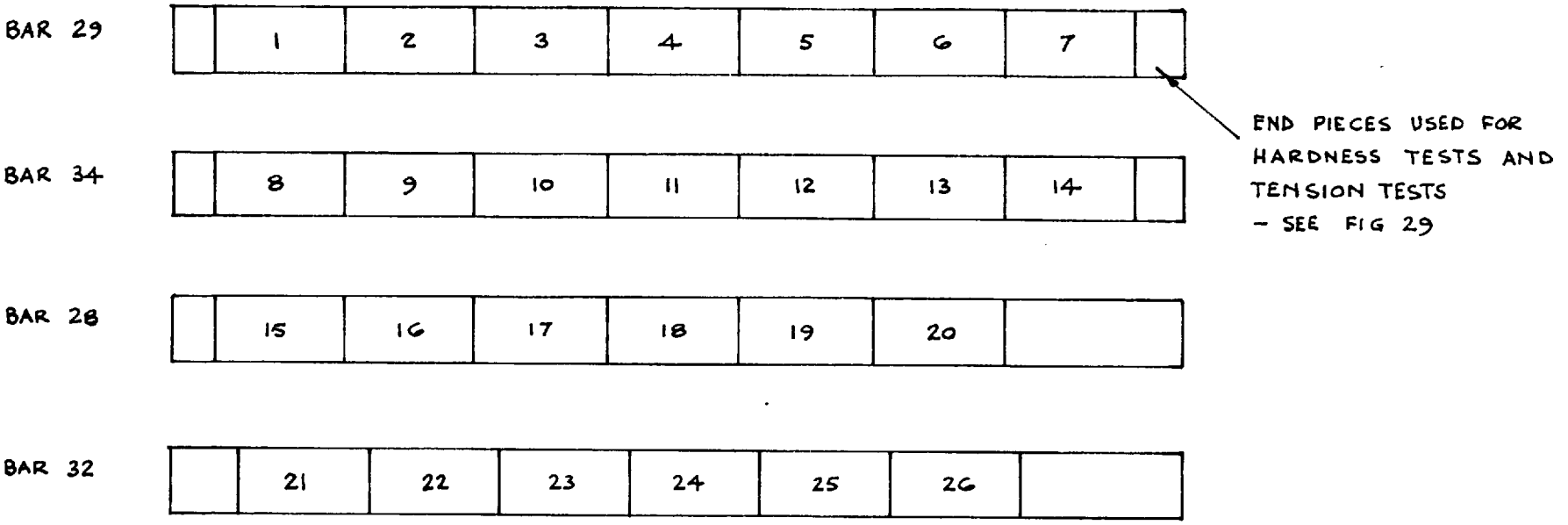



FIG 28 CUTTING OF CYLINDER SPECIMENS FROM BARS

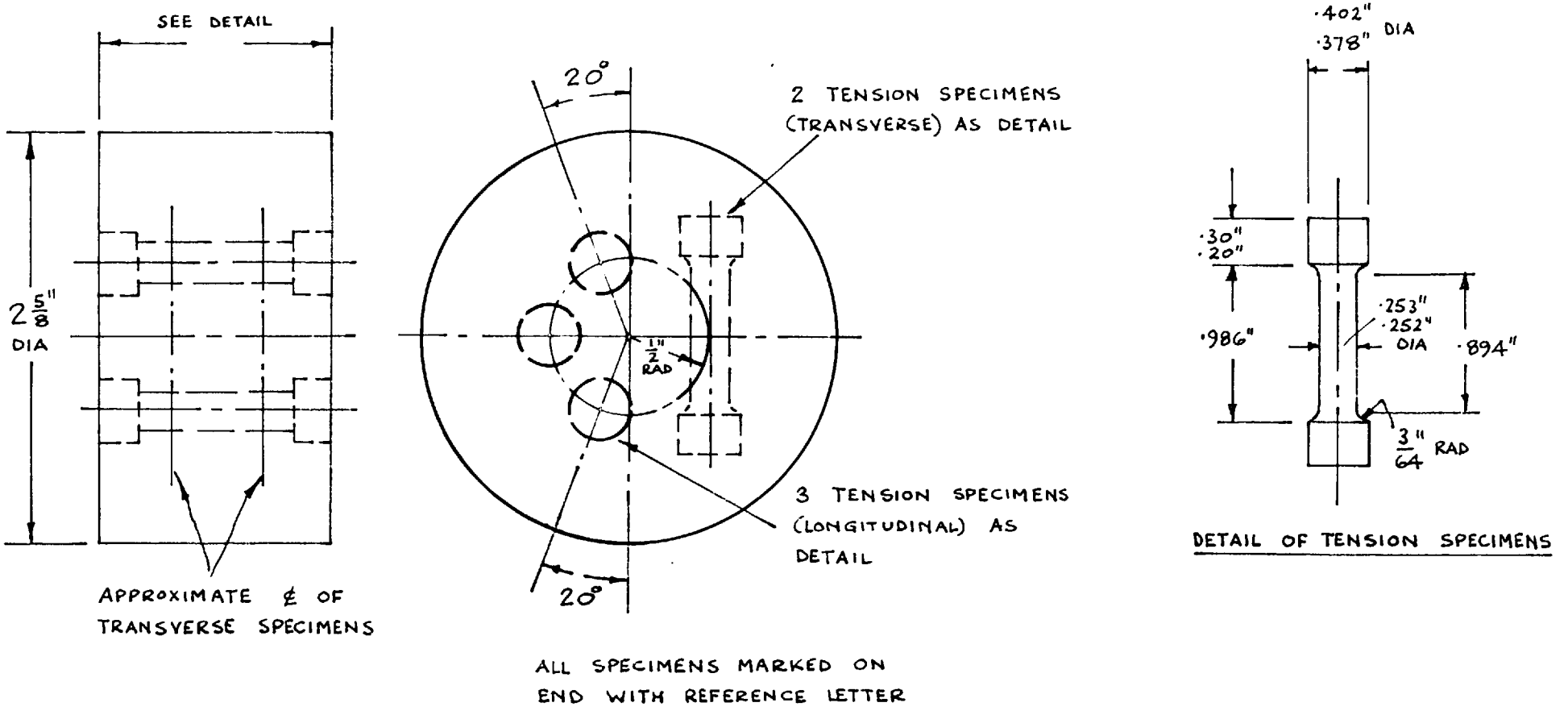



FIG 29 CUTTING OF TENSION SPECIMENS FROM BAR ENDS

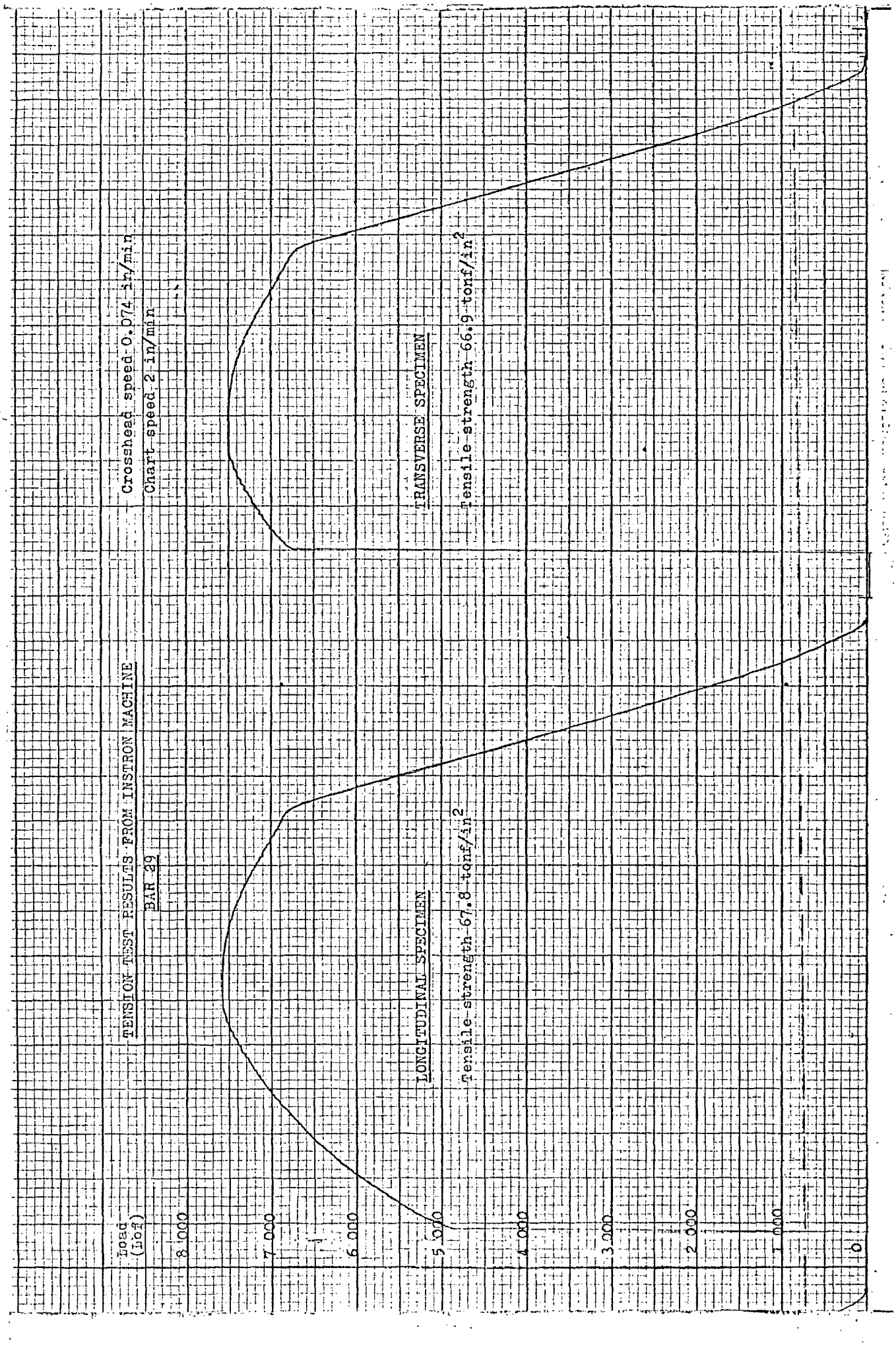



FIG 30 TENSION TEST RESULTS FROM INSTRON MACHINE

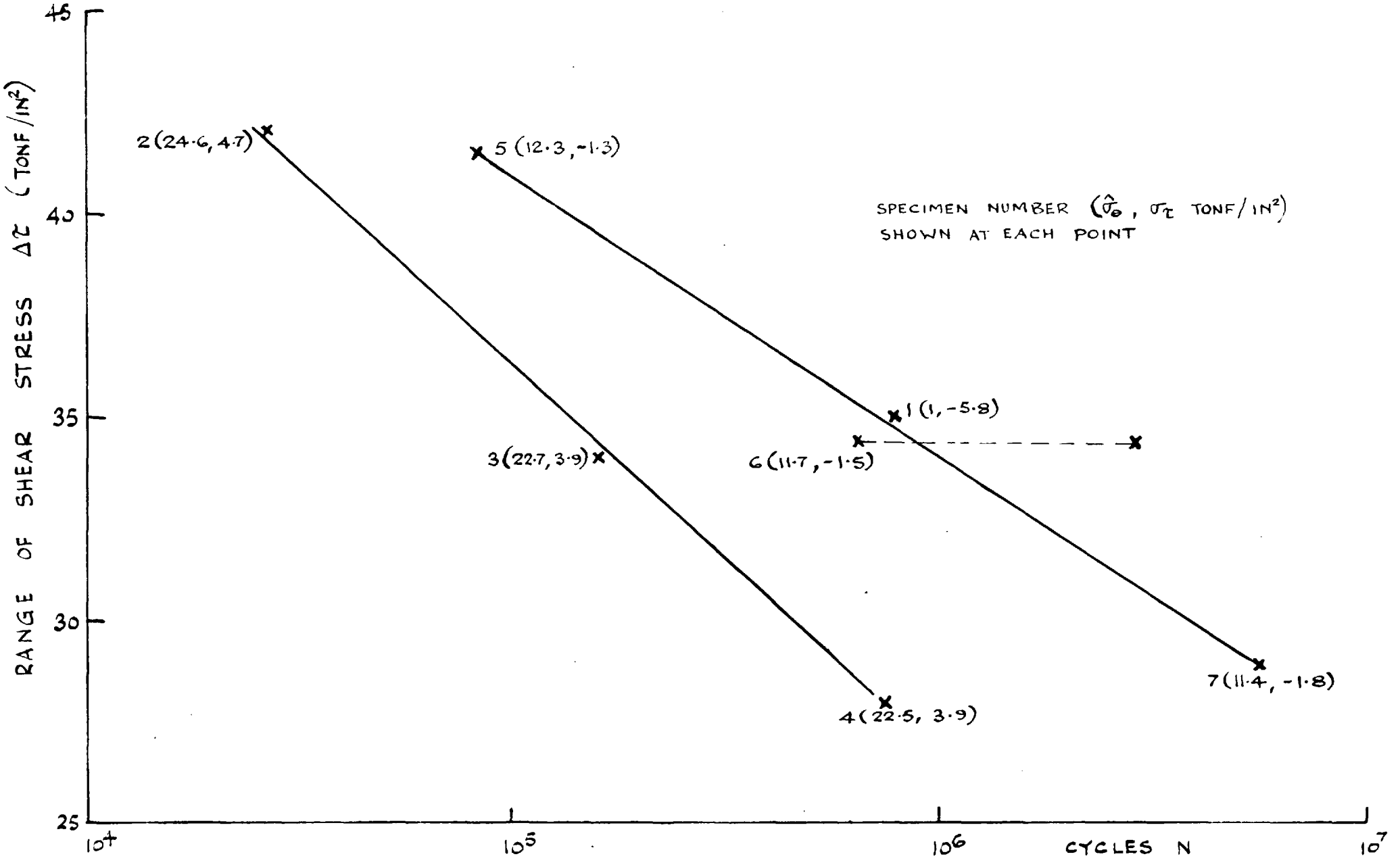



FIG 31 Δτ AGAINST N SPECIMENS 1 TO 7 TEST SERIES 3

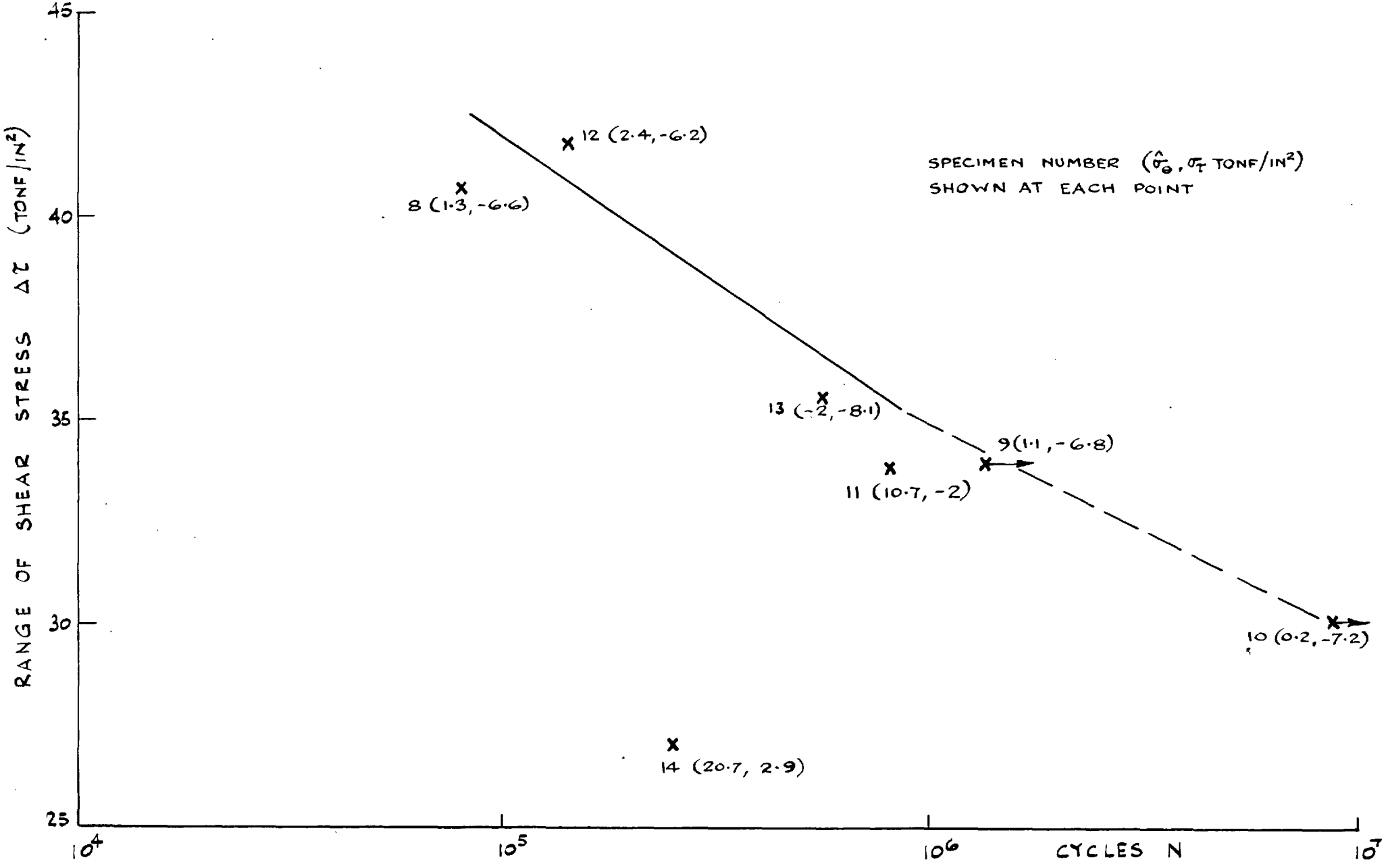



FIG 32 Δτ AGAINST N SPECIMENS 8 TO 14 TEST SERIES 3

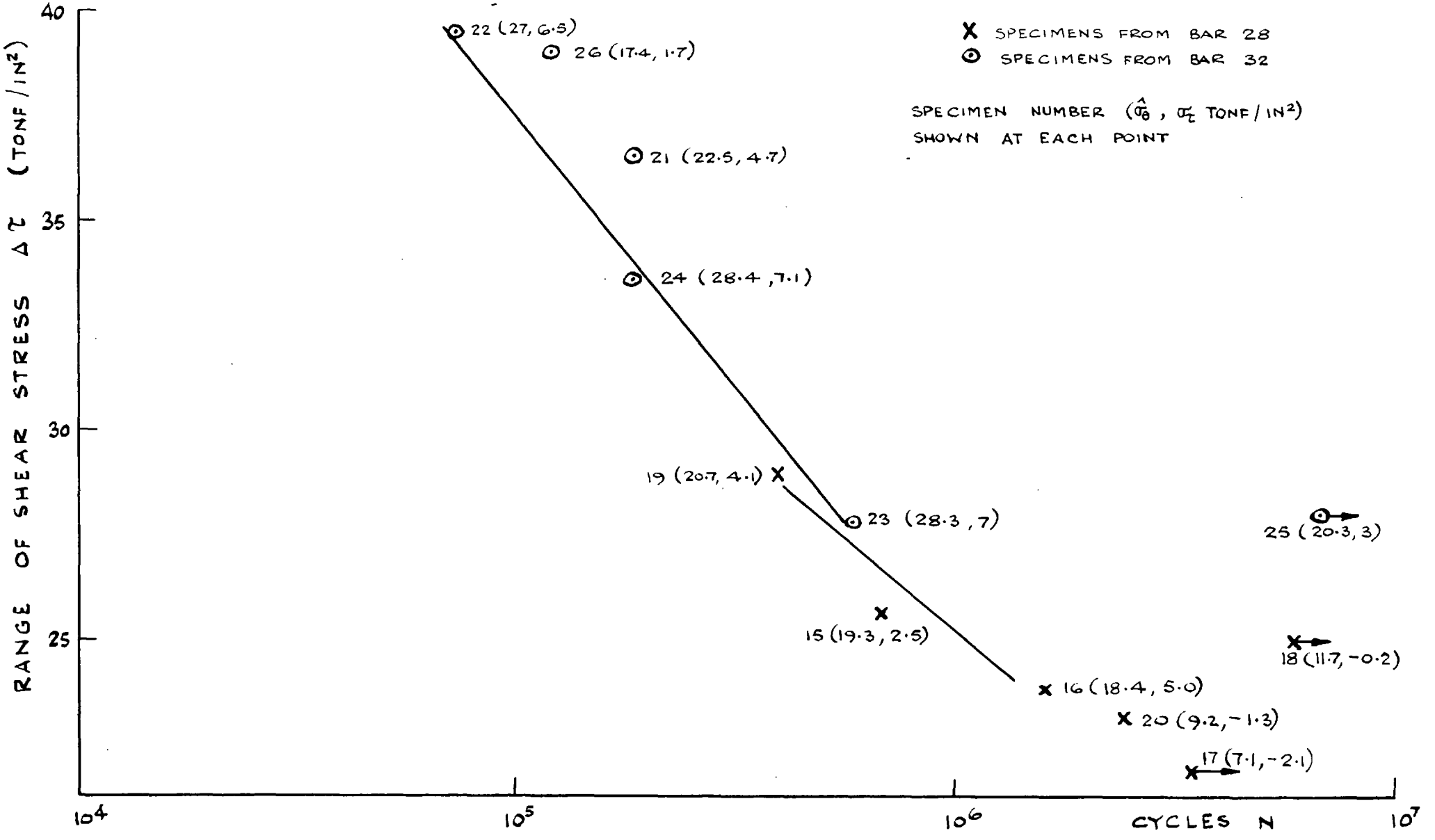



FIG 33 ΔT AGAINST N SPECIMENS 15 TO 26 TEST SERIES 3

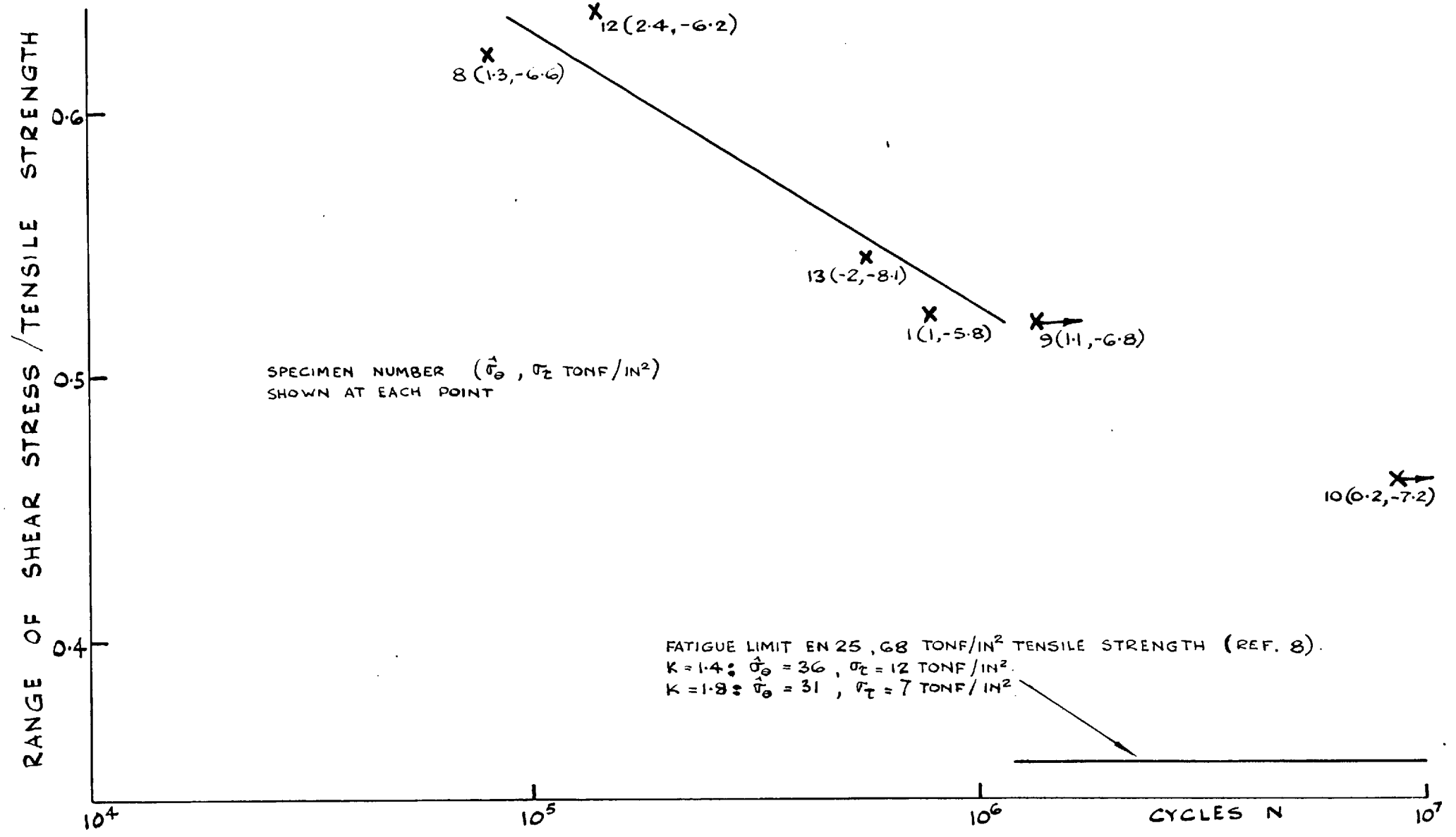



FIG 34 $\Delta\tau$/TENSILE STRENGTH AGAINST N TEST SERIES 3 $-2 \leq \hat{\sigma}_\theta \leq 2{\cdot}4$ $-8{\cdot}1 \leq \sigma_t \leq -5{\cdot}8$

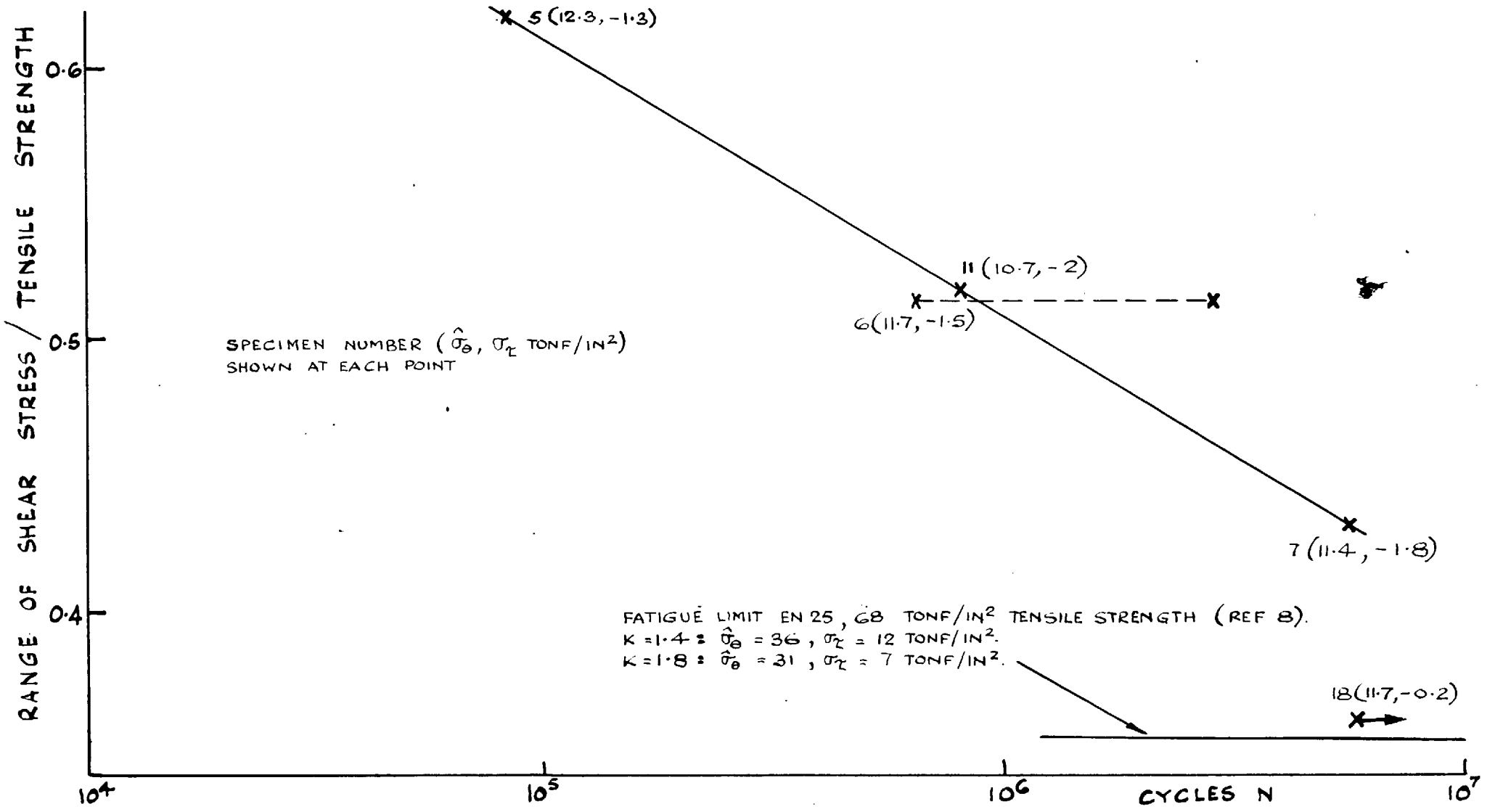



FIG 35 $\Delta\tau$/TENSILE STRENGTH AGAINST N TEST SERIES 3 $10{\cdot}7 \leq \hat{\sigma}_\theta \leq 12{\cdot}3$ $-2 \leq \sigma_\tau \leq -1{\cdot}3$

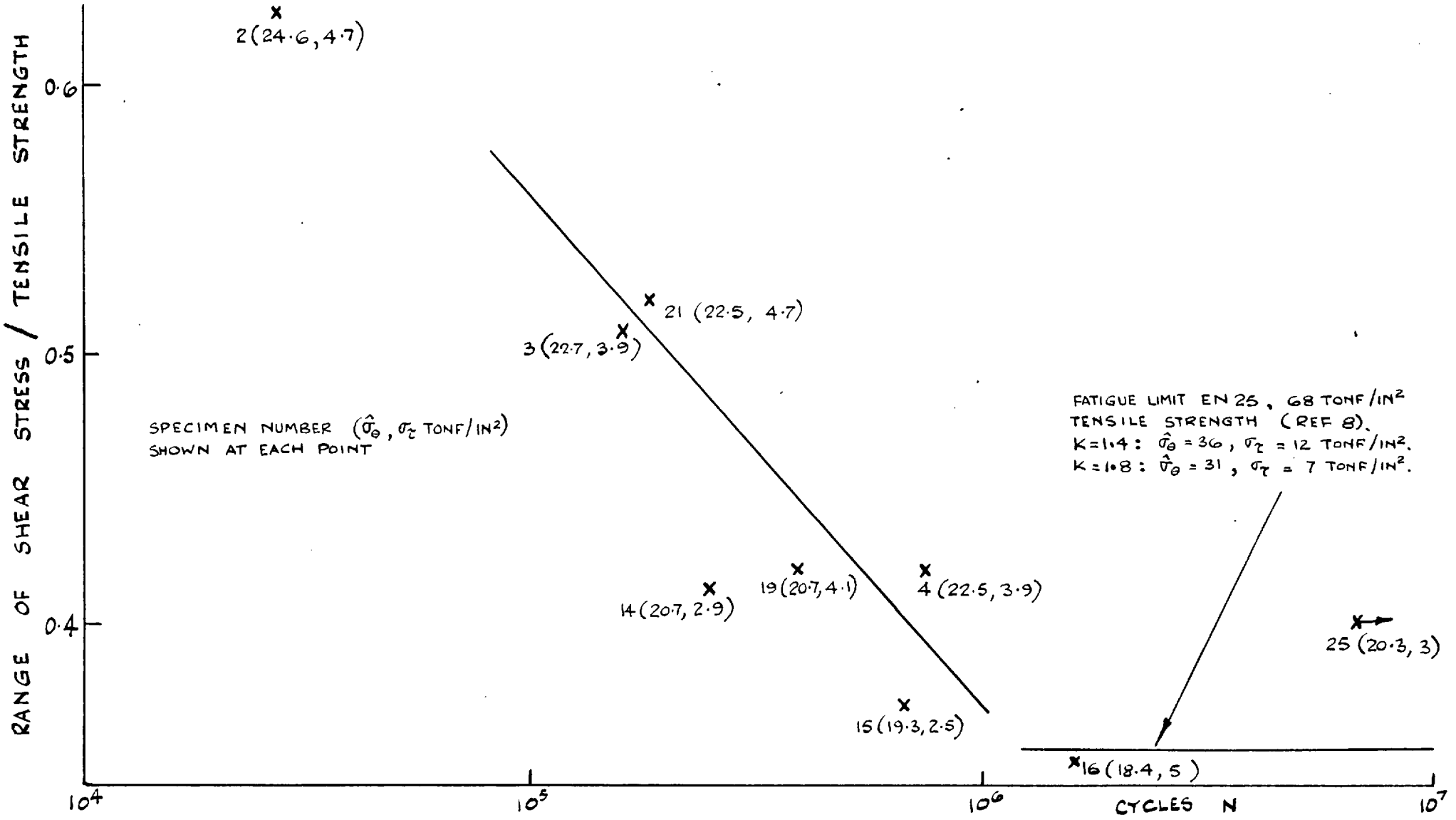



FIG 36 $\Delta\tau$ / TENSILE STRENGTH AGAINST N TEST SERIES 3 $18{\cdot}4 \leq \hat{\sigma}_\theta \leq 22{\cdot}7$ $2{\cdot}5 \leq \sigma_\tau \leq 5$

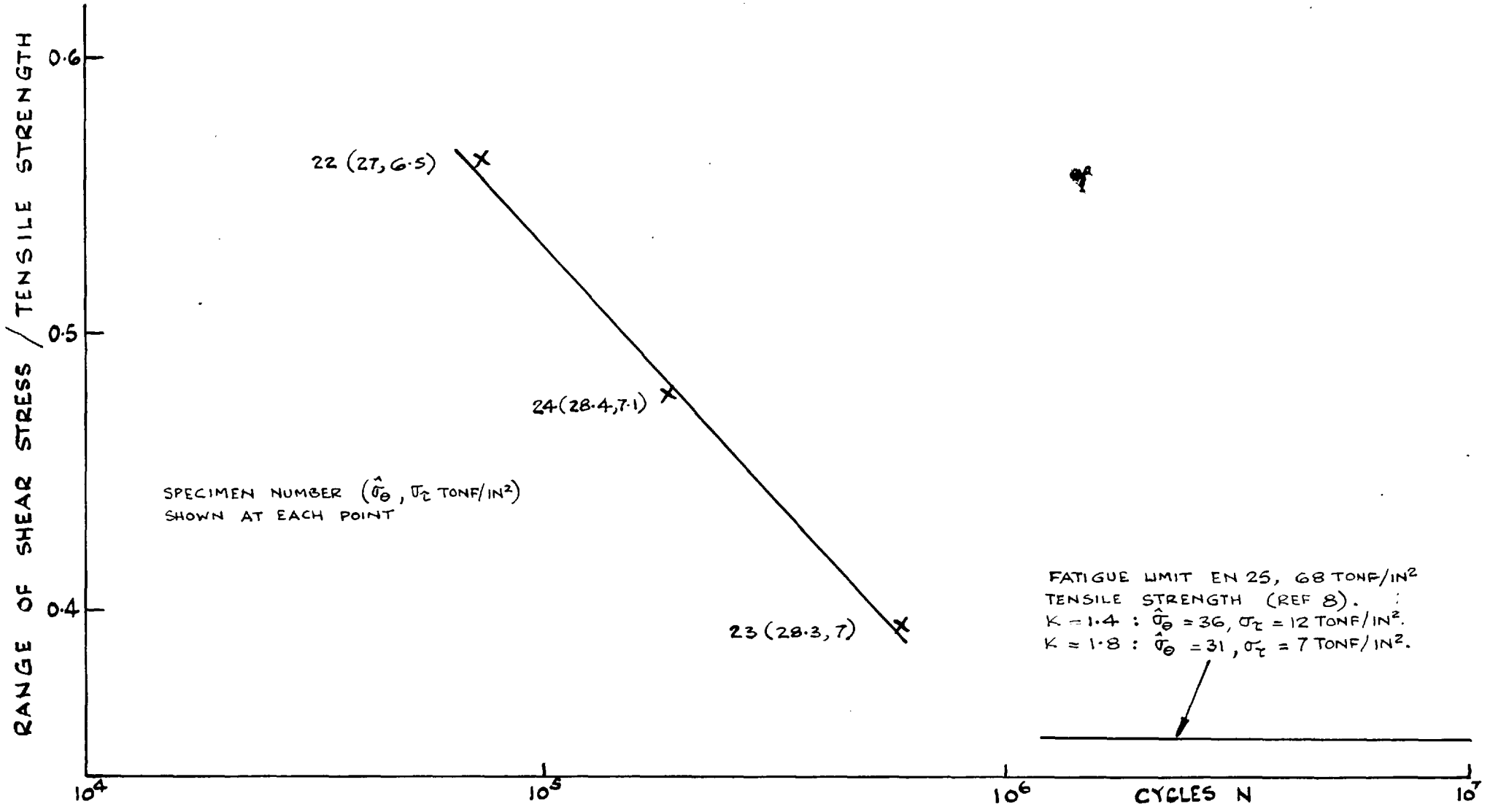



FIG 37 $\Delta\tau$/TENSILE STRENGTH AGAINST N TEST SERIES 3 $27 \leq \hat{\sigma}_\theta \leq 28.4$ $6.5 \leq \sigma_\tau \leq 7.1$

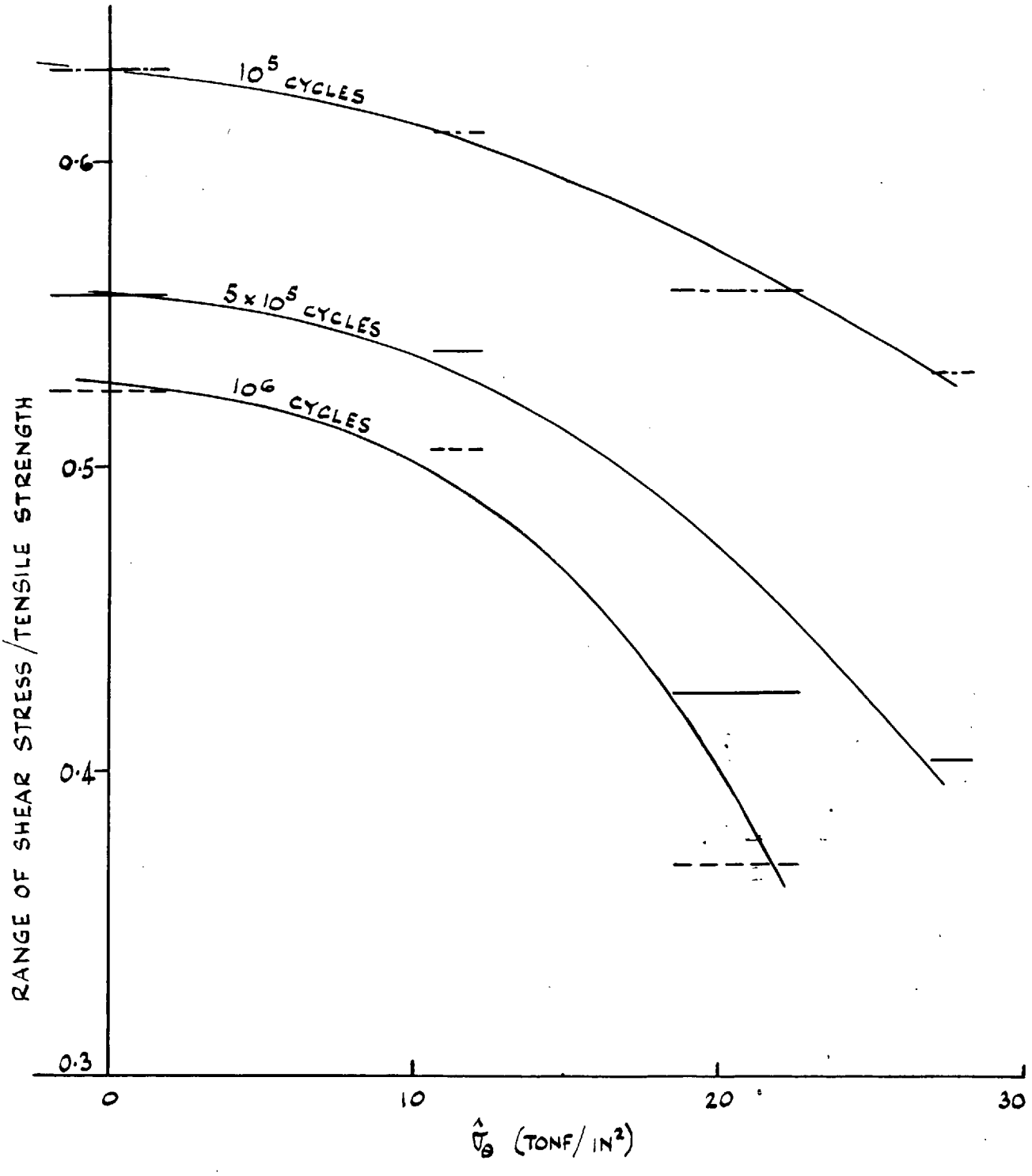



FIG 38 $\Delta\tau$/TENSILE STRENGTH AGAINST $\hat{\sigma}_\theta$

TEST SERIES 3
LIVES OF $10^5$, $5 \times 10^5$ AND $10^6$ CYCLES

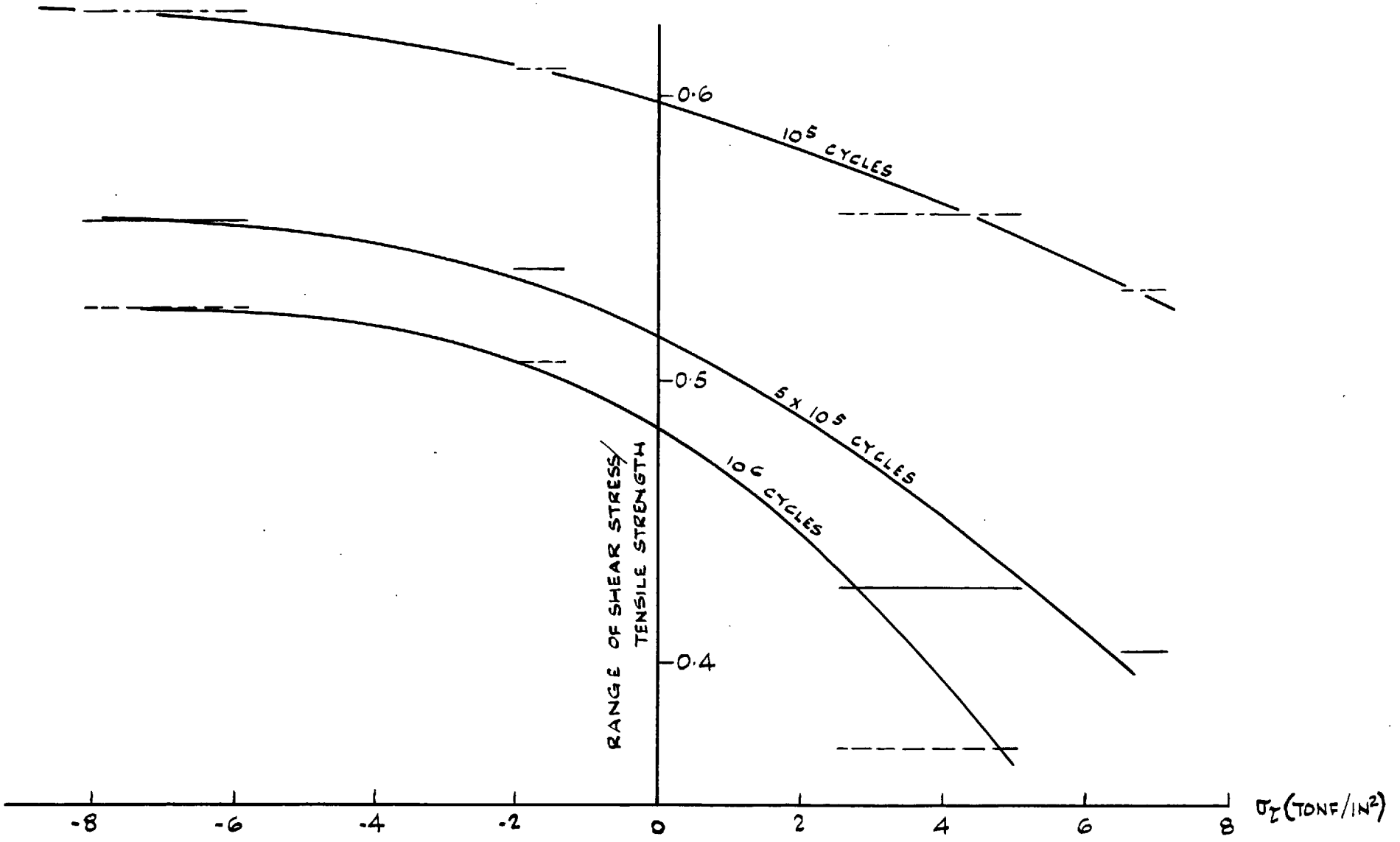



FIG 39 $\Delta\tau$/TENSILE STRENGTH AGAINST $\sigma_t$

TEST SERIES 3
LIVES OF $10^5$, $5\times10^5$ AND $10^6$ CYCLES

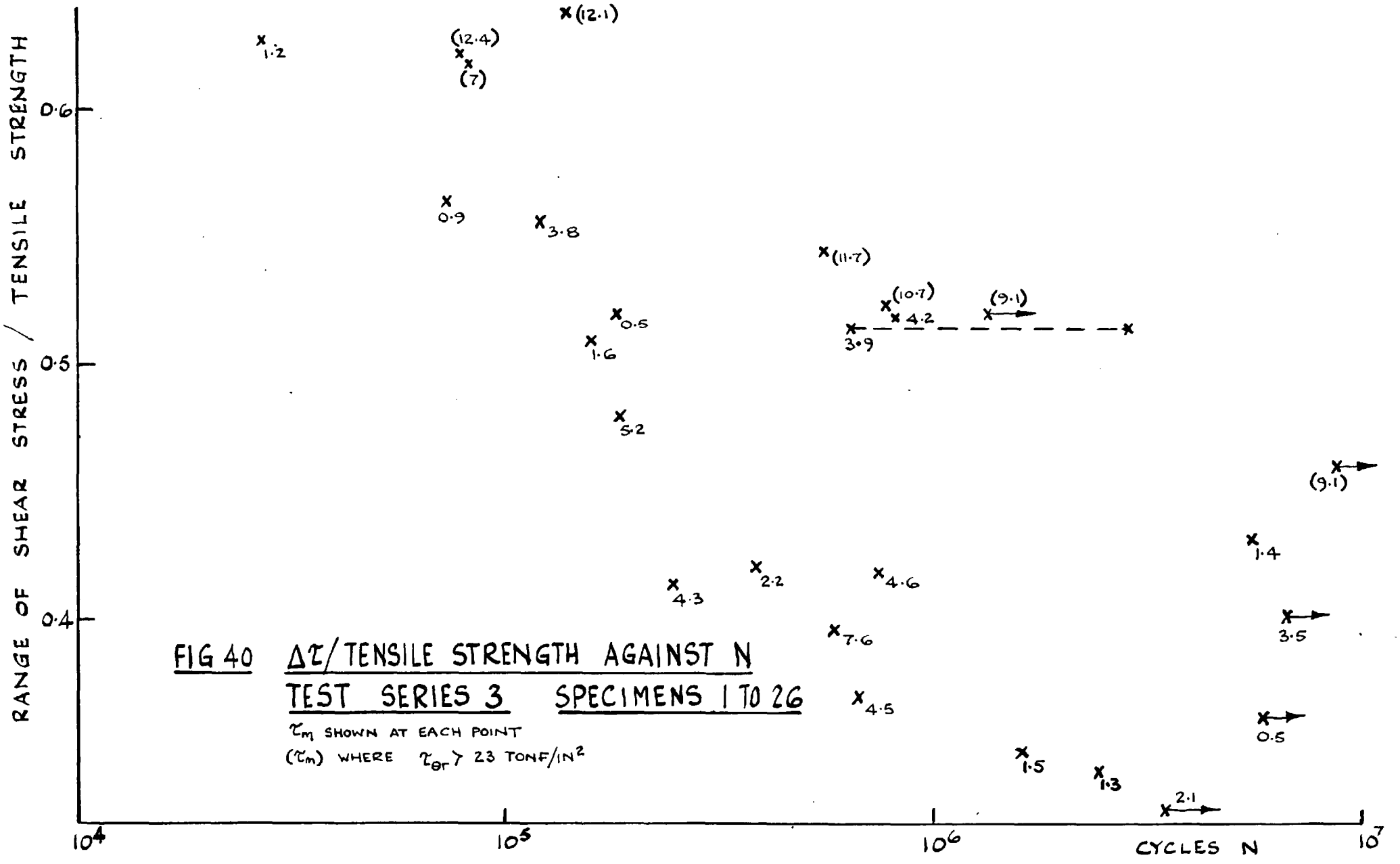



FIG 40 $\Delta\tau$/TENSILE STRENGTH AGAINST N

TEST SERIES 3 SPECIMENS 1 TO 26

$\tau_m$ SHOWN AT EACH POINT

($\tau_m$) WHERE $\tau_{0r} > 23$ TONF/IN$^2$

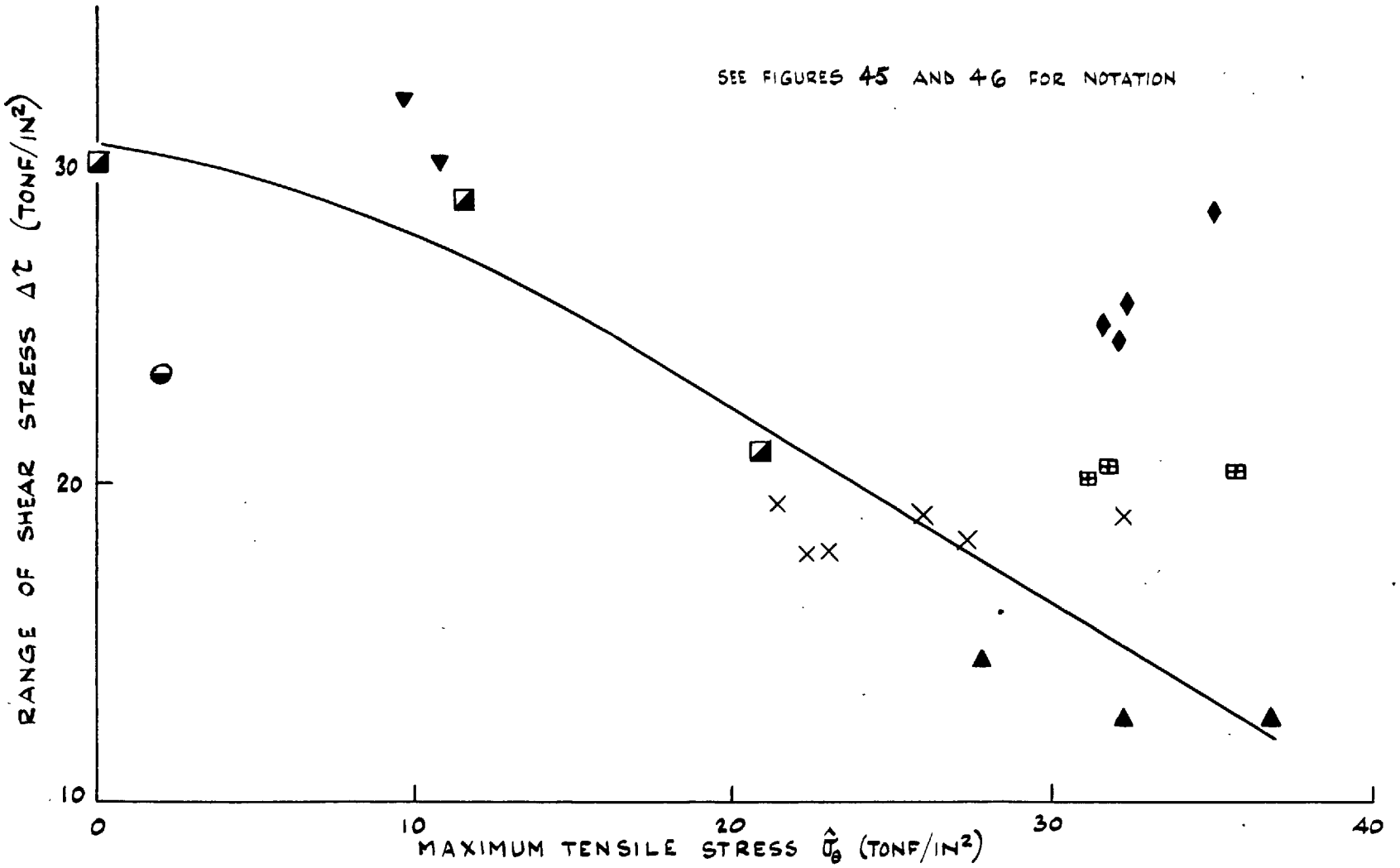



FIG 41 EFFECT OF TENSILE STRESS ON FATIGUE STRENGTH OF EN 25 STEEL CYLINDERS $10^6$ CYCLES

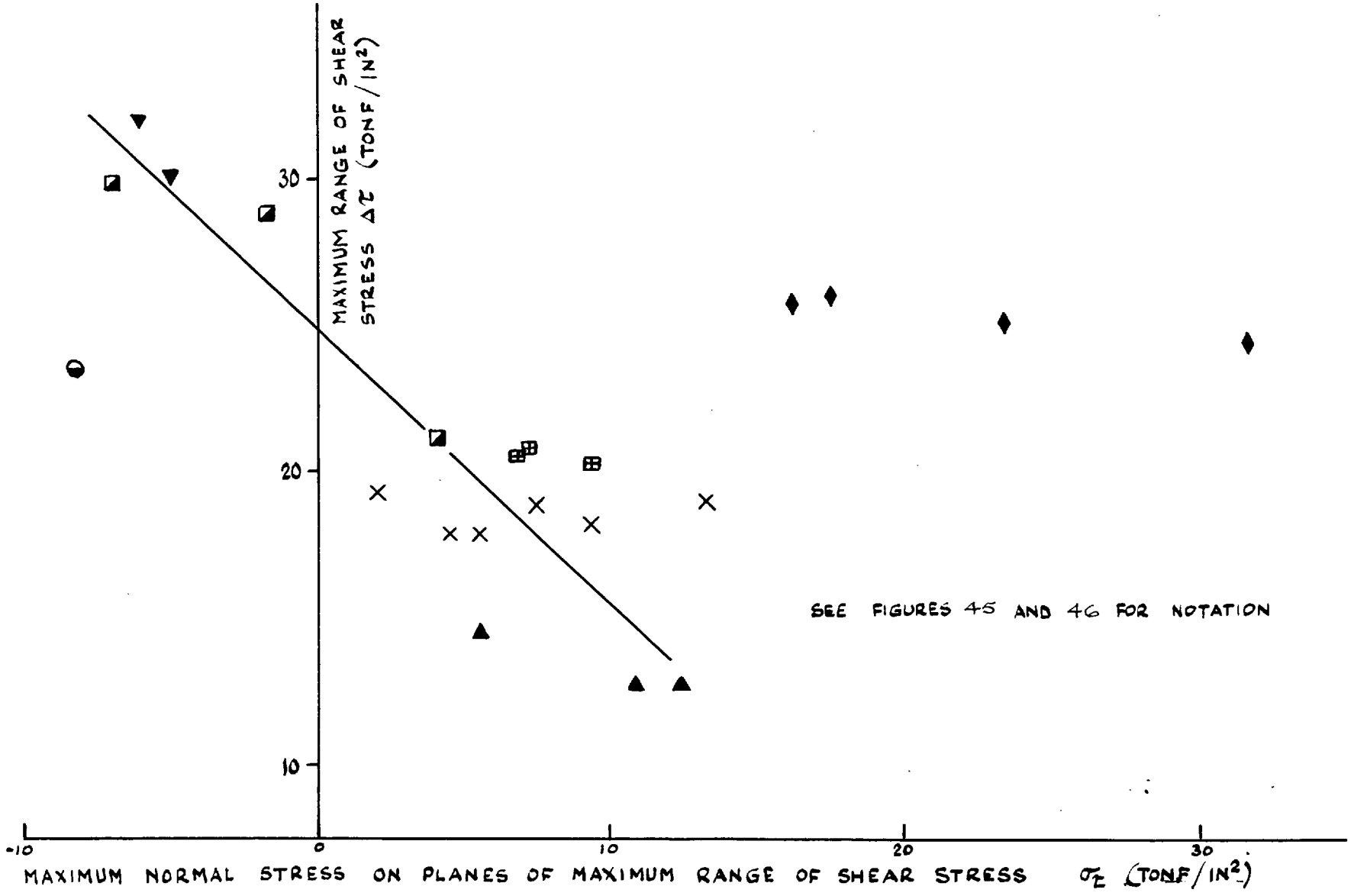



FIG 42 EFFECT OF NORMAL STRESS ON FATIGUE STRENGTH OF EN 25 STEEL CYLINDERS $10^6$ CYCLES

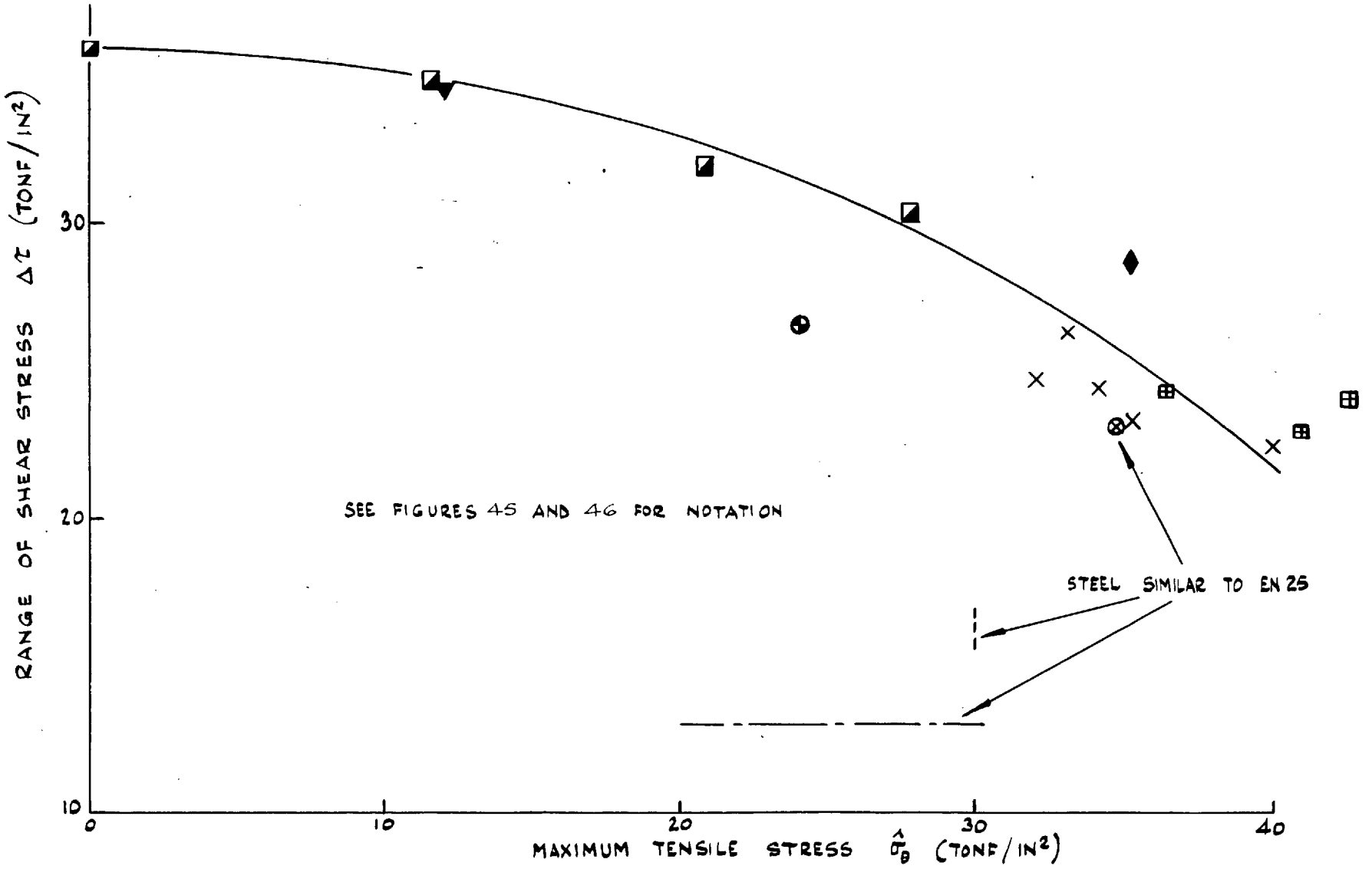



FIG 43 EFFECT OF TENSILE STRESS ON FATIGUE STRENGTH OF EN 25 STEEL CYLINDERS $10^5$ CYCLES

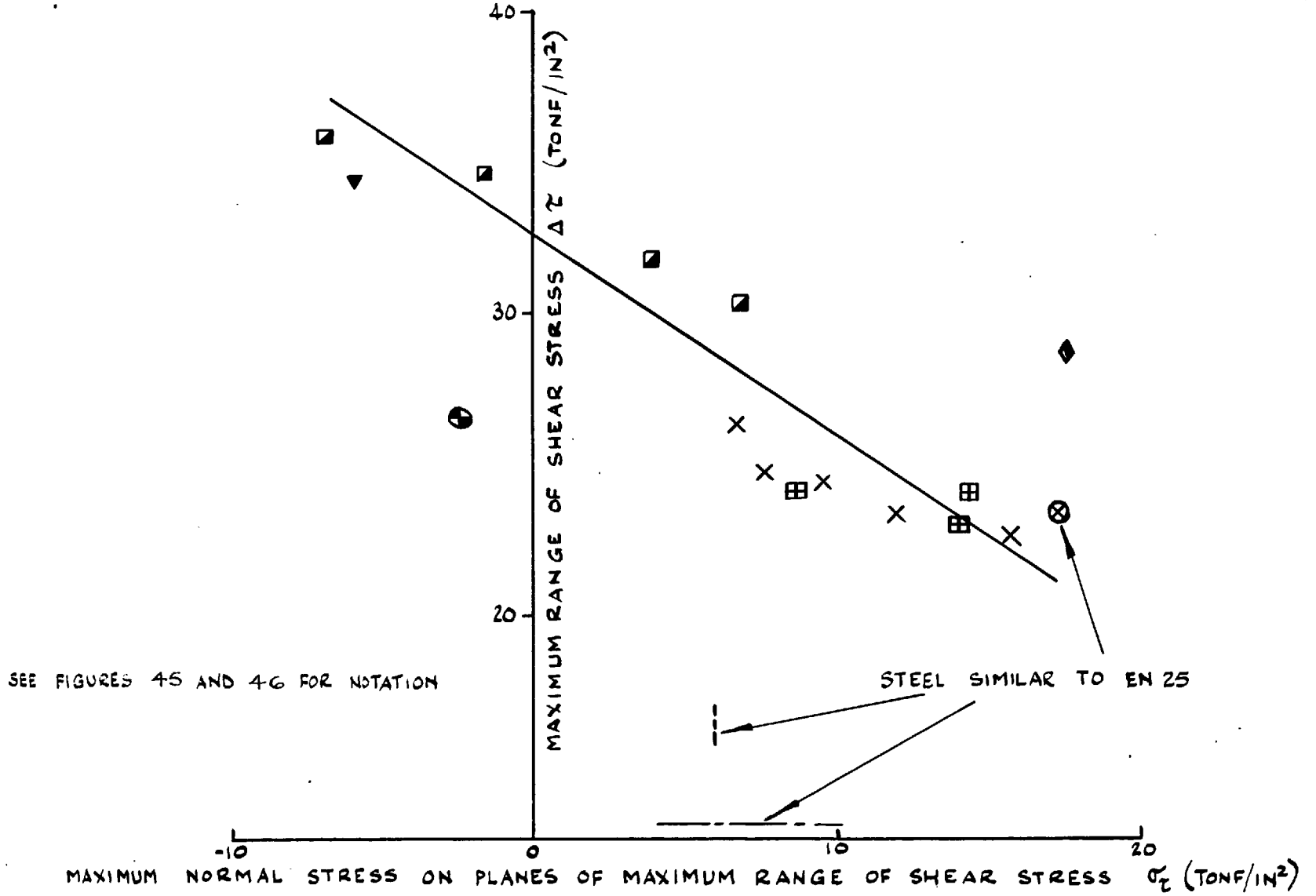



FIG 44 EFFECT OF NORMAL STRESS ON FATIGUE STRENGTH OF EN25 STEEL, CYLINDERS $10^5$ CYCLES

Hanway.
Robert tests

NOTATION USED IN FIGURES 18 TO 23 AND 41 TO 44

Material En 25

| SYMBOL | TEST | REFERENCE |
|---|---|---|
| □ | Solid torsion (Hydrostatic pressure) | Burns and Parry (24) |
| ■ | Thin walled tube torsion (Hydrostatic pressure) | |
| + | Solid torsion (Varying mean stress) | Chodorowski (25) |
| ● | Thin walled tube torsion (Varying mean stress) | |
| △ | Solid push-pull (Hydrostatic pressure and/or mean stress) | White, Crossland and Morrison (27) |
| ♦ | Cylinder push-pull (Static internal pressure) | Frost and Burns (15) |
| ▲ | Cylinder (Pulsating internal pressure) | Burns and Parry (14) |
| ▼ | Compound cylinder (Repeated internal pressure) | |
| × | Cylinder (Repeated internal pressure) | Morrison, Crossland and Parry (8) |
| ⊞ | Cylinder (Repeated internal pressure) Material in harder state than above. | |
| ⊖ | Autofrettaged cylinder (Repeated internal pressure) | |

FIGURE 45

## NOTATION USED IN FIGURES 18 TO 23 AND 41 TO 44

| SYMBOL | TEST | REFERENCE |
|---|---|---|
| ◓ | Cylinder (Repeated internal pressure and repeated external pressure) En 25 | Harvey and Lengyel (34) |
| ◪ | Cylinder (Fluctuating internal pressure and supporting external pressure) En 25 | Present tests series 3 |
| ⊗ | Cylinder (Repeated internal pressure and in-phase axial tension or compression) 4340 steel | Blass and Findley (13) |
| ! ! ! | Cylinder (Repeated internal pressure) 4330 steel | Austin, Reiner and Davidson (16) |
| —·—·— | Cylinder (Repeated internal pressure) $\overline{4340}$ steel | Davidson, Eisenstadt and Refner (10) |

P denotes protected.

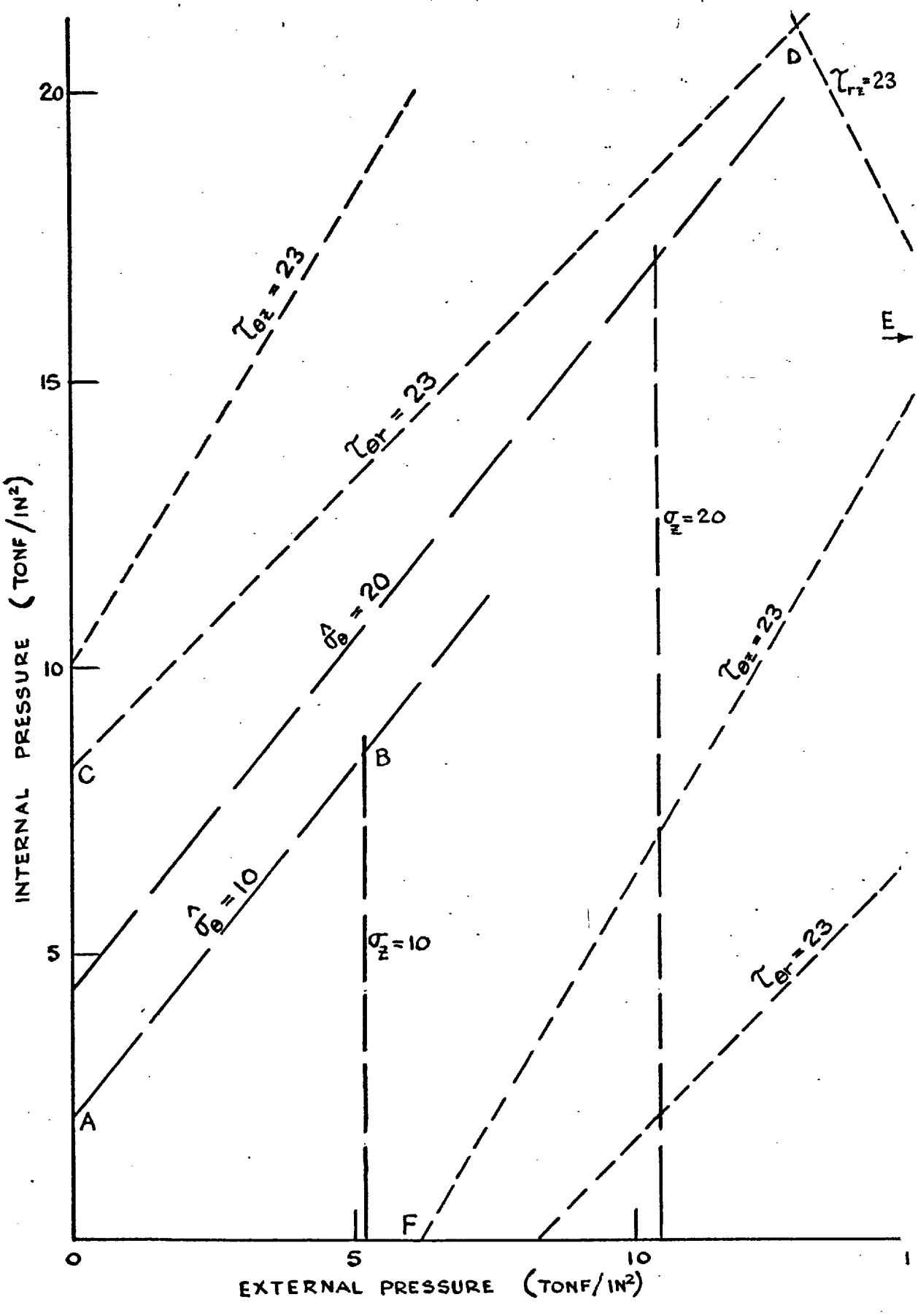
Figures adjacent to symbols are values of mean shear stress on planes of maximum range of shear stress.

TENSILE STRENGTHS

| Reference | 8 | 10 | 13 | 14 | 15 | 16 | 24 | 25 | 27 | 34 |
|---|---|---|---|---|---|---|---|---|---|---|
| Tensile strength ($Tonf/in^2$) | 56 and 66.4 | 71.5 to 85 | 58.5 | 57 | 55 to 62 | 81 to 87.5 | 57 | 54 to 56 | 55 to 59 | 58 |

Results for references 10 and 16, the harder material in reference 8 and the present tests have been modified, by the ratio 57/tensile strength ($tonf/in^2$), for comparison purposes in figures 41 to 44.

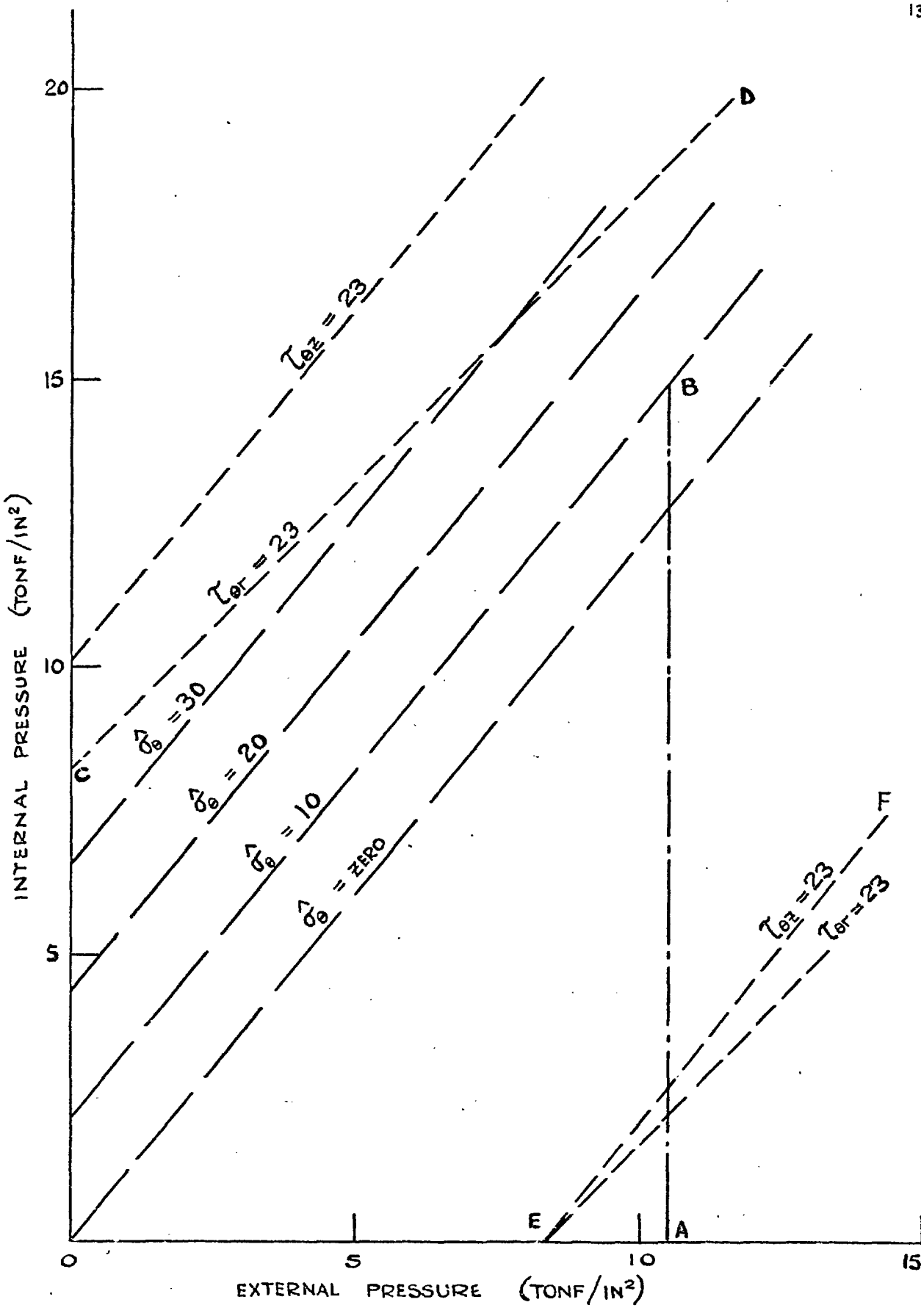
FIGURE 46




CYLINDER ELASTIC WHEN TESTED WITHIN ZONE CDEF

ALL STRESSES IN TONF/IN² EN 25 K = 1·25

FIG 47 — INTERNAL PRESSURE AGAINST EXTERNAL PRESSURE - CYLINDER WITH LONGITUDINAL STRESS

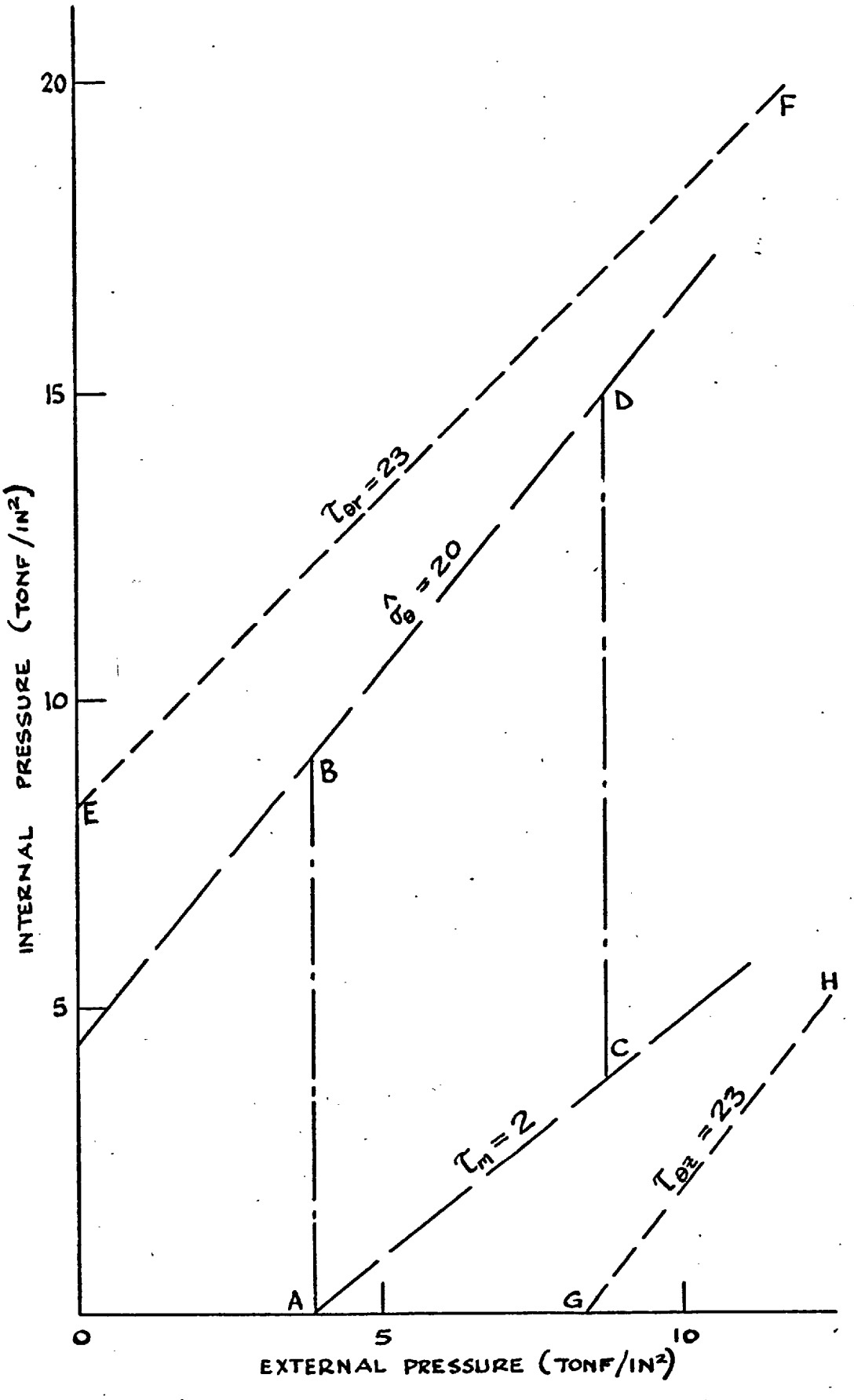



CYLINDER ELASTIC WHEN TESTED BETWEEN LINES CD AND EF

ALL STRESSES IN TONF / IN² EN 25 K = 1·25

TESTS AT CONSTANT $\hat{\sigma}_\theta$ AND $\sigma_t$ REPRESENTED BY LINE AB

FIG 48 - INTERNAL PRESSURE AGAINST EXTERNAL PRESSURE - CYLINDER WITHOUT LONGITUDINAL STRESS




CYLINDER ELASTIC WHEN TESTED BETWEEN LINES EF AND GH

ALL STRESSES IN TONF/IN² EN 25 K = 1·25

TESTS AT CONSTANT $\hat{\sigma}_\theta$ AND $\tau_m$ REPRESENTED BY LINES AB AND CD

FIG 49 - INTERNAL PRESSURE AGAINST EXTERNAL PRESSURE - CYLINDER WITHOUT LONGITUDINAL STRESS

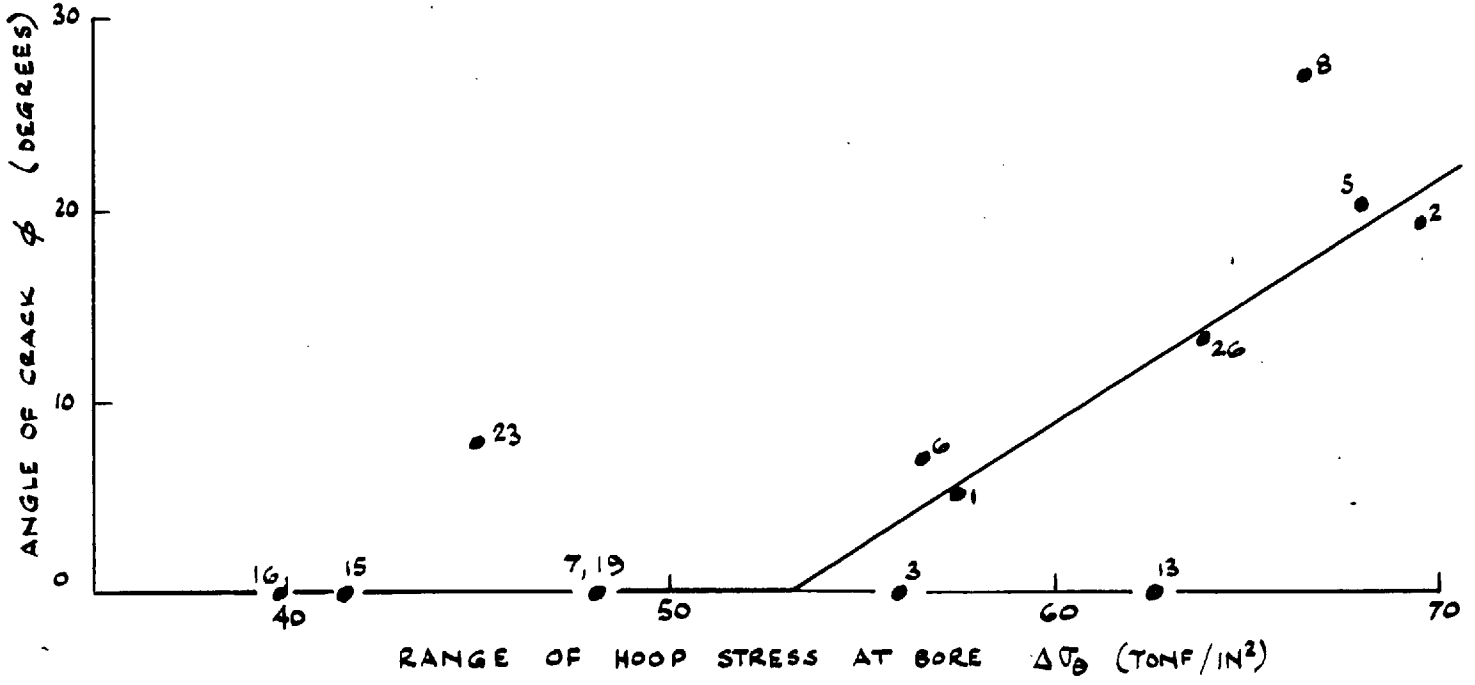



FIG 50 - φ AGAINST $\Delta\sigma_\theta$

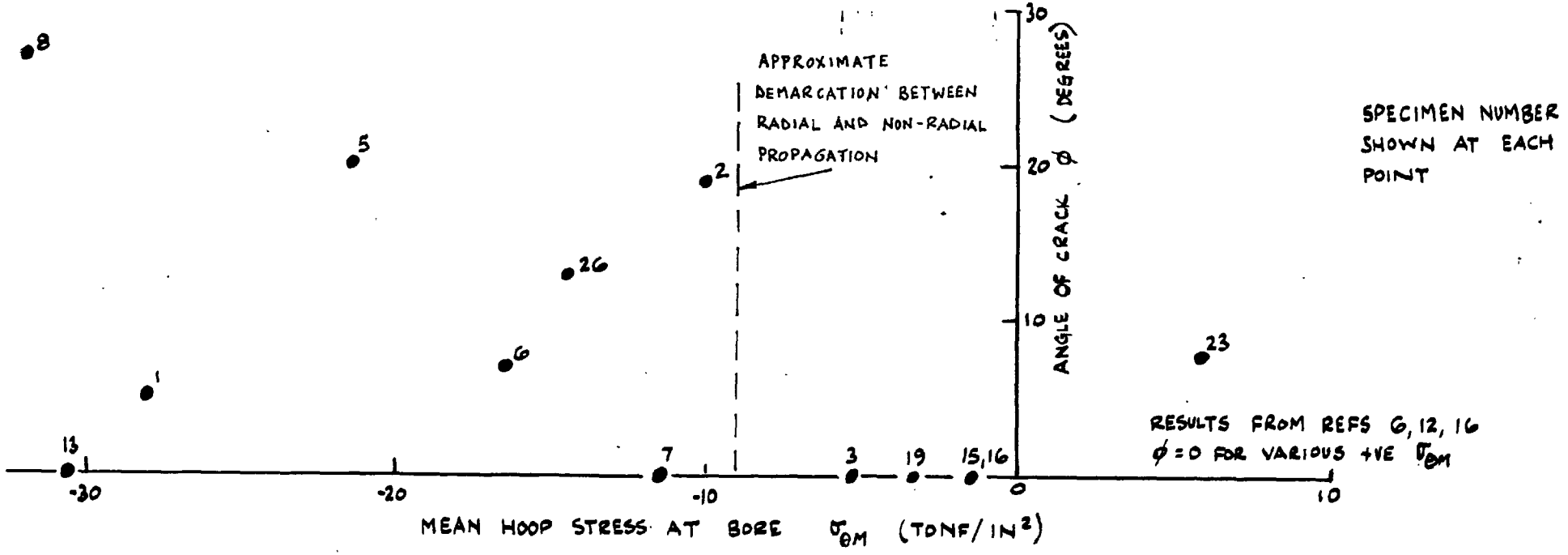



FIG 51 - $\phi$ AGAINST $\sigma_{\theta M}$

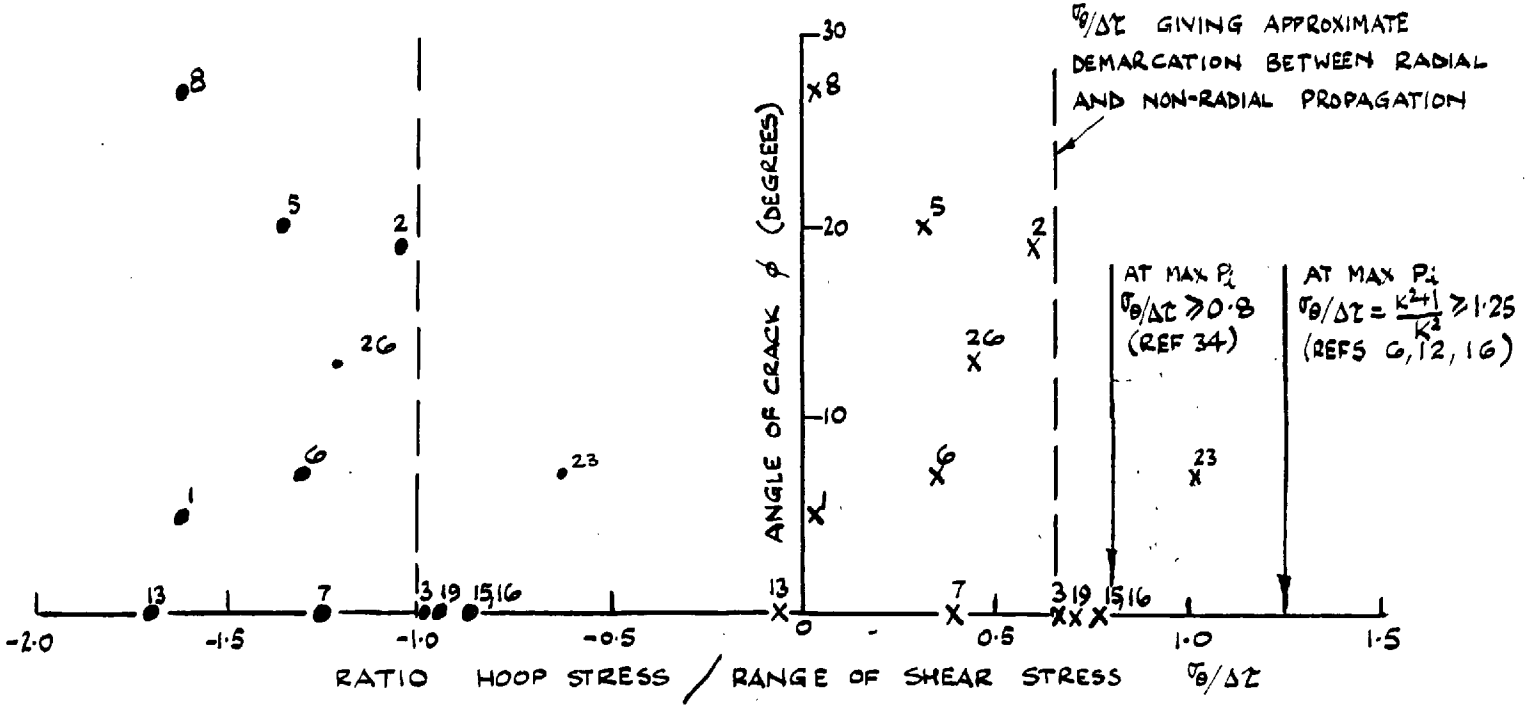



FIG 52 - $\phi$ AGAINST $\sigma_\theta/\Delta\tau$